

POLITECNICO DI TORINO

M.Sc. in Aerospace Engineering



Jet Propulsion Laboratory
California Institute of Technology

Hydrodynamics
Modeling and Simulation

FloBoS – A Time Domain Floating Bodies Simulator

Supervisor

Prof. Lorenzo CASALINO
Politecnico di Torino

Student

Orazio PINTI

Mentor

Dr. Marco B. QUADRELLI
NASA Jet Propulsion Laboratory – California Institute of Technology

March 2018

Contents

I	Introduction	7
1	Ship operational condition and reference frames	8
1.1	Reference frames	9
2	Mathematical background	12
3	Kinematic models	16
3.1	Maneuvering theory	17
3.2	Seakeeping theory	18
II	Sea loads and Equations of motion	20
4	Hydrostatic reactions	22
5	Hydrodynamic interactions	26
5.1	Frequency Domain formulation	26
5.2	Time Domain formulation	27
5.3	Ogilvie relations	30
5.4	Alternative representations of the radiation force	30
6	Potential theory	31
6.1	Incident wave potential flow	32
6.2	Potential flow around a vessel	36
6.2.1	Hydrodynamic forces and moments	39
6.2.2	Linearization of the hydrodynamic problem: Strip Theory	40
7	Rigid-body equation of motion	42
7.1	Seakeeping equation of motion	42
7.2	Maneuvering equation of motion	43
III	Time domain simulation	46
8	Linear systems representation	46

CONTENTS

9 Seakeeping simulation	48
9.1 Convolution term properties	48
9.2 Frequency domain identification problem	50
9.3 Identification of \mathbf{A}_∞ and Fluid Memory Effect	51
9.3.1 Order choice of $\hat{K}_{ik}(s)$, Model quality and Passivity	53
9.4 Alternative identification method for non-zero forward speed	54
9.5 Cummins equation resolution	58
10 Maneuvering simulation	61
10.1 Identification of $\mathbf{M}_{A,\infty}$, \mathbf{N}_∞ and Fluid Memory Effect	62
10.2 Cummins equation resolution	65
10.3 Sideslip stability	67
10.4 <i>PD</i> Controller	67
11 Integration with WAFO	69
11.1 Wave Spectrum	70
11.2 Directional spectrum	71
11.3 Spectra sampling	73
IV FloBoS - An overview	74
12 Simulation setting	77
12.1 <i>FloBoS</i> folders structure	77
12.2 <i>PDSTRIP</i> folder and cases subfolders	78
12.3 FloBoS.m settings	80
13 Code Logic description	82
14 Examples	90
15 Conclusions	102

Abstract

The aim of this work is the development of a time domain ship simulator called *FloBoS* – Floating Bodies Simulator.

Starting from the shape of an object, discretized by strips and defined by points, and the state of the sea, the simulator integrates the motion dynamical equations and reproduces the response in time domain. The advantage with respect to a pure frequency domain simulator consists in being able of capturing non periodic and transient motions.

FloBoS is structured in two sub-simulators:

- *SeaBoS* – Seakeeping Bodies Simulator, for *seakeeping*, which means to analyze the free response of a vessel trying to keep his path, or while it is at rest, in a wavy sea;
- *ManBoS* – Maneuvering Bodies Simulator, for *maneuvering*, i.e. simulating a controlled vessel, evaluating its capabilities to move above the free surface of a wavy sea.

After an in-depth theoretical overview on classical hydrodynamics mathematical and physical methods, these very models have been implemented in Matlab. The complexity of the equations governing these phenomena is notable and the hypothesis of linearity has been assumed.

The work includes both the implementation of known vessel motion models and the development of independent variations of these methods, designed *ad hoc* for the purpose and the nature of *FloBoS*.

The simulator reproduces the behavior of the vessel under the action of the waves hydrodynamics and excitation forces. The output comprises plots of the position, velocity and acceleration response; furthermore, a realistic graphic animation feature is present in the simulator, in order to help to have a good analysis, interpretation and understanding of the dynamics results.

FloBoS is also supported by other toolbox and software like PDSTRIP, MSS and WAFO: the first, based on potential theory, solves a set of bidimensional boundary values problems and provides data ready to be processed by *FloBoS*; the second, the Marine Systems Simulator – MSS, is a Matlab/Simulink library and simulator for marine systems; the last one, WAFO, is another Matlab toolbox able to generate, inter alia, realistic sea states and waves spectra: his integration in *FloBoS* allows to recreate more accurate vessels operational conditions.

The possible applications of *FloBoS* are:

- to evaluate the response of a vessel – with its dimensions, geometry and inertia characteristics, to a certain sea state;
- to evaluate the maneuvering capabilities of a vessel under certain environment conditions;

On the other hand, the restrictions to be applied to the simulations, in order to trust the results, are:

- slender bodies;
- small angles approximation;
- small wave amplitude;
- convex hull;
- speed range limited by a low Froude number.

Nomenclature

$\mathbf{A}(\omega)$ and $\mathbf{B}(\omega)$ – Frequency-dependent Added Mass and Potential Damping matrices
 \mathbf{A}_∞ and \mathbf{B}_∞ – Infinite frequency Added Mass and Potential Damping constant matrices
 $\tilde{\mathbf{A}}(j\omega)$ and $\tilde{\mathbf{B}}(j\omega)$ – Complex matrices for alternative description of the radiation forces
 \mathbf{A}_s , \mathbf{B}_s and \mathbf{C}_s – State-space Model matrices
 A_{wp} – Vessel water plane area
 β – Wave heading direction
 $D(\theta)$ – Directional waves spectrum
 δ – Sideslip angle
 η and $\xi \equiv \delta\eta$ – Generalized Position vectors
 φ – Velocity Potential function
 Fr – Froude number
 \mathbf{G} – Restoring matrix
 g – Gravity acceleration
 $\overline{GM}_{T/L}$ – Transverse and Longitudinal Metacentric heights
 H_{m0} – Significant waves height
 j – Imaginary unit
 k – Wave number
 $\mathbf{K}(t)$ and $\mathbf{K}(s)$ – Retardation matrix in time and frequency domain
 L_{pp} , B and d – Vessel Length, Beam and Draft
 \mathbf{M}_{RB} – Generalized Mass matrix
 $\mu(t)$ – Retardation convolution forces matrix
 ν and $\delta\nu$ – Generalized Velocity vectors
 ω – Wave frequency
 Ω – Fluid displaced volume
 p and ρ – Fluid pressure and density
 \hat{Q} – Approximated value of the variable Q
 s – Frequency variable
 $S^+(\omega)$ – JONSWAP waves spectrum
 t and t' – Time variables
 T_p – Peak period
 τ_{rad} and τ_{res} – Generalized radiation and restoring force vectors
 $\tau_{exc} \equiv \tau_{FK+Diff}$ – Froude-Krilov and Diffraction (or Excitation) force vector
 θ_0 – Waves main direction
 U – Vessel velocity
 \mathbf{u}^a – Coordinate form of the coordinate free vector \vec{u} , expressed in the $\{a\}$ frame of reference
 \mathbf{x} and \mathbf{y} – State variables
 ζ – Wave elevation

Part I

Introduction

In the past few years the number of applications of surface marine vessels simulators has seen a growing interest, thanks to the increasing of computational power and the improvement of mathematical models for ship dynamics. Indeed, simulators reliability continues to rise, against the always expensive acquisitions of experimental data.

Nevertheless, reliability of simulators models is usually a crucial and difficult point. The reason is that a hydrodynamics model can fit just a limited range of operational conditions, and defining the limit of a mathematical model is never a simple task. Each condition of the vessel is associated with particular physical phenomena and, at the same time, with other negligible ones. One should emphasize the right interactions in order to manage simple equations, but, at the same time, be capable to describe properly the motion of the vessel.

Nowadays many commercial seakeeping codes, most of whom based on potential theory, are usable for the prediction of loads and responses of a ship. Results are often provided in frequency domain, so, to implement a time domain simulation, they are just a starting point.

During my time at *JPL*, I developed *FloBoS* – *Floating Bodies Simulator* – a time domain simulator for ships, vessels and slender bodies in general. The purpose is to obtain the dynamical response in position, attitude, velocity and acceleration, given a certain sea state.

To define the state of the sea, it is possible to add manually a certain number of simple harmonics – specifying each amplitude, period and direction, or to exploit the integration with WAFO, a toolbox of Matlab routines for statistical analysis and simulation of random waves. The first option is useful in the validation process; if we have some available data concerning a particular ship, we can act on the ship with just one harmonic, i.e. a frequency well defined periodic force vector, and easily check if the results agree or not. If we see a good correlation, the particular analyzed case fits all the model constraints and we can trust more complicated simulation of the same ship too. Indeed WAFO creates a whole realistic spectrum of the sea, starting from the significant wave height H_{m0} , the peak period T_p and the main direction of the waves.

FoBoS is a user setting routine which can run two different simulators, depending of the aim of the simulation: *SeaBoS* – Seakeeping Bodies Simulator, or *ManBoS* – Maneuvred Bodies Simulator. The difference is about the reference frames where the equations of motions are expressed in; it depends if we want to analyze his free response to a particular sea state or to control the ship and validate his performance in maneuvering.

In this work we want to illustrate the process we carried out to design *FloBoS* and to implement every features in his framework, as well as outline the mathematical and physical apparatus the simulator is based on.

1 Ship operational condition and reference frames

The bearing hypothesis of the simulator’s mathematical model is the *linearity* of the problem, which is, of course, a very strong assumption in this kind of context. However, with a ship shape slender enough, the experimental data show that the above one is a good working approximation for small to moderate oscillations.

The motion of marine vessels is traditionally studied splitting the physical problem in two different areas: a ship-controlled motion in the absence of wave excitation – *maneuvering* – and a motion at a uniform speed with wave excitation – *seakeeping* –. This separation allows making different assumptions specific for each case, simplifying even more the analysis. We start describing these two fundamental type of motion.

In **maneuvering** the ship motion is considered developed in a horizontal plane, due to the action of control devices (propulsion systems and control surfaces) in calm water. The mathematical models one obtains from this assumption are aimed at assessing the ship capabilities to change attitude and velocity by the action of the control system. The main application finds place in ship simulators field, with the purpose of determining the ship’s directional stability and designing autopilots.

On the other hand, in **seakeeping** the dynamics of a vessel trying to keep its course and its speed constant, in presence of wave excitation, is studied; that naturally includes the case of zero speed. In seakeeping the control surfaces may be used to stabilize the vessel while sailing, reducing the motion induced by the waves. The aim is to analyze the ship response and the consequent motion when the sea state is no longer considerable calm. Performing these analysis, six degrees of freedom are often considered.

Splitting the problem this way leads to the definition of two operation regions for the ship, based on the speed of the ship itself and on the state of the sea.

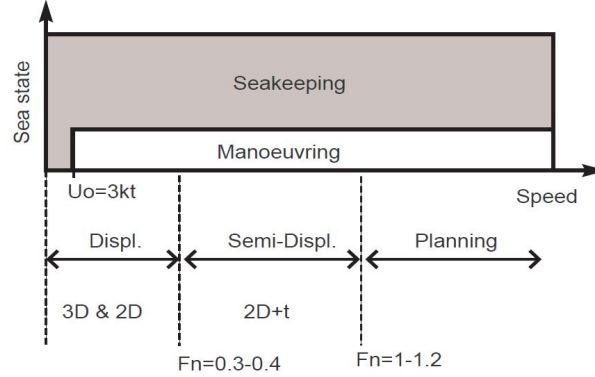


Figure 1: Sea state and range of speed covered in maneuvering and seakeeping.

Three regimes are also defined by the means of the *Froude number*, that characterizes a ship with a length L in a particular speed condition U : $Fr = \frac{U}{\sqrt{gL}}$. The behavior of a hull is strongly dependent on this number, which ponders the hydrodynamic effects – dictated by the speed U , with the hydrostatic ones – driven by the gravity g . For $Fr < 0.3$ the buoyancy effect is primarily due to the hydrostatic force: vessels operating in this regime are called *displacement vessels*. For $0.3 < Fr < 1$ hydrodynamic pressure acting on the bow of the hull generates a no longer negligible lift; this regime is for *semi-displacement vessels*. Finally, operating at $Fr > 1$ the flow under the hull becomes really complex and neither vorticity nor viscosity are negligible; this regime's name is *planning vessels*.

1.1 Reference frames

For convenience, *maneuvering* and *seakeeping* use different reference frames and coordinate systems to express the equations of motion, to make them easy to manage. In *maneuvering* the equations of motion are written relative to a body-fixed coordinate system.

To describe motion in *seakeeping* it's common to define a particular frame of reference, fixed to a virtual vessel in steady equilibrium and moving at the average speed and heading of the real vessel. Equations are formulated by means of the instantaneous waves-induced perturbations with respect to this equilibrium frame.

Since this frame follows an uniform path, corresponding to the average real motion, it's usable only if the ship has a zero-mean acceleration.

Most hydrodynamics programs compute the forces due to the interaction with the sea in the seakeeping equilibrium frame. When time domain simulations and motion control system designs are considered, it is necessary to use a unified framework and a body-fixed coordinate system is the natural choice. This calls for kinematic models that characterize the transformation of variables and forces among different coordinate systems. An overview on these reference frames and transformations models is therefore necessary, and it can be done recalling the work of [Perez&Fossen] and [Perez&Fossen2007].

Marine craft dynamics provides for a complete motion in six degrees of freedom. Indeed, a ship can experience interdependently three displacements and three rotations with respect three axes. The longitudinal displacement is called *surge*, the one who goes from starboard to port is *sway* and the one from the deck to the hull is called *heave*. The corresponding rotations are called: *roll*, *pitch* and *yaw*.

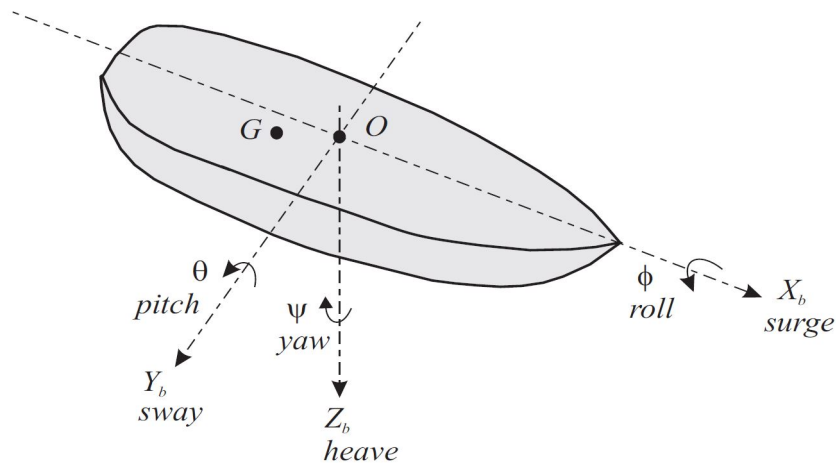


Figure 2: Definition of motions with respect to all degrees of freedom.

To express position and orientation of a ship, the following dextral orthogonal coordinate systems are commonly used:

- North-East-Down: $\{n\}$;
- Body-fixed: $\{b\}$;
- Seakeeping: $\{s\}$;

The **North-East-Down coordinate system** $\{n\} \equiv \{O_n, \vec{n}_1, \vec{n}_2, \vec{n}_3\}$ is a system fixed to the Earth and based on the local geographic properties. The origin O_n of this system lies on a plane tangent to the geodetic reference ellipsoid (*WGS84*) at a point of interest. The first unit vector \vec{n}_1 points towards the true North, \vec{n}_2 points towards the East and \vec{n}_3 points towards the interior of the earth perpendicular to the tangent plane, defining a dextral orthogonal system. This frame is considered inertial, which is a justified assumption thanks to the relative small velocity of a ship: hydrodynamic forces are prevalent with respect the fictitious ones like Coriolis and centrifugal forces, caused by the rotation of the Earth.

The **Body-fixed coordinate system** $\{b\} \equiv \{O_b, \vec{b}_1, \vec{b}_2, \vec{b}_3\}$ is fixed to the vessel, with \vec{b}_1 pointing towards the bow, \vec{b}_2 towards starboard and \vec{b}_3 downwards, completing the dextral orthogonal system. The typical convention for marine vehicles wants the origin O_b located at a half of the vessel along \vec{b}_1 , (*amidships*), and at the intersection of the longitudinal plane of symmetry ($\vec{b}_1 - \vec{b}_3$) and the design water line. It's important to point out that the equations of motion are typically formulated with respect this frame of reference.

The **Seakeeping coordinate systems** $\{s\} \equiv \{O_s, \vec{s}_1, \vec{s}_2, \vec{s}_3\}$ moves at the average speed of the vessel in linear motion. One can define and use this particular coordinate system only when the vessel sails with a straight average path at a constant average speed. Indeed, this frame moves fixed to a virtual vessel which reproduces the average motion of the real one. The hydrodynamics interaction with the water and the waves displaces the vessel with respect this equilibrium.

For the nature of this reference frame, it needs to be just a translation of the body-fixed system, when the instantaneous vessel position coincides with the equilibrium one. Because of that, the unit vector \vec{s}_1 points forward and is aligned with the average velocity vector, \vec{s}_2 points towards starboard and \vec{s}_3 downwards completing the dextral orthogonal system. The origin O_s is usually located such that the \vec{s}_3 axis passes through the center of gravity of the vessel at the equilibrium position and the horizontal plane $\vec{s}_1 - \vec{s}_2$ coincides with the mean free surface of the water.

Moreover, in a flat Earth approximation, this coordinate system position with respect the NED one is identified just by a translation on the N-E plane and a rotation about the D axis.

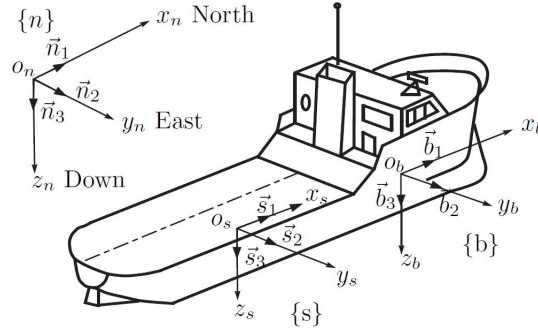


Figure 3: Reference frames used in classic ship motion theory

2 Mathematical background

It's important to specify the mathematical notation used to describe vectors, equations and models, and then report some basic notions and results before getting to the heart of the matter. Concerning the kinetic models, and their formalism and notation, we exploit the work done by [Perez&Fossen2007]; furthermore Einstein notation is used, which implies summation over a set of same-indexed terms in the same formula.

A vector is a physical entity, totally independent from a particular choice of a frame of reference: to refer to a vector itself, without considering its expression in a coordinate system, we will use the notation of a *coordinate free vector* \vec{u} .

When this vector is expressed by the means of a set of independent unit vectors \vec{a}_j , forming a generic reference frame $\{a\}$, one can write $\vec{u} = u_j^a \vec{a}_j$, where u_j^a are the measures of \vec{u} along \vec{a}_j , and $u_j^a \vec{a}_j$ are the components of \vec{u} in $\{a\}$. The *coordinate form* of the vector \vec{u} in $\{a\}$, which is the sorted collection of u_j^a , is represented by a column vector whom notation will be:

$$\mathbf{u}^a \equiv [u_1^a, u_2^a, u_3^a]^T$$

One should remember that the coordinate form is an expression of a vector quantity relative to a particular basis, that enables to manipulate and make operations with other vectors or matrices expressed in the same basis. On the other hand, the physical properties of vectors are basis-independent; when managing operations that hold whatever basis, one can simply use \mathbf{u} . For example $\vec{u} \cdot \vec{v} = \mathbf{u}^T \mathbf{v} = (\mathbf{u}^a)^T \mathbf{v}^a$, independently from the basis $\{a\}$.

Given a certain coordinate vector $\mathbf{u} = [u_1, u_2, u_3]^T$, one can define a matrix $\mathbf{S}(\mathbf{u})$ which represents his

skew-symmetric form:

$$\mathbf{S}(\mathbf{u}) \triangleq \begin{bmatrix} 0 & -u_3 & u_2 \\ u_3 & 0 & -u_1 \\ -u_2 & u_1 & 0 \end{bmatrix}$$

such that one can write a cross product as $\mathbf{u} \times \mathbf{v} = \mathbf{S}(\mathbf{u}) \mathbf{v}$.

The same vector can be expressed in different frames of reference: one can consider the problem to describe it in a certain coordinate system, knowing its expression in another one. In order to perform that, one needs to use an appropriate transformation matrix. The construction of these kind of matrix can be derived in different ways. For example, given two orthogonal basis $\{a\}$ and $\{b\}$, one can write:

$$\vec{r} = r_j^a \vec{a}_j = r_j^b \vec{b}_j$$

Expressing every unit vector \vec{a}_j forming the basis $\{a\}$, relative to the other basis $\{b\}$, like $\vec{a}_j = (\vec{a}_j \cdot \vec{b}_k) \vec{b}_k$, one can compute the frame transformation straightforward:

$$\sum_j r_j^a \left[\sum_k (\vec{a}_j \cdot \vec{b}_k) \vec{b}_k \right] = \sum_j r_j^b \vec{b}_j$$

Manipulating the last expression one can write for every index i :

$$\sum_j r_j^a \left[(\vec{a}_j \cdot \vec{b}_i) \vec{b}_i + \sum_{k \neq i} (\vec{a}_j \cdot \vec{b}_k) \vec{b}_k \right] = r_i^b \vec{b}_i + \sum_{j \neq i} r_j^b \vec{b}_j \implies \sum_j r_j^a (\vec{a}_j \cdot \vec{b}_i) = r_i^b$$

So, defining the *rotation matrix* that takes the expression of \vec{r} relative to $\{a\}$ into $\{b\}$ as

$$\mathbf{R}_a^b \triangleq [R_{ij} = \vec{a}_j \cdot \vec{b}_i], \quad (1)$$

one finds the fundamental relation:

$$\mathbf{r}^b = \mathbf{R}_a^b \mathbf{r}^a. \quad (2)$$

Rotation matrices are elements of the special orthogonal group: $\mathbf{R}\mathbf{R}^T = \mathbf{I}$, and $|\mathbf{R}| = 1$, so that $\mathbf{R}^{-1} = \mathbf{R}^T$.

Another way to derive the rotation matrix between two reference frames is considering *Euler angles*, a set of consecutive rotations around the main axes of a continuously transformed frame, until that one will coincide with the second one. The overall rotation matrix is created by means of *simple rotation matrices*, whose form is known, multiplied together.

These rotations can be performed in a different order, and each triplet is a different set of Euler angles. The set most commonly used in navigation is that of *roll*, *pitch* and *yaw*, which corresponds to the rotations performed in the following order:

1. Rotation about the z -axis of $\{b\}$ with a yaw angle ψ , resulting in the frame $\{b'\}$. The corresponding simple rotation matrix is:

$$\mathbf{R}_{z,\psi} = \begin{bmatrix} \cos \psi & -\sin \psi & 0 \\ \sin \psi & \cos \psi & 0 \\ 0 & 0 & 1 \end{bmatrix}$$

2. Rotation about the y -axis of $\{b'\}$ with a pitch angle θ , resulting in the frame $\{b''\}$. The corresponding simple rotation matrix is:

$$\mathbf{R}_{y',\theta} = \begin{bmatrix} \cos \theta & 0 & \sin \theta \\ 0 & 1 & 0 \\ -\sin \theta & 0 & \cos \theta \end{bmatrix}$$

3. Rotation about the x -axis of $\{b''\}$ with a roll angle ϕ , resulting in the frame $\{a\}$. The corresponding simple rotation matrix is:

$$\mathbf{R}_{x'',\phi} = \begin{bmatrix} 1 & 0 & 0 \\ 0 & \cos \phi & -\sin \phi \\ 0 & \sin \phi & \cos \phi \end{bmatrix}$$

and defines the relative attitude vector $\Theta_{ab} \triangleq [\phi, \theta, \psi]^T$.

The positive angle convention corresponds to a righthanded screw advancing in the positive direction of the axis of rotation. Using these consecutive single rotations, the overall rotation matrix can be expressed as:

$$\mathbf{R}_a^b = \mathbf{R}_{z,\psi} \mathbf{R}_{y',\theta} \mathbf{R}_{x'',\phi} = \begin{bmatrix} c_\psi c_\theta & -s_\psi c_\phi + c_\psi s_\theta s_\phi & s_\psi s_\phi + c_\psi c_\phi s_\theta \\ s_\psi c_\theta & c_\psi c_\phi + s_\phi s_\theta s_\psi & -c_\psi s_\phi + s_\psi c_\phi s_\theta \\ -s_\theta & c_\theta s_\phi & c_\theta c_\phi \end{bmatrix} \quad (3)$$

with $s_x \equiv \sin x$ and $c_x \equiv \cos x$. The two forms 1 and 3, derived with these two different approaches,

of course coincide.

Another important topic, with useful applications, is the one concerning the relative angular rate between two frames of reference. Given two frames $\{a\}$ and $\{b\}$, one can notice that, since the rotation matrix \mathbf{R}_b^a is orthogonal, the time derivative of $\mathbf{R}_a^b (\mathbf{R}_a^b)^T = \mathbf{I}$ must be zero. Computing the derivative

$$0 = \frac{d}{dt} \left[\mathbf{R}_a^b (\mathbf{R}_a^b)^T \right] = \dot{\mathbf{R}}_a^b (\mathbf{R}_a^b)^T + \mathbf{R}_a^b (\dot{\mathbf{R}}_a^b)^T = \dot{\mathbf{R}}_a^b (\mathbf{R}_a^b)^T + \left[\dot{\mathbf{R}}_a^b (\mathbf{R}_a^b)^T \right]^T$$

it's evident that the matrix $\dot{\mathbf{R}}_a^b (\mathbf{R}_a^b)^T$ is skew-symmetric. Thanks to that, all its properties can be described by a column vector and by the already mentioned linear operator \mathbf{S} .

The vector ω_{ab}^a of angular velocity of the frame $\{a\}$ with respect the frame $\{b\}$, with coordinates in $\{a\}$, is indeed defined as:

$$\omega_{ba}^a : \mathbf{S}(\omega_{ba}^a) = \dot{\mathbf{R}}_a^b (\mathbf{R}_a^b)^T$$

A physical interpretation of the former relation is that $\dot{\mathbf{R}}_a^b = \mathbf{S}(\omega_{ba}^a) \mathbf{R}_a^b$.

Given two frames $\{a\}$ to $\{d\}$ rotating one with respect the other, it may be useful is to find the relationship between the angular velocity ω_{ad} and the Euler angles time derivatives. In order to achieve this objective, let us consider three simple rotations from $\{a\}$ to $\{d\}$:

$$\mathbf{R}_b^a = \mathbf{R}_{z,\psi}, \quad \mathbf{R}_c^b = \mathbf{R}_{y,\theta}, \quad \mathbf{R}_d^c = \mathbf{R}_{x,\phi}$$

The three corresponding angular velocities are

$$\begin{cases} \omega_{ab}^a = [0, 0, \dot{\psi}]^T \\ \omega_{bc}^b = [0, \dot{\theta}, 0]^T \\ \omega_{cd}^c = [\dot{\phi}, 0, 0]^T \end{cases}$$

Thanks to linearity of the operator \mathbf{S} , the overall angular velocity is $\vec{\omega}_{ad} = \vec{\omega}_{ab} + \vec{\omega}_{bc} + \vec{\omega}_{cd}$ ([WAFO2017]).

Expressing this relation in the frame $\{a\}$ one obtain:

$$\omega_{ad}^a = \omega_{ab}^a + \mathbf{R}_b^a \omega_{bc}^b + \mathbf{R}_b^a \mathbf{R}_c^b \omega_{cd}^c$$

Computing the multiplication and isolating the vector $\dot{\Theta}_{ad} \triangleq [\dot{\phi}, \dot{\theta}, \dot{\psi}]^T$ one can finally reach the

following expression:

$$\dot{\Theta}_{ad} = \mathbf{T}_a(\Theta_{ad}) \omega_{ad}^a, \quad \mathbf{T}_a(\Theta_{ad}) = \begin{bmatrix} \frac{c_\psi}{c_\theta} & \frac{s_\psi}{c_\theta} & 0 \\ -s_\psi & c_\psi & 0 \\ c_\psi t_\theta & s_\psi t_\theta & 1 \end{bmatrix}. \quad (4)$$

Expressing the former in the $\{d\}$ frame, the analogous relation is:

$$\dot{\Theta}_{ad} = \mathbf{T}_d(\Theta_{ad}) \omega_{ad}^d, \quad \mathbf{T}_d(\Theta_{ad}) = \begin{bmatrix} 1 & s_\phi t_\theta & c_\phi t_\theta \\ 0 & c_\phi & -s_\phi \\ 0 & \frac{s_\phi}{c_\theta} & \frac{c_\phi}{c_\theta} \end{bmatrix}. \quad (5)$$

Note that neither $\mathbf{T}_a(\Theta_{ad})$ nor $\mathbf{T}_d(\Theta_{ad})$ are orthogonal. Further details can be found in [Perez&Fossen2007].

3 Kinematic models

To indicate relative position and velocity coordinate vectors among frames of reference it's necessary to use a three-script notation. Indeed, given two frames $\{a\}$ and $\{b\}$, the relative position coordinate vector have to bring both the information of the orientation and the system where it's expressed. If \vec{r}_{ab} is the vector from $\{a\}$ to $\{b\}$, which indicates the position of $\{b\}$ relative to $\{a\}$, the coordinate form \mathbf{r}_{ab}^a , indicates the same vector expressed in $\{a\}$. That is, the upper script indicates in which coordinate system the vector is expressed, while the order of the lower scripts indicate the orientation of the relative position. If one needs this relative position expressed in $\{b\}$, with the rotation matrix the computation is immediate: $\mathbf{r}_{ab}^b = \mathbf{R}_a^b \mathbf{r}_{ab}^a$.

Concerning the velocity, the notation is similar: \mathbf{v}_{ab}^a indicates the velocity of $\{b\}$ relative to $\{a\}$, expressed in $\{a\}$. This notation should be used only if the frame with respect to which the derivative is taken is inertial. If that is verified, then

$$\mathbf{v}_{ab}^a \triangleq \dot{\mathbf{r}}_{ab}^a \equiv \frac{{}^a d}{dt} \vec{r}_{ab} = \dot{r}_j^a \vec{a}_j$$

One must always specify with respect to what coordinate system a derivative of a vector is taken. The well known coordinate-free relationship between the derivatives of a vector in two coordinate systems is:

$$\frac{{}^a d}{dt} \vec{r} = \frac{{}^b d}{dt} \vec{r} + \vec{\omega}_{ab} \times \vec{r}$$

It is possible to derive the same relation in coordinate form, expressing every vector in $\{b\}$ for example, reaching the following one:

$${}^a\dot{\mathbf{r}}^b = {}^b\dot{\mathbf{r}}^b + \mathbf{S}(\omega_{ab}^b) \mathbf{r}^b$$

where the upper-left script indicates the coordinate system with respect to which the derivative is taken.

3.1 Maneuvering theory

In maneuvering theory, the position of a ship is given by the position of the origin of $\{b\}$ relative to $\{n\}$ \vec{r}_{nb} . When expressed in coordinate form in $\{n\}$, this vector gives the North, East and Down positions:

$$\mathbf{r}_{nb}^n \triangleq [N, E, D]^T$$

The attitude of the vessel will be given by the angles or roll, pitch and yaw that take $\{n\}$ into $\{b\}$, $\Theta_{nb} \triangleq [\psi, \theta, \phi]^T$

The linear velocities are usually expressed in the body-fixed frame: the *linear velocity* in $\{b\}$ is given by

$$\mathbf{v}_{nb}^b \triangleq [u, v, w]^T = \mathbf{R}_n^b \dot{\mathbf{r}}_{nb}^n = \mathbf{R}_n^b [\dot{N}, \dot{E}, \dot{D}]^T$$

whose component are called *surge*, *sway* and *heave speeds*.

On the other hand, the angular velocity in $\{b\}$, formed by *surge*, *sway* and *heave rates*, is given by

$$\omega_{nb}^b = [p, q, r]^T$$

Exploiting the relation 4, the dependence of ω_{nb}^b from the time derivative of the Euler angle can be written as

$$\dot{\Theta}_{nb} = \mathbf{T}_b(\Theta_{nb}) \omega_{nb}^b$$

Please note that the trajectory of the vessel can be computed only with the velocity in an inertial frame, like $\{n\}$:

$$\mathbf{r}_{nb}^n(t) = \mathbf{r}_{nb}^n(t_0) + \int_{t_0}^t \mathbf{R}_b^n \mathbf{v}_{nb}^b dt'$$

Before writing the kinetic model, one can join linear and angular variables, defining the *generalized coordinate position* and *velocity vectors*, as suggested by [Fossen2002]:

$$\eta \triangleq \begin{bmatrix} \mathbf{r}_{nb}^n \\ \Theta_{nb} \end{bmatrix} = [N, E, D, \psi, \theta, \phi]^T \quad \nu \triangleq \begin{bmatrix} \mathbf{v}_{nb}^b \\ \omega_{nb}^b \end{bmatrix} = [u, v, w, p, q, r]^T. \quad (6)$$

From relations already derived, the *maneuvering kinematic model* follows:

$$\dot{\eta} = \begin{bmatrix} \mathbf{R}_n^b & \mathbf{0}_{3 \times 3} \\ \mathbf{0}_{3 \times 3} & \mathbf{T}_b \end{bmatrix} \nu = \mathbf{J}_b^n(\eta) \nu \quad (7)$$

3.2 Seakeeping theory

In seakeeping the motion of the vessel is described relative to the inertial seakeeping coordinate system $\{s\}$. As long as the sea is calm and there are no waves, the vessel remains in equilibrium condition, with zero relative linear and angular velocity with respect to $\{s\}$. However, in presence of waves, excitation forces are experienced by the marine vehicle and it oscillates with respect to this equilibrium. The virtual equilibrium vessel state is defined by a constant heading $\bar{\psi}$ and speed U :

$$\begin{cases} \mathbf{v}_{ns}^n = \dot{\mathbf{r}}_{ns}^n = [U \cos \bar{\psi}, U \sin \bar{\psi}, 0]^T \\ \omega_{ns}^n = [0, 0, 0]^T \\ \Theta_{nb} = [0, 0, \bar{\psi}]^T \end{cases}$$

That means that the velocity of $\{s\}$ relative to $\{n\}$ expressed in $\{s\}$ is $\mathbf{v}_{ns}^s = [U, 0, 0]^T$.

For the analysis of the motion of a vessel, a $\{b\}$ to $\{s\}$ kinetic model derivation is required; the linear and angular velocity of the vessel $\{b\}$ relative to $\{s\}$ and expressed in $\{b\}$ are:

$$\begin{cases} \mathbf{v}_{sb}^b = \mathbf{R}_s^b \dot{\mathbf{r}}_{sb}^s \triangleq [\delta u, \delta v, \delta w]^T \\ \omega_{sb}^b \triangleq [\delta p, \delta q, \delta r]^T \end{cases}$$

They represent instantaneous perturbations of the vessel position and attitude with respect the average trajectory. To identify the instantaneous attitude of $\{b\}$ we can use, as usual, Euler angles that take $\{s\}$ to $\{b\}$, related with ω_{sb}^b thanks to the 5:

$$\begin{cases} \Theta_{sb} \triangleq [\delta\psi, \delta\theta, \delta\phi]^T \\ \dot{\Theta}_{sb} = \mathbf{T}_b(\Theta_{sb})\omega_{sb}^b \end{cases}$$

Merging the variables, as done for maneuvering, we can define the *perturbation generalized position* and *velocity* vectors:

$$\delta\eta \triangleq \begin{bmatrix} \mathbf{r}_{sb}^s \\ \Theta_{sb} \end{bmatrix} \quad \delta\nu \triangleq \begin{bmatrix} \mathbf{v}_{sb}^b \\ \omega_{sb}^b \end{bmatrix}. \quad (8)$$

It's common to find the notation $\xi \equiv \delta\eta$ in hydrodynamics literature. From the definition we gave, the kinetic model became:

$$\delta\dot{\eta} = \begin{bmatrix} \mathbf{R}_b^s & \mathbf{0}_{3 \times 3} \\ \mathbf{0}_{3 \times 3} & \mathbf{T}_b \end{bmatrix} \delta\nu = \mathbf{J}_b^n(\delta\eta) \delta\nu \quad (9)$$

Another useful model are the one that relates velocities ν and $\delta\nu$ and accelerations $\dot{\nu}$ and $\delta\dot{\nu}$. With small angle approximations and linearization, the following relations can be derived (see [Perez&Fossen2007]):

$$\begin{cases} \nu = \bar{\nu} + \delta\nu \\ \nu \approx U(-\mathbf{L}\delta\eta + \mathbf{e}_1) + \delta\nu \\ \dot{\nu} \approx -U\mathbf{L}\delta\nu + \delta\dot{\nu}. \end{cases} \quad (10)$$

with

$$\mathbf{L} = \begin{bmatrix} 0 & 0 & 0 & 0 & 0 & 0 \\ 0 & 0 & 0 & 0 & 0 & 1 \\ 0 & 0 & 0 & 0 & -1 & 0 \\ 0 & 0 & 0 & 0 & 0 & 0 \\ 0 & 0 & 0 & 0 & 0 & 0 \\ 0 & 0 & 0 & 0 & 0 & 0 \end{bmatrix} \quad \mathbf{e}_1 = [1, 0, \dots, 0]^T.$$

Part II

Sea loads and Equations of motion

Before formulating the laws of motions and the models through which a ship simulator can be implemented, an overview about the nature of the interactions between a moving vessel and a rough sea is required.

The total interaction can be written as a generalized vector τ , by assembling both force and torque components. The fluid field around the hull of a moving vessel creates a time dependent vector τ , which can be seen as the superposition of different effects.

The physical phenomena of sea waves excites the ship with a time dependent force, because of the change in pressure of the fluid field around the hull. The ship starts moving and oscillating under their action, producing a feedback reaction which perturbs in turn the water, changing the momentum of the fluid. This reaction has a conservative part, proportional to the accelerations of the vessel, and a non-conservative part proportional to the velocities. The former reflects the loss of energy carried away from the hull, becoming itself a source of radiated waves.

Thanks to linearity, we can consider separately these effects. Therefore we are assuming that the system behaves as if the simple linear superposition of all these kind of forces differs from the overall effect when they act at the same time, interacting each other, by a negligible factor, if the sea condition is not extreme.

So one can identify multiple contributions which compose the global problem:

- The first is the zero mean linear **excitation contribution**: the waves encounter a vessel bound to be at rest, which experiences a time dependent force τ_{exc} , called first order *waves excitation force* or *load*, caused by the changing of the pressure field. This effect can, in turn, be splitted in two more basic interactions: *Froude-Krilov forces*, the pressure field the sea would generate without ship, and *diffraction force*, due to the fact that the ship behaves as an obstacle against the incoming waves, modifying the conformation of the waves structure.
- The second is the **radiation contribution**: as mentioned, this effect is equivalent of the forced oscillation of the ship, in the same way as it would do in presences of the waves, but in calm water. By setting in motion the sea, these oscillations cause *radiation forces* τ_{rad} on the vessel.

The total reaction can be splitted in the in-phase and out-of-phase components. The first one is due to the *added mass* phenomena, i.e. the mass of fluid bounded to the hull that accelerates with it, because of the adherence condition; this component results proportional to the linear and rotational accelerations of the vessel. On the other hand, the out-of-phase component is the *damping force*, proportional to the instantaneous velocities. This force includes a memory effect term: the instantaneous changing in momentum affects the force in future. In other words, the radiation forces at a particular time depend on the whole history of the velocity of the vessel up to that time. Due to the fact that we are not considering viscous and rotational effects, the damping effect is also called in literature *potential damping*; the reason is to specify that this force comes just from potential theory.

- Finally, the last effect is the static pressure field contribution: the **hydrostatics reaction**. It's proportional to water displaced volume and it's caused by the gravity acting on the fluid. The change in position of the center of buoyancy, caused by the action of the other time dependent forces on the vessel, implies the variation of this hydrostatics effect. This tends to re-establish the stable static position of the vessel: that's why this force is called restoring force, τ_{res} . A problem that can arise, concerning the stability of the ship dynamics, is that this restoring force is not present in every degree of freedom. To avoid the possibility to manage unstable dynamics equations, some mathematical manipulations are needed; as shown by [Cummins1962], one have to set the right initial conditions, exploiting the asymptotic limit of the response function, in order to rewrite an equivalent stable differential problem.

Hence, the following separation of the *generalized force vector* τ is considered:

$$\tau = \tau_{exc} + \tau_{rad} + \tau_{res}. \quad (11)$$

The non-linear effect of viscous force τ_{visc} , generated by friction and vortex shedding phenomena, is not directly computed. In our models we will use empirical formulas, accepting the consequent approximation error that will affect the results.

Another non-linear contribution due to second order excitation forces is also present. This contribution is composed both by non-oscillatory forces, *mean wave drift forces*, and oscillatory forces. The

oscillatory components act at lower and higher frequencies than the linear wave loads one. The force acting at lower frequencies is known as *slow wave drift load*, which constitutes with the *mean wave drift* and the first order wave load the main disturbances for the ship control system. On the other hand the high frequencies forces can result in structure oscillation of the ship; this phenomena is named *springing*.

4 Hydrostatic reactions

When a body is partially or completely submerged in a fluid, it experiments buoyancy forces and moments, which are also called *restoring forces*. Indeed the external gravitational field induces a pressure gradient in the fluid, and the pressure field is not constant along the local gravity vector direction. It holds the *Stevino* law, that, in the simple case of flat Earth approximation, considering a NED reference frame, can be written as $p = p_0 + \rho g z$, where p_0 is the atmospheric pressure on the free surface and z is the vertical coordinate: pressure increases linearly with the depth of the fluid, because of its own weight. This non uniformity of the pressure field generates a non-zero net force and moment when integrating it on the surface of a partially or completely submerged body. The buoyancy center does not correspond in general with the center of mass of the body, that leads to the net moment. The force depends only on the position of the body, and in particular it's proportional to the volume of displaced fluid Ω . Indeed, using *Gauss theorem*, the net force due to the pressure field acting on a body Ω , with a surface Σ and external normal vector \vec{n} , is written as:

$$\vec{F} = - \int_{\Sigma} p \vec{n} d\sigma = - \int_{\Omega} \nabla p d\Omega = - \int_{\Omega} (0, 0, \rho g) d\Omega = -\rho g \Omega \vec{k}$$

where \vec{k} is the unit vector pointing downwards and ρ is the density of the fluid. To assure floating equilibrium it must holds $W = \rho g \Omega$, with W indicating the weight of the body. For a partially submerged body, the mathematical surface Σ , where the integration is carried out, is the wet hull and the water plane area, where the static pressure is considered identical to the constant atmosphere one. Note that for a surface integral on a closed surface, the component p_0 of the pressure does not affect the result, because its integration is identical null. By its definition, Σ is the boundary of the volume of the fluid displaced, in general different with respect to the one of the whole body.

For the static analysis we need to identify the hydrostatic derivatives, which give the static reaction of the fluid due to displacements in the 6 degrees of freedom.

Considering surface vessels, static stability, also known as *Metacentric stability*, is an important requirement: the vessel should respond to any inclination with an opposite moment, naturally generated by its weight.

For surface vessels, the restoring forces will depend on the vessel's metacentric heights (transverse \overline{GM}_T and longitudinal \overline{GM}_L), the location of the center of gravity – CG , the center of buoyancy – CB , as well as size of the water plane A_{wp} .

The *metacenter* is defined as the theoretical point of intersection between a vertical line through the center of buoyancy of a floating body and a vertical line through the new center of buoyancy when the body is tilted, as shown in figure.

Basically, when the vessel heels the buoyancy force gets shifted towards the most submerged side of the hull; its displacement generates a rolling moment with respect to the center of mass. If the submerged volume increasing appears at the same side of the hull which rolls down, with respect to the center of mass, the consequent moment will restore the initial equilibrium, otherwise it will amplify the tilt. That means that, in order to have static stability, the center of mass must be placed low enough.

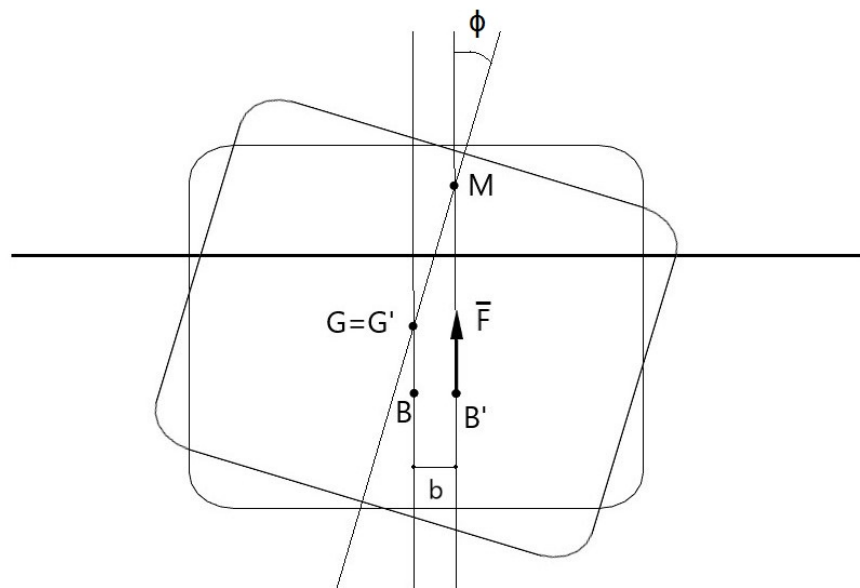


Figure 4: Transverse metacentric stability

As long as the load of a ship remains stable, G is fixed. For small angles M_T can also be considered to be fixed, while B moves as the ship heels. In order to assure static stability, M_T must be above the center of gravity. The distance \overline{GM}_T , dynamically equivalent to a spring stiffness, measures the stability capacity of the ship and remains constant for small angles. Indeed, the restoring moment K , due to the integration of the static pressure on the wet hull surface, is linear with the roll angle ϕ when the former is small enough: $K(\phi) = K_\phi \phi$. The restoring moment, on the other hand, can be also written as the product of the buoyancy force F and a certain arm b ; furthermore F must be always equal to the weight W for the static equilibrium analysis, so it's constant. From the equality $|K_\phi| \phi = Wb$ and the small angle approximation, simple considerations lead to:

$$\frac{Wb}{|K_\phi|} = \phi \approx \sin \varphi \triangleq \frac{b}{\overline{GM}_T}$$

which means

$$\overline{GM}_T = \frac{|K_\phi|}{W}.$$

Same considerations may be carried out for the longitudinal static stability, reaching a similar relation for \overline{GM}_L :

$$\overline{GM}_L = \frac{|M_\theta|}{W}.$$

In literature more classical ways to calculate the *metacenter heights* can be found, with formulas that exploit the second moments of area of the water plane J_T , J_L : the distance of the *metacenter* from the *buoyancy center* is determined by the ratio between the inertia resistance of the boat and the fluid displaced volume of the boat

$$\overline{BM}_{T/L} = \frac{J_{T/L}}{\Omega}$$

So, knowing the vertical position of the center of buoyancy, which is the one of the center of mass of the displaced volume, one can compute:

$$\overline{GM}_{T/L} = (z_b - z_g) + \overline{BM}_{T/L}$$

Starting from the equilibrium position, any vertical displacement of the vessel z implies a variation of the displaced volume of the fluid $\Omega(z) = \Omega(0) + \delta\Omega(z)$, being the equilibrium volume $\Omega = \Omega(0) = \frac{W}{\rho g}$.

A displaced volume changing reflects on the hydrostatic force:

$$Z = W - \rho g \Omega(z) = -\rho g \delta \Omega(z)$$

Indicating as $A_{wp}(\zeta)$ the water plane area of the vessel as a function of the vertical coordinate, the volume variation $\delta \Omega(z)$ is written as $\delta \Omega(z) = \int_0^z A_{wp}(\zeta) d\zeta$; however, for conventional vessel, the assumption $A_{wp}(\zeta) \approx A_{wp}(0)$ is a good approximation for small perturbation. Hence the approximated restoring force is linear in z :

$$Z \approx -\rho g A_{wp}(0) z = Z_z z.$$

The hydrostatic derivative Z_z is correctly negative, meanings that for a positive (downwards) displacement z , the buoyancy force becomes larger than the equilibrium one, since the submerged volume is increased. If the body is non symmetrical with respect to the $y - z$ plane, other static restoring forces appear: we modelise them with the same linear approximation by the means of the hydrostatics derivatives Z_θ and M_z .

When a pitch angle θ appears, the submerged volume increases because of the part of the vessel who pitch down and decrease for the part who pitch up: the net change $\delta \Omega(\theta)$ can be computed integrating the function of every single infinitesimal volume $h \cdot dA_{wp} = \theta x \cdot dA_{wp}$ all over the wet area. The hydrostatics force will change proportionally to $\delta \Omega(\theta)$:

$$Z = -\rho g \delta \Omega(\theta) = - \left(\rho g \int_{A_{wp}} x \cdot dA_{wp} \right) \theta = Z_\theta \theta$$

That means $Z_\theta = -\rho g \int_{A_{wp}} x \cdot dA_{wp}$.

The last hydrostatic derivative to identify is M_z , which will result identical to Z_θ . The resulting pitch moment M , caused by a perturbation in heave z , can be computed by integrating every single change in force Z multiplied by the arm, which is x ; at every station x , the force depends on the local submerged volume, which is $z \cdot dA_{wp}$, and the resulting moment is $\rho g \cdot z \cdot dA_{wp} \cdot x$. Hence

$$M = \left(\int_{A_{wp}} \rho g \cdot x \cdot dA_{wp} \right) z = M_z z$$

The whole linear restoring force vector can be written as

$$\tau_{res} = -\mathbf{G} \cdot \boldsymbol{\eta} = \begin{bmatrix} 0 & 0 & 0 & 0 & 0 & 0 \\ 0 & 0 & 0 & 0 & 0 & 0 \\ 0 & 0 & Z_z & 0 & Z_\theta & 0 \\ 0 & 0 & 0 & K_\phi & 0 & 0 \\ 0 & 0 & M_z & 0 & M_\theta & 0 \\ 0 & 0 & 0 & 0 & 0 & 0 \end{bmatrix} \begin{bmatrix} x \\ y \\ z \\ \phi \\ \theta \\ \psi \end{bmatrix}$$

with:

$$\begin{aligned} Z_z &= -\rho g A_{wp}(0) \\ K_\phi &= -\rho g \overline{GM}_T \\ M_\theta &= -\rho g \overline{GM}_L \\ Z_\theta &= -\rho g \int_{A_{wp}} x \cdot dA_{wp} \\ M_z &= \rho g \int_{A_{wp}} x \cdot dA_{wp} \end{aligned}$$

5 Hydrodynamic interactions

5.1 Frequency Domain formulation

Assuming a ship sailing at a forward speed U in a pure sinusoidal regime of the waves, radiation force can be expressed in the frequency domain, as shown by [Newman1997, Faltinsen1990], as follows:

$$\tau_{rad}(j\omega) = -\mathbf{A}(\omega, U) \ddot{\eta}(j\omega) - \mathbf{B}(\omega, U) \dot{\eta}(j\omega) \quad (12)$$

The matrices $\mathbf{A}(\omega)$ and $\mathbf{B}(\omega)$ are the *frequency dependent added mass* and *potential damping matrices* respectively. The motion of the ship will be a combination of oscillations in every degree of freedom, carried out at the same frequency ω of the waves: $\eta(j\omega) = \bar{\eta}e^{j\omega t}$. That leads to the following formulation:

$$\tau_{rad}(j\omega) = [\omega^2 \mathbf{A}(\omega, U) - \omega \mathbf{B}(\omega, U)] \eta(j\omega) \quad (13)$$

Concerning the excitation force τ_{exc} , we can express it as: $\bar{\tau}_{exc}$

$$\tau_{exc}(j\omega) = \bar{\tau}_{KF}(\omega, U, \beta) e^{j\omega t} + \bar{\tau}_{Diff}(\omega, U, \beta) e^{j\omega t} = \bar{\tau}_{exc}(\omega, U, \beta) e^{j\omega t} \quad (14)$$

where β the sideslip angle between \vec{U} and the x body axis. The approach to achieve this formulation is to find the velocity potential for the fluid field of the excitation sub problem, identifying then the contributions. A deeper analysis of the derivations of 12 and 14 will be given in the next section, after treating the potential theory.

To conclude, we recall the restoring forces, only function of the position and the attitude of the ship with respect his point of stable equilibrium. The linear approximation of the hydrostatics effects may be written, as we saw, as:

$$\tau_{res}(j\omega) = -\mathbf{G}\eta(j\omega) \quad (15)$$

As explained in [Faltinsen1990], when $Fr < 0.3$ the only important terms are G_{33} , $G_{35} = G_{53}$, G_{44} , and G_{55} .

These expressions of the interaction forces can be directly used in the equations of motion, implementing a frequency domain model for solving the dynamics of a vessel.

5.2 Time Domain formulation

The former formulation can correctly describe ship motion only under a pure sinusoidal regime of waves; that is because of the frequency dependent coefficients. If the sea state is representable only as a spectrum, i.e. if there is no a well defined frequency, a Fourier analysis must be performed to make the mathematical model fit the reality. This approach leads to a large number of equations, required to describe the motion properly. In this context, the development of a time domain mathematical model becomes very desirable. That was the main reason who encouraged W. E. Cummins to accomplish his famous work, writing a fundamental paper concerning ship motion, [Cummins1962], which has been, is and probably will continue to be the basis of every linear time domain model. The crucial points of his work were:

- To be able to represent the response of a ship in six degree of freedom, to an arbitrary forcing function in all the degree of freedom, avoiding the use of any frequency dependent parameter;
- To separate and identify in an explicit way all the factors governing the response.

In addition, during the last years, an increasing interest for linear time domain models, based on frequency domain data, became widespread. The strength of this *modus operandi* is the possibility to develop models for the dynamics of a ship by necessitating of a limited amount of data. The key element of these models is the so-called *Cummins equation*, presented in his paper. The peculiarity of this integro differential equation is that, expliciting the waves radiation forces, it appears a convolution term imputable to the fluid memory effect, that takes into account the variations of the fluid momentum at every instants, along all the time history of the motion.

The starting point to derive *Cummins equation* is the assumption of linearity. Under this hypothesis, one can exploit the theory of the *Green function* to state that, given the response of a linear stable system to a unit impulse, the computation of the response to an arbitrary time dependent force is also directly available. That means that if $R(t)$ is the impulse response, then the response $x(t)$ to a general excitation $f(t)$ is:

$$x(t) = \int_{-\infty}^t R(t-t') f(t') dt' = \int_0^{\infty} R(t') f(t-t') dt'$$

The other fundamental assumption is that the fluid field is rotational free, so that one can use potential theory to model and describe the behavior of the sea water.

Using impulses in the components of motion, the first step is to find the potential function of the fluid field φ . Cummins approached the problem dividing the time in two intervals, one during the impulses and one other after the impulses are extinguished. Defining the right boundary conditions, both on the water free surface and on the moving or still hull, as well as the initial physical condition about the state of the pressure, Cummins wrote the function φ . Once that is done, the linearized dynamic pressure is straight calculable as:

$$p = -\rho \frac{\partial \varphi}{\partial t}$$

Integrating this function over the surface of the hull, one can find the hydrodynamic action, a force and a moment.

By proceeding with all the mathematical apparatus and manipulations, the following form for the radiation force is found:

$$\tau_{rad} = -\mathbf{A}_\infty \ddot{\xi} - \mathbf{B}_\infty \dot{\xi} - \int_0^t \mathbf{K}(t-t') \dot{\xi}(t') dt' \quad (16)$$

with

$$\mathbf{K}(t) = \int_0^\infty (\mathbf{B}(\omega) - \mathbf{B}_\infty) \cos(\omega t) d\omega \quad (17)$$

\mathbf{A}_∞ is the *added mass matrix*, which takes into account the amount of mass accelerating with the ship during the motion. \mathbf{B}_∞ is the *damping matrix*, the out-of-phase reaction force of the water: during the ship oscillations the water follows the hull, but the inertia of the fluid, obviously not rigidly bound to the ship, causes a certain delay to the change in his direction. The convolution term represents the fluid memory effect that incorporate the energy dissipation due to the radiated waves, consequent of the motion of the hull. The *kernel* of the convolution, $\mathbf{K}(t)$, is the retardation matrix, function of the hull geometry and the forward speed. The fluid memory effect appears due to the free surface: waves generated by the motion of the hull will persist at all subsequent times, affecting the motion of the ship.

By the way, the convolution term is really inconvenient concerning simulations. Hence an interest in parametric models for its replacement has grown up. Indeed, thanks to the linearity and the nature of the convolution operator, it can be approximated with a linear-time invariant *state-space* model:

$$\mu(t) = \int_0^t \mathbf{K}(t-t') \dot{\xi}(t') dt' \approx \begin{cases} \dot{\mathbf{x}} = \mathbf{A}_s \mathbf{x} + \mathbf{B}_s \dot{\xi} \\ \mu = \mathbf{C}_s \mathbf{x} \end{cases} \quad (18)$$

[Taghipour2008] provides an overview on the various methods to implement such a model. It concludes that a state-space model for a time domain simulation gives comparable results of the same quality of a direct computation of the convolution term. However, this work indicates also a potential simulation speed gain of the order of 40 times, when using state-space models.

Indeed, the computation of the memory convolution term implies the need to store and process at each time step a large number of past response data. On the other hand, the state-space model incorporates all the time history in the state variable, making possible the computation of the subsequent state just by processing the former.

For zero input, the state-space formulation indicates that the dynamic variables are expressed as a linear combination of exponential functions of time. On the other hand it's been proved that the free

vertical motion of a floating body, immersed on deep water, decays slower, more like the inverse of a power of time. However, in many cases, the difference of these solutions is negligible, and the state-space system represent an excellent approximation.

5.3 Ogilvie relations

By applying the Fourier transform, [Ogilvie1964] found the following relationships between the frequency dependent added mass and damping matrices the and time domain model invariant ones:

$$\begin{cases} \mathbf{A}(\omega) = \mathbf{A}_\infty - \frac{1}{\omega} \int_0^\infty \mathbf{K}(t) \sin(\omega t) dt \\ \mathbf{B}(\omega) = \mathbf{B}_\infty + \int_0^\infty \mathbf{K}(t) \cos(\omega t) dt \end{cases} \quad (19)$$

The notation for \mathbf{A}_∞ and \mathbf{B}_∞ is now understandable: evaluating the limit $\omega \rightarrow \infty$ in 19, from the Riemann-Lebesgue lemma it follows that:

$$\begin{aligned} \mathbf{A}_\infty &= \lim_{\omega \rightarrow \infty} \mathbf{A}(\omega) \\ \mathbf{B}_\infty &= \lim_{\omega \rightarrow \infty} \mathbf{B}(\omega) \end{aligned}$$

In frequency domain, the former relations allow to write:

$$\begin{aligned} \mathbf{K}(j\omega) &= \int_0^\infty \mathbf{K}(t) e^{-j\omega t} dt = \int_0^\infty \mathbf{K}(t) \cos(\omega t) dt - j \int_0^\infty \mathbf{K}(t) \sin(\omega t) dt = \\ &= \mathbf{B}(\omega) - \mathbf{B}_\infty + j\omega [\mathbf{A}(\omega) - \mathbf{A}_\infty] \end{aligned} \quad (20)$$

5.4 Alternative representations of the radiation force

When we will face the problem of the approximation of the convolution term, it will be useful exploiting other representations of $\tau_{rad}(j\omega)$. From the relation 12, the total hydrodynamic radiation force vector can be expressed in the frequency domain as:

$$\tau_{rad}(j\omega) = -\mathbf{A}(\omega) \ddot{\eta}(j\omega) - \mathbf{B}(\omega) \dot{\eta}(j\omega)$$

Taking the derivative of the velocity vector, $\dot{\eta}(j\omega) = j\omega\dot{\eta}(j\omega)$, it also holds:

$$\begin{aligned}\tau_{rad}(j\omega) &= -[j\omega\mathbf{A}(\omega) + \mathbf{B}(\omega)]\dot{\eta}(j\omega) = -\tilde{\mathbf{B}}(j\omega)\dot{\eta}(j\omega) \\ &= -\left[\mathbf{A}(\omega) + \frac{\mathbf{B}(\omega)}{j\omega}\right]\dot{\eta}(j\omega) = -\tilde{\mathbf{A}}(j\omega)\dot{\eta}(j\omega)\end{aligned}\quad (21)$$

From 20:

$$j\omega\mathbf{A}(\omega) + \mathbf{B}(\omega) = \tilde{\mathbf{B}}(j\omega) = \mathbf{K}(j\omega) + \mathbf{B}_\infty + j\omega\mathbf{A}_\infty,$$

so it follows:

$$\tau_{rad}(j\omega) = -\mathbf{A}_\infty\dot{\eta}(j\omega) - [\mathbf{K}(j\omega) + \mathbf{B}_\infty]\dot{\eta}(j\omega)\quad (22)$$

6 Potential theory

For our analysis we will consider potential theory applicable, by assuming that the fluid field around the vessel is incompressible, inviscid and irrotational. That allows to define the function of the velocity potential φ such that, for every point of the fluid domain, it holds:

$$V(t, \mathbf{x}) = \nabla\varphi(t, \mathbf{x})\quad (23)$$

Euler's equation for the conservation of momentum of incompressible fluids, with the irrotational hypothesis $\nabla \times V(t, \mathbf{x}) = 0$, is written as:

$$\frac{\partial V}{\partial t} + (V \cdot \nabla)V = \frac{\partial V}{\partial t} + \frac{1}{2}\nabla(V^2) = -\nabla\left(\frac{p}{\rho}\right) + \mathbf{g}\quad (24)$$

Using a flat earth approximation, one can write the gravitational field in a gradient form, $\mathbf{g} = (0, 0, -g) = -\nabla gz$, and by replacing 23 in 24, it turns into:

$$\nabla\left(\frac{\partial\varphi}{\partial t} + \frac{1}{2}\nabla\varphi \cdot \nabla\varphi + \frac{p}{\rho} + gz\right) = 0$$

which becomes the unsteady Bernoulli's equation, the first integral for the potential flow:

$$\frac{\partial\varphi}{\partial t} + \frac{1}{2}\nabla\varphi^2 + \frac{p}{\rho} + gz = f(t)\quad (25)$$

where $f(t)$ is an arbitrary function of time. This function can be put equal to zero without loss of generality, because of the non-uniqueness of the potential function: if $\varphi(t, \mathbf{x})$ satisfies 23 then $\varphi(t, \mathbf{x}) + \delta(t)$ does it to, and we can always impose $\delta'(t) = f(t)$.

Morover, expressing the conservation of mass by the continuity equation

$$\frac{\partial \rho}{\partial t} + \nabla \cdot (\rho V) = \frac{D\rho}{Dt} + \rho \nabla \cdot V = 0$$

the incompressible hypothesis $\rho = \text{const}$ on the flow means also $\nabla \cdot V(t, \mathbf{x}) = 0$; that can be interpreted stating that for any given closed volume inside the domain, the net amount of fluid mass which instantaneously enters is zero. Being the velocity field divergence free, the potential must also satisfies the Laplace equation:

$$\Delta \varphi = 0 \tag{26}$$

6.1 Incident wave potential flow

In our case we want to find the potential function for a perturbed ideal sea. We will call this function the incident waves potential φ_I . Let's consider a fluid with a free surface in equilibrium with the gravitational field. If any perturbation occurs and the surface is moved from its equilibrium state, the motion is propagated. Under the same assumption of linearity, we will consider small waves which can be superposed to define a general spectrum.

If the waves amplitude is small compared to the wavelengths, the term $\nabla \varphi^2$ can be neglected in comparison with $\frac{\partial \varphi}{\partial t}$: the velocity varies more rapidly at a fixed point with the time than spatially at a fixed moment. Putting $f(t) = 0$, equation 25 becomes:

$$p = -\rho \frac{\partial \varphi}{\partial t} - \rho g z = p_{dyn} - \rho g z \tag{27}$$

Defining a reference system with the vertical z -axis pointing upwards and the $x - y$ plane coincident with the equilibrium surface of the fluid, we will denote as $\zeta = \zeta(t, x, y)$ the vertical coordinate of a point on the surface, so its displacement during the oscillations from the equilibrium position $z = 0$.

The physical condition of the free surface is that the pressure must be the same everywhere and equal to the atmospheric p_0 : $p(t, x, y, \zeta) = p_0$. Equation 27 becomes

$$p_0 = -\rho \frac{\partial \varphi}{\partial t} - \rho g \zeta$$

We can easily eliminate the constant p_0 redefining the potential as $\varphi - \frac{p_0}{\rho}t$, which can be also seen as putting $f(t) = \frac{p_0}{\rho}t$. We obtain the condition on the surface as:

$$g\zeta + \frac{\partial\varphi}{\partial t} = 0 \quad (28)$$

For small oscillations, with the same degree of approximation, we can say that the vertical velocity $\frac{\partial\varphi}{\partial z}$ on the surface is simply the time derivative of ζ :

$$\frac{\partial\varphi}{\partial z} = \frac{\partial\zeta}{\partial t} \quad (29)$$

The derivatives in 29 should be taken in $z = \zeta$, but since the displacements are small we can take them at the equilibrium point in $z = 0$.

Combining together 28 and 29, we reach the following system for the potential function:

$$\begin{cases} \Delta\varphi = 0, & z < 0; \\ \frac{\partial^2\varphi}{\partial t^2} + g\frac{\partial\varphi}{\partial z} = 0, & z = 0; \\ \nabla\varphi \rightarrow 0, & z \rightarrow -\infty. \end{cases}$$

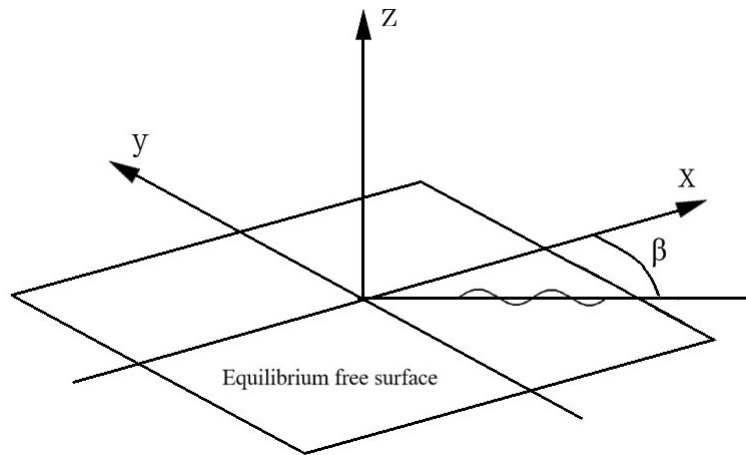
Where the condition $\nabla\varphi \rightarrow 0$ for $z \rightarrow -\infty$ is valid for infinitely deep fluid. Note that the hypothesis of infinite depth is equivalent to consider small enough wavelengths. Moreover, considering an unlimited free surface, we can omit boundary conditions. Solving the system for a general pure sinusoidal wave, with frequency equal to ω_0 and wave number k , traveling in a direction dictated by the heading angle $\beta = \arctan\left(-\frac{y}{x}\right)$, brings to the function:

$$\varphi_I(t, x, y, z) = \frac{\zeta g}{\omega_0} e^{kz} e^{jk(x \cos \beta - y \sin \beta)} e^{j\omega_0 t} \quad (30)$$

with the dispersion relation

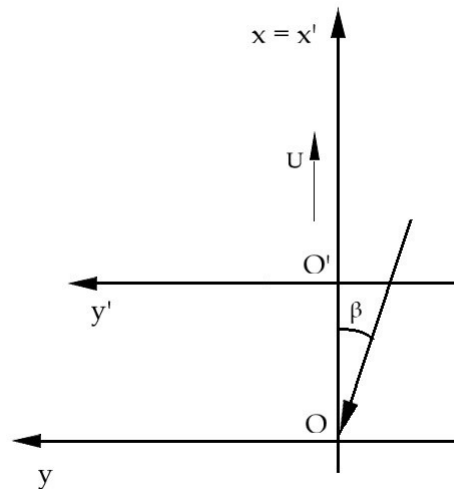
$$\omega_0^2 = kg$$

One have to consider only the real part of 30, and after finding the velocity components $\nabla\varphi_I$, it results that the trajectories of the particles are circles about fixed equilibrium points, with a radius which exponentially decreases with the depth.

Figure 5: Inertial reference frame and definition of heading angle β

For the analysis of floating bodies moving at a constant speed on the free surface, it can be useful to apply to 30 a transformation. Defining a moving right-handed coordinate system, that will be our seakeeping reference frame $\{s\} = O' x' y' z'$, which translates with respect to the first inertial one $\{n\} = O x y z$ with a constant speed U along the x direction, we want find the expression of the potential with respect to $\{s\}$.

The origins of the frames are located in the plane of the undisturbed free surface, the z -axes are positive vertically upwards, the x -axes point towards the stern and the y -axes complete the dextral coordinate systems. The $x - z$ plane of the moving frame is assumed to be a symmetry plane for the ship in its mean oscillatory position.

Figure 6: The seakeeping frame $\{s\}$ translates parallel to the inertial one $\{n\}$

The linear transformation between the two frames is:

$$\Lambda = \begin{cases} x' = x - Ut, \\ y' = y, \\ z' = z. \end{cases}$$

The velocity field, both seen and expressed with respect to $\{n\}$, V_n^n , and his potential φ^n are:

$$\begin{cases} \varphi_I^n(t, x, y, z) = \frac{\zeta g}{\omega_0} e^{kz} e^{jk(x \cos \beta - y \sin \beta)} e^{j\omega_0 t} \\ V_n^n = \nabla \varphi_I^n(t, x, y, z) \end{cases}$$

The time derivative of the transformation Λ leads to the kinetic relation $V_s^n = V_n^n - \vec{U}^n$, $\vec{U}^n = (U, 0, 0)$, which is the velocity field seen by $\{s\}$ expressed in the $\{n\}$ frame of reference; by the means of the potential function one can write:

$$V_s^n = \nabla \varphi_I^n - \vec{U}^n$$

Applying Λ^{-1} to the former relation we can find the velocity field both seen and expressed with respect to $\{s\}$, obtaining:

$$\nabla \varphi_I^s = V_s^s = \Lambda^{-1}(V_s^n) = \nabla [\Lambda^{-1}(\varphi_I^n)] - \vec{U}^n$$

i.e.:

$$\begin{aligned} \varphi_I^s &= \frac{\zeta g}{\omega_0} e^{kz'} e^{jk(x' \cos \beta + Ut \cos \beta - y' \sin \beta)} e^{j\omega_0 t} - Ux' = \\ &= \frac{\zeta g}{\omega_0} e^{kz'} e^{jk(x' \cos \beta - y' \sin \beta)} e^{j(\omega_0 + kU \cos \beta)t} - Ux' \end{aligned}$$

The gradient in (x', y', z') of this function give us the velocity field of the wave seen by the $\{s\}$. The physical meaning is studying the equivalent behavior of a body at rest in the same flow with also an opposite speed $-U$. We can define the encounter frequency of the wave as $\omega_e = \omega_0 + kU \cos \beta$, describing the fact that if the body moves against the waves, it experiences a higher impact frequency.

We showed that it is possible to reduce the seakeeping analysis to a steady body analysis. Renaming the variables of $\{s\}$ as $(x', y', z') \rightarrow (x, y, z)$, and calling φ_I^* just as φ_I , i.e. the incident waves potential, we can find the velocities and the accelerations of the flow:

$$\varphi_I = \frac{\zeta g}{\omega_0} e^{kz} e^{jk(x \cos \beta - y \sin \beta)} e^{j\omega_e t} - Ux = \varphi_I^* - Ux \quad (31)$$

$$\begin{cases} v &= \frac{\partial \varphi_I}{\partial y} = -i\zeta\omega_0 \sin \beta e^{kz} e^{jk(x \cos \beta - y \sin \beta)} e^{j\omega_e t} \\ w &= \frac{\partial \varphi_I}{\partial z} = \zeta\omega_0 e^{kz} e^{jk(x \cos \beta - y \sin \beta)} e^{j\omega_e t} \\ a_y &= \frac{\partial v}{\partial t} = \zeta\omega_e\omega_0 \sin \beta e^{kz} e^{jk(x \cos \beta - y \sin \beta)} e^{j\omega_e t} \\ a_z &= \frac{\partial w}{\partial t} = i\zeta\omega_e\omega_0 e^{kz} e^{jk(x \cos \beta - y \sin \beta)} e^{j\omega_e t} \end{cases}$$

Please note that $\nabla^2 \varphi_I$ can not be considered negligible anymore, because of the presence of the speed U , and the linearized dynamic pressure requires a better analysis; indeed $\nabla \varphi_I = \left(\frac{\partial \varphi_I^*}{\partial x} - U, \frac{\partial \varphi_I}{\partial y}, \frac{\partial \varphi_I}{\partial z} \right)$ and $\nabla^2 \varphi_I \approx -2 \frac{\partial \varphi_I^*}{\partial x} U + U^2$.

So, starting from the 25, we should modify the pressure equation 27 as:

$$p = -\rho \frac{\partial \varphi_I}{\partial t} - \frac{1}{2} \rho \nabla^2 \varphi_I - \rho g z \approx -\rho \frac{\partial \varphi_I}{\partial t} + \rho \frac{\partial \varphi_I^*}{\partial x} U - \rho g z = -\rho \left(\frac{\partial}{\partial t} - U \frac{\partial}{\partial x} \right) \varphi_I^* - \rho g z \quad (32)$$

thanks to the fact that $\frac{\partial \varphi_I}{\partial t} = \frac{\partial \varphi_I^*}{\partial t}$; furthermore we included, as usual, the constant term $\frac{1}{2} \rho U^2$ in the function $f(t)$.

6.2 Potential flow around a vessel

Assuming a ship traveling at a constant speed U and heading β with the presence of waves, we want to solve the problem of finding the overall potential of the resulting flow.

We can reformulate the problem in a reference frame where with the ship is at rest and experiences a flow with an opposite velocity $-U$. The total potential can be expressed as the sum of a steady part and an oscillatory one:

$$\Phi(t, \mathbf{x}) = \varphi_S(\mathbf{x}) + \varphi_T(t, \mathbf{x})$$

The steady part φ_S is caused only by the presence of the ship, which perturbs the flow incoming with a velocity $-U$, creating a time-independent sea structure around the hull; on the other hand, the unsteady

part φ_T is due to the incoming waves. The former φ_T can be decomposed in three contributions:

$$\varphi_T(t, \mathbf{x}) = \varphi_I(t, \mathbf{x}, \beta, \omega_0) + \varphi_{Diff}(t, \mathbf{x}, \beta, \omega_0) + \sum_k \eta_k \varphi_k(t, \mathbf{x}, U, \omega_e)$$

where φ_I is the potential of the incident waves, the one we already found in 31, φ_{Diff} is the potential of the diffracted waves and φ_k and η_k are the radiation potential and the complex amplitude.

To find the potential function Φ , we have to add the right boundary conditions: for a rigid body advancing on the free surface of the fluid, which is infinite in all horizontal directions, the conditions to impose are:

- Incompressibility condition: velocity field is divergence free in all the fluid domain and every potential component must satisfy

$$\Delta \{\varphi_S, \varphi_I + \varphi_{Diff}, \varphi_k\} = 0$$

so, evidently

$$\Delta \Phi = 0$$

- Tangential condition on the body wet surface: no fluid can flows through the body. Concerning the steady potential φ_S , referred to the flow generated by the ship when it is at rest, this condition is equivalent to zero normal velocity on the hull surface: $\frac{\partial \varphi_S}{\partial n} = 0$ on Σ_{hull} . The incident and diffracted potential $\varphi_I + \varphi_{Diff}$, representative of the wavy sea perturbed by a steady vessel, must satisfy the same condition. On the other hand, the radiation potential is caused by the oscillations of the hull, so for each φ_k the tangential condition is more complicated: it implies the oscillations of the potential too.

The mathematical conditions, for $\mathbf{x} \in \Sigma_{hull}$, are written as:

$$\begin{cases} \frac{\partial \varphi_S}{\partial n} & = 0 \\ \frac{\partial(\varphi_I + \varphi_{Diff})}{\partial n} & = 0 \end{cases}$$

For the radiation potential, in regular sinusoidal waves, every component φ_k must satisfy:

$$\left\{ \begin{array}{l} \frac{\partial \varphi_k}{\partial n} = j\omega n_k - U m_k \\ (n_1, n_2, n_3) = \vec{n} \\ (n_4, n_5, n_6) = \vec{r} \times \vec{n} \\ m_j = 0, \quad j = 1, \dots, 4; \\ m_5 = n_3 m_6 = -n_2 \\ m_6 = -n_2 \end{array} \right.$$

with \vec{r} and \vec{n} are respectively the position vector with respect to the origin of the coordinate system and the outward unit normal vector, pointing into the fluid.

- Free surface condition: the pressure must be the same on it, so $\frac{Dp}{Dt} = 0$. Equation 32 is valid for each potential part $\{\varphi_S, \varphi_I, \varphi_{Diff}, \varphi_k\}$, so calling the generic component just as φ and computing the total derivative, the following is reached

$$\begin{aligned} \frac{1}{\rho} \frac{Dp}{Dt} &= \frac{D}{Dt} \left(-\frac{\partial \varphi}{\partial t} + U \frac{\partial \varphi}{\partial x} - gz \right) = \\ &= \frac{\partial}{\partial t} \left(-\frac{\partial \varphi}{\partial t} + U \frac{\partial \varphi}{\partial x} - gz \right) + \nabla \varphi \cdot \nabla \left(-\frac{\partial \varphi}{\partial t} + U \frac{\partial \varphi}{\partial x} - gz \right) = \\ &= -\frac{\partial^2 \varphi}{\partial t^2} + U \frac{\partial^2 \varphi}{\partial t \partial x} + \left(\frac{\partial \varphi}{\partial x} - U, \frac{\partial \varphi}{\partial y}, \frac{\partial \varphi}{\partial z} \right) \cdot \left(-\frac{\partial^2 \varphi}{\partial t \partial x} + U \frac{\partial^2 \varphi}{\partial x^2}, -\frac{\partial^2 \varphi}{\partial t \partial y} + U \frac{\partial^2 \varphi}{\partial x \partial y}, -\frac{\partial^2 \varphi}{\partial t \partial z} + U \frac{\partial^2 \varphi}{\partial x \partial z} - g \right) = \\ &= -\frac{\partial^2 \varphi}{\partial t^2} + U \frac{\partial^2 \varphi}{\partial t \partial x} + U \frac{\partial^2 \varphi}{\partial t \partial x} - U^2 \frac{\partial^2 \varphi}{\partial x^2} - g \frac{\partial \varphi}{\partial z} + \mathcal{O}(d^3 \varphi) \approx \\ &\approx -\frac{\partial^2 \varphi}{\partial t^2} + 2U \frac{\partial^2 \varphi}{\partial t \partial x} - g \frac{\partial \varphi}{\partial z} - U^2 \frac{\partial^2 \varphi}{\partial x^2} \end{aligned}$$

For each potential term the former must be satisfied in $z = \zeta$, but with the small oscillation hypothesis the derivative can be taken in $z = 0$. This condition is clearly satisfied also by the overall potential Φ , so one can shortly write

$$\frac{\partial^2 \Phi}{\partial t^2} - 2U \frac{\partial^2 \Phi}{\partial t \partial x} + U^2 \frac{\partial^2 \Phi}{\partial x^2} + g \frac{\partial \Phi}{\partial z} = 0, \quad z = 0.$$

but always bearing in mind that this condition must be satisfied by each potential contribution, not just by their sum.

- Bottom condition: velocity must be tangential in $z = -h$, if the depth h is finite, or zero as $z \rightarrow -\infty$, for infinitely depth sea; so for $\varphi \in \{\varphi_S, \varphi_I, \varphi_{Diff}, \varphi_k\}$ one the following conditions also

holds

$$\frac{\partial \varphi}{\partial z} = 0, \quad z = -h$$

or

$$\frac{\partial \varphi}{\partial x} = \frac{\partial \varphi}{\partial y} = \frac{\partial \varphi}{\partial z} = 0, \quad z \rightarrow -\infty$$

- Radiation condition: the flow is undisturbed far away from the moving body. Hence

$$\nabla \varphi \rightarrow 0, \quad \|\mathbf{x}\| \rightarrow \infty, \quad t < \infty$$

6.2.1 Hydrodynamic forces and moments

After finding the potential, the linearized time-dependent pressure on the hull is:

$$p = -\rho \left(\frac{\partial}{\partial t} - U \frac{\partial}{\partial x} \right) \varphi_T(t, \mathbf{x}), \quad \mathbf{x} \in \Sigma_{hull}$$

The integration of the pressure over the mean position of the hull leads to the hydrodynamics forces $H_{1,2,3}$ and moments $H_{4,5,6}$. Considering each simple sinusoidal harmonics of the sea, with a well defined frequency ω , we can write $\varphi_T(t, \mathbf{x}) = \tilde{\varphi}_T(\mathbf{x}) e^{j\omega t}$, so consider just the amplitudes of the forces and moments:

$$H_j = \int_{\Sigma_{hull}} \rho \left(\frac{\partial}{\partial t} - U \frac{\partial}{\partial x} \right) \tilde{\varphi}_T(\mathbf{x}) n_j d\sigma$$

with $(n_1, n_2, n_3) = \vec{n}$ and $(n_4, n_5, n_6) = \vec{r} \times \vec{n}$.

The vector H can be divided into two parts: the exciting forces and moments F and the ones due to the body motions G :

$$\begin{aligned} H_j &= F_j + G_j \\ F_j &= \int_{\Sigma_{hull}} \rho \left(\frac{\partial}{\partial t} - U \frac{\partial}{\partial x} \right) (\tilde{\varphi}_I + \tilde{\varphi}_{Diff}) n_j d\sigma \\ G_j &= \int_{\Sigma_{hull}} \rho \left(\frac{\partial}{\partial t} - U \frac{\partial}{\partial x} \right) \left(\sum_k \eta_k \tilde{\varphi}_k \right) n_j d\sigma = \sum_k T_{jk} \eta_k \end{aligned}$$

F_j can be clearly divided into two components, the Froude-Krilov and the diffraction terms:

$$\begin{aligned}
 F_j &= F_{FK,j} + F_{Diff,j} \\
 F_{FK,j} &= \int_{\Sigma_{hull}} \rho \left(\frac{\partial}{\partial t} - U \frac{\partial}{\partial x} \right) \tilde{\varphi}_I n_j d\sigma \\
 F_{Diff,j} &= \int_{\Sigma_{hull}} \rho \left(\frac{\partial}{\partial t} - U \frac{\partial}{\partial x} \right) \tilde{\varphi}_{Diff} n_j d\sigma
 \end{aligned}$$

Finally, T_{jk} denotes the hydrodynamic reaction in the j th direction per unit oscillatory displacement in the k th mode, and for each harmonic can be separated in his real and imaginary part:

$$\begin{aligned}
 T_{jk} &= \int_{\Sigma_{hull}} \rho \left(\frac{\partial}{\partial t} - U \frac{\partial}{\partial x} \right) \tilde{\varphi}_k n_j d\sigma \\
 T_{jk} &= \omega^2 A_{jk} - j\omega B_{jk}
 \end{aligned}$$

where A_{jk} and B_{jk} are the added mass and damping coefficients.

6.2.2 Linearization of the hydrodynamic problem: Strip Theory

The numerical solution of the nonlinear boundary value problem is possible, but very complex and computationally expensive. To simplify the problem resolution, one can carry out the linearization of the boundary conditions. In order to proceed, some restrictions on the nature of the problem are necessary:

- The wet hull must be slender;
- The speed of the ship can't be too high;
- Waves amplitude must be small;
- Motions amplitude of the ship must be small.

Different combinations of restrictions result on different linear formulations; the adequacy of the simplification depends on the physical problem intended to represent. In our case we will use the *Strip Theory*.

Indeed, for slender bodies, a good approximation is that the fluid motion field varies much slower in the longitudinal direction of the ship than in the cross-directional plane. Hence, the problem can be reformulated bidimensionally.

The principle of strip theory, a low Froude number theory, is to divide the submerged part of the vessel into a finite number of strips and analyze each one separately. After solving a set of bidimensional boundary value problems, one can compute the frequency dependent bidimensional coefficients of added masses and damping for each strip.

Hence, integrating the action of each 2D coefficient along the length of the vessel, one can estimate the overall tridimensional coefficients of the whole hull.

For more details see for example [Faltinsen1990].

One of the problem of the strip theory is that we can not trace back to the surge force, because is not present in the bi-dimensional problems from which we obtain the tridimensional quantities.

To add the drag force we will use empirical formulas, based on the geometry of the ship, the operational conditions and the characteristic Reynolds number.

Moreover, in *FloBoS*, the steady part of the potential φ_S is neglected. The steady perturbation due to the presence of the hull at rest is considered negligible with respect to the sea waves, or of the same approximation degree of the linear hypothesis: this approach is also called of the *ghost vessel*.

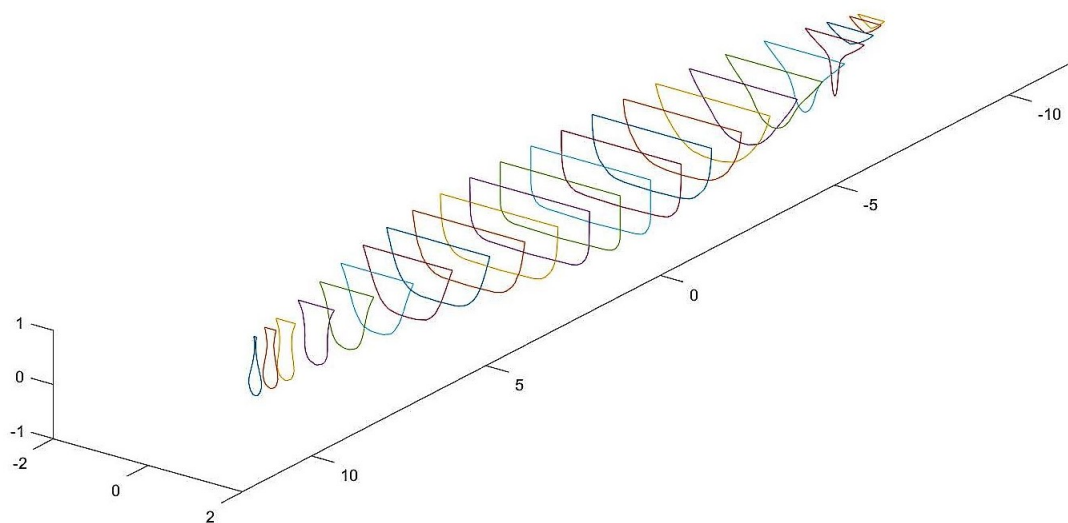


Figure 7: Strip Theory – discretization example of a 10% scaled container ship S175

7 Rigid-body equation of motion

In order to implement kinematics and dynamics models in a time domain marine vehicles simulator, by having seakeeping data from PDSTRIP, a transformation of the equations of motion used in seakeeping theory to body-fixed coordinates is required. The following transformations are the ones derived by [Perez&Fossen2007].

The vessel rigid-body generalized mass matrix, computed with respect the origin of $\{b\}$, is of the form

$$\mathbf{M}_{RB}^b = \begin{bmatrix} m\mathbf{I}_{3 \times 3} & -m\mathbf{S}(\mathbf{r}_{bg}^b) \\ m\mathbf{S}(\mathbf{r}_{bg}^b) & \mathbf{I}_{b/b}^b \end{bmatrix},$$

where m is the mass of the vessel, $\mathbf{I}_{b/b}^b$ is the inertia tensor about $\{b\}$ and \mathbf{r}_{bg}^b gives the coordinates of the *center of gravity* in $\{b\}$. From the conservation of the angular momentum, one can demonstrate that the inertia tensor will not be constant in an inertial frame if the vessel rotates with respect this frame. Therefore, it is always convenient to formulate the equations of motion in a body-fixed rather than inertial coordinate system (see [Perez&Fossen2007]).

Expressing in $\{b\}$ the Newton's fundamental second law for rigid bodies, the 6 degrees of freedom motion is governed by the following equation:

$$\mathbf{M}_{RB}^b \dot{\nu} + \mathbf{C}_{RB}(\nu) \nu = \tau^b \quad (33)$$

where τ^b is the *generalized external force vector*, which includes both the interaction forces with water and the control and propulsive forces; lastly, $\mathbf{C}_{RB}(\nu)$ is the *Coriolis-Centripetal matrix*, which appears because the body-fixed frame is not inertial. The terms of this matrix are:

$$\mathbf{C}_{RB}(\nu) = \begin{bmatrix} \mathbf{0}_{3 \times 3} & -m\mathbf{S}(\nu_1) - m\mathbf{S}(\mathbf{S}(\nu_2) \mathbf{r}_{bg}^b) \\ -m\mathbf{S}(\nu_1) - m\mathbf{S}(\mathbf{S}(\nu_2) \mathbf{r}_{bg}^b) & m\mathbf{S}(\mathbf{S}(\nu_1) \mathbf{r}_{bg}^b) - \mathbf{S}(\mathbf{I}_{b/b}^b \nu_2) \end{bmatrix}$$

7.1 Seakeeping equation of motion

Describing the motion by the means of perturbations of $\{b\}$ with respect to $\{s\}$, using 9, leads to the following kinetic model for the *seakeeping equation*:

$$\begin{cases} \delta\dot{\eta} = \mathbf{J}_b^s(\delta\eta) \delta\nu \\ \mathbf{M}_{RB}^b \delta\dot{\nu} + \mathbf{C}_{RB}(\delta\nu) \delta\nu = \delta\tau \end{cases}$$

One should notice that for small angles both \mathbf{R}_b^s and \mathbf{T}_b tend to the identity matrix, and therefore also $\mathbf{J}_b^s(\delta\eta)$. It follows that a linear approximation of the former model is

$$\begin{cases} \delta\dot{\eta} \approx \delta\nu \\ \mathbf{M}_{RB} \delta\dot{\nu} \approx \delta\tau \end{cases}$$

which results simply in

$$\mathbf{M}_{RB} \delta\ddot{\eta} = \delta\tau \quad (34)$$

Changing notation and splitting the forces in the two main contribution, the equation (11) can be written expressed in $\{s\}$, with a same order approximation, as:

$$\mathbf{M}_{RB} \ddot{\xi} = \tau_{rad}^s + \tau_{exc}^s + \tau_{res}^s \quad (35)$$

By writing the forces in the frequency domain, this equation is:

$$[\mathbf{M}_{RB} + \mathbf{A}(\omega)] \ddot{\xi} + \mathbf{B}(\omega) \dot{\xi} + \mathbf{G}\xi = \tau_{FK+Diff}^s \quad (36)$$

Exploiting *Cummins* work, radiation force can be rewritten achieving the linear seakeeping vector equation of motion in time domain, called *Cummins Equation*:

$$(\mathbf{M}_{RB} + \mathbf{A}_\infty) \ddot{\xi} + \mathbf{B}_\infty \dot{\xi} + \int_0^t \mathbf{K}(t-t') \dot{\xi}(t') dt' + \mathbf{G}\xi = \tau_{FK+Diff}^s \quad (37)$$

7.2 Maneuvering equation of motion

When treating the design and the implementation of an autopilot and a control system, it becomes indispensable to treat equations written with respect to an inertial reference frame. Indeed, in maneuvering theory, a ship changes his attitude and position and an equilibrium inertial frame does not exist and can

not be identified. Furthermore, to control the ship trajectory, control forces (propulsive system thrust or forces and moments due to the deflection of a control surface like the rudder) are applied directly on the body

That leads, in summary, to the necessity of writing the dynamics equations in an inertial fixed reference frame, for example the NED one, but express them in the body frame, in order to apply easily control forces.

Following [Fossen2005], we can express the relation between $\nu \triangleq \left[(\mathbf{v}_{nb}^b)^T, (\boldsymbol{\omega}_{nb}^b)^T \right]^T = \bar{\nu} + \delta\nu$, where $\bar{\nu} = [U, 0, 0, 0, 0, 0]^T$, and ξ as:

$$\begin{cases} \dot{\xi} = \mathbf{J}^* \delta\nu - \frac{U}{\omega_e^2} \mathbf{L}^* \delta\dot{\nu} \\ \ddot{\xi} = \mathbf{J}^* \delta\dot{\nu} + U \mathbf{L}^* \delta\nu \end{cases}$$

with:

$$\mathbf{L}^* \triangleq \begin{bmatrix} 0 & \cdots & 0 & 0 \\ 0 & \cdots & 0 & 1 \\ 0 & \cdots & -1 & 0 \\ \vdots & \ddots & \vdots & \vdots \\ 0 & \cdots & 0 & 0 \end{bmatrix} \quad \mathbf{J}^* \triangleq \begin{bmatrix} 1 & 0 & 0 & 0 & z_w & 0 \\ 0 & 1 & 0 & -z_w & 0 & x_w \\ 0 & 0 & 1 & 0 & -x_w & 0 \\ 0 & 0 & 0 & 1 & 0 & 0 \\ 0 & 0 & 0 & 0 & 1 & 0 \\ 0 & 0 & 0 & 0 & 0 & 1 \end{bmatrix}$$

Applying the former transformation to the 36, premultiplicating it for \mathbf{J}^{*T} , changing notation for the rigid body inertial tensor $\mathbf{M}_{RB} \rightarrow \mathbf{J}^{*T} \mathbf{M}_{RB} \mathbf{J}^*$ and adding the control forces, we reach:

$$[\mathbf{M}_{RB} + \mathbf{M}_A(\omega)] \delta\dot{\nu} + \mathbf{N}(\omega) \delta\nu + \mathbf{C}_{RB} \delta\nu + \mathbf{G}\xi = \tau_{FK+Diff}^b + (\tau_{PID} - \bar{\tau}) \quad (38)$$

with:

$$\begin{aligned} \mathbf{M}_A(\omega) &= \mathbf{J}^{*T} \left[\mathbf{A}(\omega) - \frac{U}{\omega_e^2} \mathbf{B}(\omega) \mathbf{L}^* \right] \mathbf{J}^* \\ \mathbf{N}(\omega) &= \mathbf{J}^{*T} [\mathbf{B}(\omega) + U \mathbf{A}(\omega) \mathbf{L}^*] \mathbf{J}^* \\ \mathbf{C}_{RB} &= U \mathbf{M}_{RB} \mathbf{L}^* \end{aligned}$$

The time domain solution of the 38 is:

$$[\mathbf{M}_{RB} + \mathbf{M}_{A,\infty}] \delta \dot{\nu} + \mathbf{N}_{\infty} \delta \nu + \mathbf{C}_{RB} \delta \nu + \int_0^t \tilde{\mathbf{K}}(t-t') \delta \nu(t') dt' + \mathbf{G} \eta = \tau_{FK+Diff}^b + (\tau_{PID} - \bar{\tau})$$

with:

$$\begin{aligned} \mathbf{M}_{A,\infty} &= \mathbf{J}^{*T} \mathbf{A}_{\infty} \mathbf{J}^* \\ \mathbf{N}_{\infty} &= \mathbf{J}^{*T} [\mathbf{B}_{\infty} + U \mathbf{A}_{\infty} \mathbf{L}^*] \mathbf{J}^* \\ \mathbf{C}_{RB} &= U \mathbf{M}_{RB} \mathbf{L}^* \end{aligned}$$

and where the impulse response matrix is

$$\tilde{\mathbf{K}}(t) = \frac{2}{\pi} \int_0^{\infty} [\mathbf{N}(\omega) - \mathbf{N}_{\infty}] \cos(\omega t) d\omega$$

Using $\delta \nu = \nu - \bar{\nu}$ and setting the constant control input $\bar{\tau} = [\mathbf{C}_{RB} + \mathbf{N}_{\infty}] \bar{\nu}$, which corresponds to the steady state $u = U$, the final dynamical model is:

$$\begin{cases} \dot{\eta} = \mathbf{J}_b^n(\eta) \nu \\ [\mathbf{M}_{RB} + \mathbf{M}_{A,\infty}] \dot{\nu} + \mathbf{N}_{\infty} \nu + \mathbf{C}_{RB} \nu + \int_0^t \tilde{\mathbf{K}}(t-t') \delta \nu(t') dt' + \mathbf{G} \eta = \tau_{FK+Diff}^b + \tau_{PID} \end{cases}$$

In order to simulate the dynamical behavior of a ship in maneuvering, these are the equations to implement and solve.

Part III

Time domain simulation

Time domain models based on frequency domain data are useful both for simulation and control systems design. Furthermore, adding non linear effects for higher accuracy is easier with a time domain formulation.

8 Linear systems representation

The means to analyze the convolution term are based on his linearity, so we will present a brief overview about how to represent linear dynamics systems. A stable linear dynamics system, with a scalar excitation $u(t)$ and a scalar response $y(t)$, can be characterized in different equivalent ways: by the means of an *ordinary differential equation* with high-order derivatives, by a *convolution* or a *state-space* representation.

For example, if one writes the relation between the dynamical response and the excitation with an *ODE*:

$$\frac{d^n y(t)}{dt^n} + \sum_{k=1}^{n-1} q_k \frac{d^k y(t)}{dt^k} + q_0 y(t) = \sum_{k=1}^m p_k \frac{d^k u(t)}{dt^k} + p_0 u(t) \quad (39)$$

by applying the Laplace transform it results:

$$Y(s) = H(s)U(s) \quad (40)$$

where $H(s)$ is a transfer function defined by:

$$H(s) = \frac{p_m s^m + p_{m-1} s^{m-1} + \dots + p_1 s + p_0}{s^n + q_{n-1} s^{n-1} + \dots + q_1 s + q_0}$$

By taking the inverse Laplace transform of 40 the relation is led back the convolution operator:

$$y(t) = \int_0^t h(t-t') u(t') dt' \quad (41)$$

where $h(t)$ is the simple impulse response of the system.

On the other hand, an equivalent state-space formulation is written as:

$$\begin{cases} \dot{\mathbf{x}}(t) = \mathbf{A}'\mathbf{x}(t) + \mathbf{B}'u(t) \\ y(t) = \mathbf{C}'\mathbf{x}(t) + \mathbf{D}'u(t) \end{cases} \quad (42)$$

with the following relationship between the matrices of the system and the transfers function:

$$H(s) = \mathbf{C}'(s\mathbf{I} + \mathbf{A}')^{-1}\mathbf{B}' + \mathbf{D}'. \quad (43)$$

The former relation is reached by taking the Laplace transform of the system 42.

Nevertheless, the equation 39 can be reduced to a system of the type of 42 by simply adding auxiliary variables. For example, with the assumption of $p_m = \dots = p_1 = 0$, one can define the components of the state vector \mathbf{x} as :

$$x_1(t) = y(t), \quad x_2(t) = \frac{dy}{dt}(t), \quad \dots \quad x_n(t) = \frac{d^{n-1}y}{dt^{n-1}}(t).$$

With these definition, using the same notation of 42, the matrices are defined by:

$$\mathbf{A}' = \begin{bmatrix} 0 & 1 & 0 & \dots & 0 \\ 0 & 0 & 1 & & 0 \\ 0 & 0 & 0 & \ddots & 0 \\ \vdots & \vdots & \vdots & & \vdots \\ 0 & 0 & 0 & \dots & 1 \\ -q_0 & -q_1 & -q_2 & \dots & -q_{n-1} \end{bmatrix}, \quad \mathbf{B}' = \begin{bmatrix} 0 \\ 0 \\ \vdots \\ p_0 \end{bmatrix}, \quad \mathbf{C}' = \begin{bmatrix} 0 \\ 0 \\ \vdots \\ 1 \end{bmatrix}^T, \quad \mathbf{D}' = 0.$$

The state-space formulation is a good alternative for simulations because of the simple form of the general solution of the system 42:

$$y(t) = \mathbf{C}' \left(\mathbf{x}(0) e^{\mathbf{A}'t} + \int_0^t e^{\mathbf{A}'(t-t')} \mathbf{B}' u(t') dt' \right) + \mathbf{D}' u(t) \quad (44)$$

The last observation is that, from the comparison of the former solution with the convolution operator 41, it follows that the response of the system to the impulse $u(t) = \delta(t)$, with zero initial condition, is:

$$h(t) = \mathbf{C}' e^{\mathbf{A}'t} \mathbf{B}' + \mathbf{D}' \delta(t)$$

For more details [Taghipour2008] presents a good summary of the linear system representation forms.

9 Seakeeping simulation

Evaluating seakeeping simulation techniques, Cummins equation expressed in the seakeeping frame is the starting point:

$$(\mathbf{M}_{RB} + \mathbf{A}_{\infty}) \ddot{\xi} + \mathbf{B}_{\infty} \dot{\xi} + \int_0^t \mathbf{K}(t-t') \dot{\xi}(t') dt' + \mathbf{G}\xi = \tau_{FK+Diff}^s$$

In order to design and code a simulator, one have to face two problems:

- The convolution term is not efficient for time domain simulations; it implies the storage of a big amount of data to compute the integral at each time step. For this reason, different methods have been proposed in the literature as approximate alternative representations of the convolutions. Because the convolution is a linear operator, different approaches can be followed to obtain an equivalent linear system in the form of either transfer function or state-space models. For an overview on the main methods for replacing the convolutions and a comparison of the different methods in terms of complexity and performance, please see [Taghipour2008] or [Perez&Fossen2008bis].
- The second problem is to approximate the infinite-frequency added mass and damping matrices \mathbf{A}_{∞} and \mathbf{B}_{∞} , due to the fact that the bidimensional hydrodynamic code PDSTRIP does not provide such estimation.

A method to identify both the convolution term and the infinite added mass matrix in one fell swoop has been proposed by [Perez&Fossen2008]; we are going to develop a method starting from their work, to find also the matrix \mathbf{B}_{∞} and then implement it in our simulator.

9.1 Convolution term properties

Before exposing the previously mentioned method of [Perez&Fossen2008], we will focus on the properties of the convolution term, useful to impose the conditions for building its estimation. The expressions both in time and frequency domain are:

$$\mathbf{K}(t) = \int_0^{\infty} (\mathbf{B}(\omega) - \mathbf{B}_{\infty}) \cos(\omega t) d\omega$$

$$\mathbf{K}(j\omega) = \mathbf{B}(\omega) - \mathbf{B}_{\infty} + j\omega [\mathbf{A}(\omega) - \mathbf{A}_{\infty}]$$

- For $t \rightarrow 0^+$ it results:

$$\mathbf{K}(0^+) = \int_0^{\infty} (\mathbf{B}(\omega) - \mathbf{B}_{\infty}) d\omega \neq \mathbf{0} < \infty \quad (45)$$

because the functions $B_{ik}(\omega) - B_{\infty ik}$ are all bounded.

- From the Riemann-Lebesgue Lemma it follows that, for $t \rightarrow \infty$:

$$\lim_{t \rightarrow \infty} \mathbf{K}(t) = \lim_{t \rightarrow \infty} \int_0^{\infty} (\mathbf{B}(\omega) - \mathbf{B}_{\infty}) \cos(\omega t) d\omega = \mathbf{0} \quad (46)$$

That implies the important input-output stability property of the convolution term: indeed, in order to have each term $\int_0^t K_{ij}(t-t') \dot{\xi}_j(t') dt'$ bounded for any bounded excitation $\dot{\xi}_j(t)$, it is necessary that $\int_0^t |K_{ij}(t)| dt < \infty$, which holds provided 46.

- Using the Riemann-Lebesgue Lemma, it is also verified that for $\omega \rightarrow 0$:

$$\lim_{\omega \rightarrow 0} \mathbf{K}(j\omega) = \mathbf{0}$$

- For $\omega \rightarrow \infty$, $\mathbf{B}(\omega) \rightarrow \mathbf{B}_{\infty}$, and from the same Lemma:

$$\lim_{\omega \rightarrow \infty} \omega [\mathbf{A}(\omega) - \mathbf{A}_{\infty}] = \int_0^{\infty} \mathbf{K}(t) \sin(\omega t) dt = \mathbf{0}$$

so it holds also:

$$\lim_{\omega \rightarrow \infty} \mathbf{K}(j\omega) = \mathbf{0}$$

- The last important property is the *passivity* of $\mathbf{K}(j\omega)$. Passivity establishes that there is no generation of energy within physical system, i.e. the system can either store or dissipate energy. In our case it derives from the fact that radiation forces are dissipative. To reflect this property in the mathematical model, thanks to the linearity, we have just to assure positive realness: the real part of the frequency response function must be non zero. The damping matrix is symmetric and

positive-semi definite – $\mathbf{B}(\omega) = \mathbf{B}^T(\omega) \succeq \mathbf{0}$, [Newman1997] – so $\mathbf{K}(j\omega)$ is positive real and thus passive. This implies that the diagonal elements of the matrix $\mathbf{K}(j\omega)$ are positive real and the off-diagonal terms needs only to be stable, [Taghipour2008].

Expression 20, given \mathbf{A}_∞ and \mathbf{B}_∞ , allows to compute the values of the frequency response function $\mathbf{K}(j\omega)$ for a finite set of available data. Thanks to linearity, one can seek a transfer function approximation $\tilde{\mathbf{K}}(s)$, using these values for the identification method:

$$\hat{K}_{ik}(s) = \frac{P_{ik}(s)}{Q_{ik}(s)} = \frac{p_r s^r + p_{r-1} s^{r-1} + \dots + p_0}{s^n + q_{n-1} s^{n-1} + \dots + q_0}, \quad i, k = 1, \dots, 6 \quad (47)$$

In order to carry out a good estimation of the approximations $\tilde{K}_{ik}(s)$, one have to exploit both the non parametric data $K_{ik}(j\omega)$ from 20, and the properties previously listed. The following table from [Perez&Fossen2008] summarizes these properties and their implications on the transfer function 47:

Properties	Implication on Parametric Models $\tilde{K}_{ik}(s)$
1 – $\lim_{t \rightarrow 0^+} \mathbf{K}(t) \neq \mathbf{0} < \infty$	Relative degree between $P_{ik}(s)$ and $Q_{ik}(s)$ is 1
2 – $\lim_{t \rightarrow \infty} \mathbf{K}(t) = \mathbf{0}$	Bounded-input, bounded-output (BIBO) stability
3 – $\lim_{\omega \rightarrow 0} \mathbf{K}(j\omega) = \mathbf{0}$	$P_{ik}(s)$ has zeros in $s = 0$
4 – $\lim_{\omega \rightarrow \infty} \mathbf{K}(j\omega) = \mathbf{0}$	$\deg(Q_{ik}(s)) > \deg(P_{ik}(s))$
5 – Passivity of $\mathbf{K}(j\omega)$	$\mathbf{K}(j\omega)$ is positive real

Table 1: Properties of retardation functions

Using these informations to set constraints on the model's structure is fundamental to fit a transfer function which will assure a good estimation.

9.2 Frequency domain identification problem

From property 3 of Table 1, it is know that $P_{ik}(s)$ must have the form $s^l P'_{ik}(s)$, so that:

$$\hat{K}_{ik}(s) = \frac{s^l P'_{ik}(s)}{Q_{ik}(s)} = \frac{s^l (p_m s^m + p_{m-1} s^{m-1} + \dots + p_0)}{s^n + q_{n-1} s^{n-1} + \dots + q_0}$$

Furthermore using property 1 and 4, the orders of the polynomials must satisfy the relation $l+m+1 = n$. Since in general $\mathbf{A}(0) \neq \mathbf{A}_\infty$, from 20 it follows that there is a unique zero of $K_{ik}(s)$ in $s = 0$, so $l = 1$ and $n - m = 2$. That also means that the lowest possible order of approximation is $m = 0$ and $n = 2$. The final form of the rational approximation is:

$$\frac{\hat{K}_{ik}(s)}{s} = \frac{P'_{ik}(s)}{Q_{ik}(s)} = \frac{p_m s^m + p_{m-1} s^{m-1} + \dots + p_0}{s^{m+2} + q_{m+1} s^{m+1} + \dots + q_0} \quad (48)$$

The problem is now reduced to find the vector of parameters $\theta = [p_m, \dots, p_0, q_{m+1}, \dots, q_0]$, which perfectly defines the (i, k) element of the approximated transfer function $\hat{\mathbf{K}}(s)$.

In order to exploit the available data $\mathbf{A}(\omega_l)$ and $\mathbf{B}(\omega_l)$, which give the exact values $\mathbf{K}(j\omega_l)$ from 20, we can define the auxiliary function

$$\tilde{K}_{ik}(j\omega_l) = \frac{K_{ik}(j\omega_l)}{j\omega} \quad (49)$$

to shape the data in a similar manner of 48, and set the identification problem to find $P'_{ik}(s)$ and $Q_{ik}(s)$. One can think to a complex least square curve fitting problem, to minimize the overall displacement of 48 with respect to the points defined by 49. The vector of parameters to choose is the argument of the result of the following minimization problem:

$$\theta^* = \arg \min_{\theta} \sum_l w_l \left| \tilde{K}_{ik}(j\omega_l) - \hat{\tilde{K}}_{ik}(j\omega_l) \right|^2 = \arg \min_{\theta} \sum_l w_l \left| \tilde{K}_{ik}(j\omega_l) - \frac{P'_{ik}(s; \theta)}{Q_{ik}(s; \theta)} \right|^2 \quad (50)$$

The weights w_l can be chosen in order to emphasize a particular range of frequencies. This kind of parameter estimation is non linear in the parameters: it can be solved with Gauss-Newton algorithms or by linearization, as proposed by [Levy1959].

For other identification methods, both in time and in frequency domain, in order to analyze other ways to estimate $\hat{\mathbf{K}}(t)$ or $\hat{\mathbf{K}}(s)$, [Taghipour2008, Perez&Fossen2008bis] provides an exhaustive summary of the state of the art.

9.3 Identification of \mathbf{A}_∞ and Fluid Memory Effect

The minimization problem can not be accomplished in the absence of the Infinite Added Mass matrix: that's because it's not possible to proceed with the computation of the discrete values of $\mathbf{K}(j\omega_k)$ through 20, so no set of available data can be generated for the fitting problem.

The method proposed by [Perez&Fossen2008] overcomes this limit by defining another minimization

problem that allows to find both terms. Indeed, it provides an extension of the previous results, putting the two identification problems into the same framework.

First of all we have to recall the relation 21:

$$\tau_{rad,i}(j\omega_l) = - \left[A_{ik}(\omega_l) + \frac{B_{ik}(\omega_l)}{j\omega} \right] \ddot{\eta}_k(\omega_l) = -\tilde{A}_{ik}(j\omega_l) \ddot{\eta}_k(\omega_l) \quad (51)$$

On the other hand, taking the Laplace transform of 22 in the case of zero speed, which implies $\mathbf{B}_\infty = 0$, with the same rational approximation of the convolution term analyzed previously, we obtain:

$$\begin{aligned} \hat{\tau}_{rad,i}(s) &= - \left[sA_{\infty,ik} + \frac{P_{ik}(s; \theta)}{Q_{ik}(s; \theta)} \right] \dot{\eta}_k(s) \\ &= - \left[A_{\infty,ik} + \frac{P'_{ik}(s; \theta)}{Q_{ik}(s; \theta)} \right] \ddot{\eta}_k(s) = -\hat{A}_{ik}(s; \theta) \ddot{\eta}_k(s) \end{aligned}$$

We can now follow the general identification problem approach, using a Least Square Optimization to find θ^* . The error to globally minimize is defined by the deviations of $\hat{A}_{ik}(j\omega_k, \theta)$ to $\tilde{A}_{ik}(j\omega_k)$. The new parametric identification problem is:

$$\theta^* = \arg \min_{\theta} \sum_l w_l \left| \tilde{A}_{ik}(j\omega_l) - \hat{A}_{ik}(j\omega_l; \theta) \right|^2$$

The rational function one have to find from the minimization problem is:

$$\hat{A}_{ik}(s; \theta) = \frac{Q_{ik}(s; \theta) A_{\infty,ik} + P'_{ik}(s; \theta)}{Q_{ik}(s; \theta)} = \frac{R_{ik}(s; \theta)}{Q_{ik}(s; \theta)} \quad (52)$$

Therefore, the optimization problem is set to find the polynomials $R_{ik}(s; \theta)$ and $Q_{ik}(s; \theta)$ such that

$$\theta^* = \arg \min_{\theta} \sum_l w_l \left| \tilde{A}_{ik}(j\omega_l) - \frac{R_{ik}(s; \theta)}{Q_{ik}(s; \theta)} \right|^2 \quad (53)$$

Being the order of $Q_{ik}(s; \theta)$ higher then $P'_{ik}(s; \theta)$, $R_{ik}(s; \theta)$ and $Q_{ik}(s; \theta)$ have the same degree n ; furthermore $Q_{ik}(s; \theta)$ is defined as monic. These two observations imply:

$$\hat{A}_{\infty,ik} = \lim_{\omega \rightarrow \infty} \frac{R_{ik}(j\omega; \theta^*)}{Q_{ik}(j\omega; \theta^*)}$$

that is: the estimated infinite-frequency added mass term $\hat{A}_{\infty,ik}$ is the coefficient of the highest order term of $R_{ik}(s; \theta^*)$. After obtaining the rational approximation 52, the memory effect polynomial

$P'_{ik}(s; \theta)$ is also deduced straightforwardly:

$$P'_{ik}(s; \theta^*) = R_{ik}(s; \theta^*) - Q_{ik}(s; \theta^*) A_{\infty, ik}$$

and also $\hat{K}_{ik}(s; \theta^*)$ is found.

This algorithm to solve the optimization problem has been implemented in the Marine Systems Simulator, so we will integrate a MSS routine in *FloBoS* to find the polynomial rational function which minimize the argument of 53.

9.3.1 Order choice of $\hat{K}_{ik}(s)$, Model quality and Passivity

As mentioned before, to remain consistent with the properties of thde Table 1, the order of the polynomials $P'_{ik}(s; \theta^*)$ and $Q_{ik}(s; \theta^*)$ have to be related by

$$n = \deg(Q_{ik}(s; \theta^*)) = \deg(P'_{ik}(s; \theta^*)) + 2$$

It implies that the minimum order transfer function is a second order one:

$$\hat{K}_{ik}^{min}(s; \theta) = \frac{sp_0}{s^2 + q_1 s + q_0}.$$

The correct order to select is based on the particular hull shape considered. The algorithm can start with the minimum order, $n = 2$, increasing it until a chosen maximum one. After having all the errors, related with the corresponding degree, we can choose the best trade off between a low error and a low order. Indeed, if the order is too high, the over-fitting would increase the computational cost.

Once the approximated transfer function $\hat{K}_{ik}(s) = \frac{P_{ik}(s)}{Q_{ik}(s)}$ is found, to compute the error a comparison among the frequency dependent coefficients $A_{ik}(\omega)$ and $B_{ik}(\omega)$, available from the set of data, and the estimated ones can be performed. Indeed, from the function $\hat{K}_{ik}(s)$, one can exploit the equation 20 to compute:

$$\begin{aligned} \hat{B}_{ik}(\omega) &= Re \left\{ \hat{K}_{ik}(j\omega) \right\} \\ \hat{A}_{ik}(\omega) &= \hat{A}_{\infty, ik} + \frac{1}{\omega} Im \left\{ \hat{K}_{ik}(j\omega) \right\} \end{aligned}$$

A low deviations of these coefficients give confidence in the fitted $\hat{\mathbf{K}}(s)$ and $\hat{\mathbf{A}}_\infty$, [Perez&Fossen2008].

To assure passivity, another control must be carried out. The diagonal terms $\hat{K}_{ii}(j\omega)$ are passive because the real parts of $B_{ii}(j\omega)$ are positive for all frequencies. For the off-diagonal terms this can be not always satisfied, because the Least Square fitting does not enforce passivity. That means that the correct order to choose is also the one which ensure:

$$\text{Re} \left\{ \frac{P_{ik}(s; \theta)}{Q_{ik}(s; \theta)} \right\} > 0$$

Until the approximation passivity is not satisfied, one should continue changing the order.

9.4 Alternative identification method for non-zero forward speed

Starting from the previous work of [Perez&Fossen2008], we can develop a method to identify also the matrix \mathbf{B}_∞ : indeed, in the case of a moving vessel, the *infinite frequency damping matrix* does not vanish.

The Laplace transform of 22 in the general case is:

$$\hat{\tau}_{rad,i}(s) = -A_{\infty,ik} \ddot{\eta}_k(s) - \left[B_{\infty,ik} + \frac{P_{ik}(s; \theta)}{Q_{ik}(s; \theta)} \right] \dot{\eta}_k(s) = - \left[A_{\infty,ik} + \frac{B_{\infty,ik}}{s} + \frac{P_{ik}(s; \theta)}{sQ_{ik}(s; \theta)} \right] \ddot{\eta}_k(s)$$

We can write the former parenthesis as a polynomial fraction $\frac{R_{ik}(s; \theta)}{S_{ik}(s; \theta)}$, such that:

$$\frac{R_{ik}(s; \theta)}{S_{ik}(s; \theta)} = \frac{sQ_{ik}(s; \theta) \hat{A}_{\infty,ik} + Q_{ik}(s; \theta) \hat{B}_{\infty,ik} + P_{ik}(s; \theta)}{sQ_{ik}(s; \theta)} \quad (54)$$

By the means of the coefficients 51, computed using the set of data, we can set the same minimization problem

$$\theta^* = \arg \min_{\theta} \sum_l w_l \left| \tilde{A}_{ik}(j\omega_l) - \frac{R_{ik}(s; \theta)}{S_{ik}(s; \theta)} \right|^2 \quad (55)$$

in order to find the polynomials of the rational function 54.

Once 55 is solved, we have both $R_{ik}(s)$ and $S_{ik}(s)$, and we can trace back to the unknowns $\hat{A}_{\infty,ik}$, $\hat{B}_{\infty,ik}$ and $\frac{P_{ik}(s)}{Q_{ik}(s)}$, to reconstruct the radiation force $\hat{\tau}_{rad,i}(s)$.

The polynomial function $Q_{ik}(s)$ is given simply by $\frac{S_{ik}(s)}{s}$; to continue the identification, we have to exploit the information a priori about $P_{ik}(s)$ and $Q_{ik}(s)$. We know that, calling n the degree of $Q_{ik}(s)$,

then the degree of $P_{ik}(s)$ is $n - 1$, and, obviously, the degree of $sQ_{ik}(s)$ is $n + 1$. That means that we easily find $\hat{A}_{\infty,ik}$ as the highest degree coefficient of $R_{ik}(s)$.

The last unknowns to find are the value of $\hat{B}_{\infty,ik}$ and the polynomial $P_{ik}(s)$. We can write the general form of the polynomials as:

$$\begin{aligned} R_{ik}(s) &= r_{n+1}s^{n+1} + r_n s^n + \cdots + r_1 s + r_0, \\ Q_{ik}(s) &= q_n s^n + q_{n-1}s^{n-1} + \cdots + q_1 s + q_0, \\ P_{ik}(s) &= p_{n-1}s^{n-1} + p_{n-2}s^{n-2} + \cdots + p_1 s + p_0. \end{aligned}$$

From 54 we know that these polynomials are related by:

$$sQ_{ik}(s; \theta) \hat{A}_{\infty,ik} + Q_{ik}(s; \theta) \hat{B}_{\infty,ik} + P_{ik}(s; \theta) = R_{ik}(s; \theta) \quad (56)$$

which, extending, turns into:

$$\begin{aligned} s [q_n s^n + q_{n-1}s^{n-1} + \cdots + q_0] \hat{A}_{\infty,ik} + [q_n s^n + \cdots + q_0] \hat{B}_{\infty,ik} + [p_{n-1}s^{n-1} + \cdots + p_0] &= \\ &= r_{n+1}s^{n+1} + \cdots + r_0 \end{aligned}$$

Furthermore we know that $P_{ik}(s)$ has a zero in $s = 0$, which means $p_0 = 0$, and $Q_{ik}(s)$ is monic, so $q_n = 1$. That leads to:

$$\begin{aligned} [s^{n+1} + q_{n-1}s^n + \cdots + q_0 s] \hat{A}_{\infty,ik} + [s^n + q_{n-1}s^{n-1} + \cdots + q_0] \hat{B}_{\infty,ik} + [p_{n-1}s^{n-1} + \cdots + p_1 s] &= \\ &= r_{n+1}s^{n+1} + \cdots + r_0 \end{aligned}$$

Comparing term by term, we reach $n + 2$ relations:

$$\left\{ \begin{array}{l} r_{n+1} = \hat{A}_{\infty,ik}, \\ r_n = q_{n-1}\hat{A}_{\infty,ik} + \hat{B}_{\infty,ik}, \\ r_{n-1} = q_{n-2}\hat{A}_{\infty,ik} + q_{n-1}\hat{B}_{\infty,ik} + p_{n-1}, \\ \vdots \\ r_k = q_{k-1}\hat{A}_{\infty,ik} + q_k\hat{B}_{\infty,ik} + p_k, \\ \vdots \\ r_1 = q_0\hat{A}_{\infty,ik} + q_1\hat{B}_{\infty,ik} + p_1, \\ r_0 = q_0\hat{B}_{\infty,ik} \end{array} \right.$$

where the coefficients r_j , q_j and the value of $\hat{A}_{\infty,ik}$ are all known. Calling $\sum_j r_j = R$, $\sum_j q_j = Q$ and $\sum_j p_j = P$, we can sum the former relations, reaching the new one:

$$R = Q \cdot \hat{A}_{\infty,ik} + Q \cdot \hat{B}_{\infty,ik} + P \quad (57)$$

With the two 56 and 57, we can set an iterative process to find both $\hat{B}_{\infty,ik}$ and $P_{ik}(s)$. Indeed the system

$$\left\{ \begin{array}{l} [P_{ik}(s; \theta)]_l = R_{ik}(s; \theta) - sQ_{ik}(s; \theta) \hat{A}_{\infty,ik} - Q_{ik}(s; \theta) [\hat{B}_{\infty,ik}]_l \\ P_l = \sum_j [p_j]_l \\ [\hat{B}_{\infty,ik}]_{l+1} = \hat{A}_{\infty,ik} + \frac{R-P_l}{Q} \end{array} \right.$$

can eventually converge to the unknowns. The first step is to initialize a value: due to the fact that we do not have any prior information about the polynomial $P_{ik}(s)$, we have to choose $[\hat{B}_{\infty,ik}]_0$; from the data set of $B_{ik}(\omega_l)$ we can take the value corresponding to the maximum frequency $\omega_{max} = \max_l \omega_l$ as a good initial approximation of $B_{\infty,ik}$, so $[\hat{B}_{\infty,ik}]_0 = B_{ik}(\omega_{max})$.

The complete algorithm becomes:

$$\begin{aligned}
A_{ik}(\omega_l), B_{ik}(\omega_l) &\rightarrow \tilde{A}_{ik}(j\omega_l); \\
\tilde{A}_{ik}(j\omega_l) &\rightarrow \frac{R_{ik}(s; \theta)}{S_{ik}(s; \theta)}; \\
S_{ik}(s) &\rightarrow Q_{ik}(s); \\
R_{ik}(s) &\rightarrow \hat{A}_{\infty, ik}; \\
[\hat{B}_{\infty, ik}]_0 &= B_{ik}(\omega_{max}) \\
\left\{ \begin{array}{l} [\hat{B}_{\infty, ik}]_l \rightarrow [P_{ik}(s; \theta)]_l \\ [P_{ik}(s; \theta)]_l \rightarrow P_l \\ P_l \rightarrow [\hat{B}_{\infty, ik}]_{l+1} \end{array} \right.
\end{aligned}$$

At the end we find $\hat{A}_{\infty, ik}$, $\hat{B}_{\infty, ik}$ and $K(s) = \frac{P_{ik}(s)}{Q_{ik}(s)}$. The evaluations about the transfer function order and the model quality check are the same described in the previous sections, exception for that, if the speed is not zero, the inverse relations to re-compute the approximated $\hat{A}_{ik}(\omega)$ and $\hat{B}_{ik}(\omega)$ are:

$$\begin{aligned}
\hat{B}_{ik}(\omega) &= \hat{B}_{\infty, ik} + Re \left\{ \hat{K}_{ik}(j\omega) \right\} \\
\hat{A}_{ik}(\omega) &= \hat{A}_{\infty, ik} + \frac{1}{\omega} Im \left\{ \hat{K}_{ik}(j\omega) \right\}
\end{aligned}$$

Once we have the approximated transfer functions of $K_{ik}(s)$, we can find the memory effect term in the time domain, exploiting the relation 43. Indeed, by taking the Laplace transform of

$$\mu(t) = \int_0^t \mathbf{K}(t-t') \dot{\xi}(t') dt'$$

we obtain

$$\mu_i(s) = K_{ik}(s) \dot{\xi}_k(s) \approx \frac{P_{ik}(s)}{Q_{ik}(s)} \dot{\xi}_k(s) \quad (58)$$

but the Laplace transform of the state-space formulation

$$\mu(t) \approx \begin{cases} \dot{\mathbf{x}} = \mathbf{A}_s \mathbf{x} + \mathbf{B}_s \dot{\xi} \\ \mu = \mathbf{C}_s \mathbf{x} \end{cases} \quad (59)$$

leads to

$$\mu(s) = \mathbf{C}_s (s\mathbf{I} - \mathbf{A}_s)^{-1} \mathbf{B}_s \dot{\xi}(s) \quad (60)$$

Hence, a correlation between 58 and 60 can be made to find the constant matrices \mathbf{A}_s , \mathbf{B}_s and \mathbf{C}_s of the state-space formulation, starting from the frequency domain transfer functions $\frac{P_{ik}(s)}{Q_{ik}(s)}$; then, \mathbf{A}_s , \mathbf{B}_s and \mathbf{C}_s can be used in 59 for the time domain approximation of $\mu(t)$.

9.5 Cummins equation resolution

Once we found a time domain approximation of the memory effect term $\mu(t)$ and the constant matrices \mathbf{A}_∞ and \mathbf{B}_∞ , we can proceed with the numerical resolution of the Cummins equation

$$(\mathbf{M}_{RB} + \mathbf{A}_\infty) \ddot{\xi} + \mathbf{B}_\infty \dot{\xi} + \mu(t) + \mathbf{G}\xi = \tau_{FK+Diff}^s$$

From potential theory we can compute the dynamic pressure due to incident and diffracted waves and, after the integration over the wet surface of the vessel, we can find the Froude-Krilov and diffraction force vector $\tau_{FK+Diff}^s$.

Writing the equation as

$$\ddot{\xi} = -(\mathbf{M}_{RB} + \mathbf{A}_\infty)^{-1} \mathbf{G}\xi - (\mathbf{M}_{RB} + \mathbf{A}_\infty)^{-1} \mathbf{B}_\infty \dot{\xi} + (\mathbf{M}_{RB} + \mathbf{A}_\infty)^{-1} (\tau_{FK+Diff}^s - \mu(t))$$

we can reduce the order of the problem defining the following state vector

$$\mathbf{y}(t) = \begin{bmatrix} \xi(t) \\ \dot{\xi}(t) \end{bmatrix}$$

Indeed, the time derivative of $\mathbf{y}(t)$ can be written in a linear system form as:

$$\dot{\mathbf{y}}(t) = \mathbf{W} \cdot \mathbf{y}(t) + \mathbf{l}(t) = \mathbf{f}(t, \mathbf{y}(t)) \quad (61)$$

where \mathbf{W} is the constant matrix

$$\mathbf{W} = \begin{bmatrix} \mathbf{0}_{6 \times 6} & \mathbf{I}_{6 \times 6} \\ -(\mathbf{M}_{RB} + \mathbf{A}_{\infty})^{-1} \mathbf{G} & -(\mathbf{M}_{RB} + \mathbf{A}_{\infty})^{-1} \mathbf{B}_{\infty} \end{bmatrix}$$

and $\mathbf{l}(t)$ the time dependent vector

$$\mathbf{l}(t) = \begin{bmatrix} \mathbf{0}_{6 \times 1} \\ (\mathbf{M}_{RB} + \mathbf{A}_{\infty})^{-1} \left(\tau_{FK+Diff}^s - \mu(t) \right) \end{bmatrix}$$

As we can see, in order to integrate the motion equation 61, we need the initial condition $\mathbf{y}(0)$, so the starting position and the velocity of the ship with respect his equilibrium position. For the memory effect term, a parallel update can be performed separately each time step, initializing the state vector \mathbf{x} to zero $\mathbf{x}(0) = \mathbf{0}$.

$$\begin{cases} \dot{\mathbf{x}}(t) = \mathbf{A}_s \mathbf{x}(t) + \mathbf{B}_s \dot{\xi}(t) \\ \mu(t) = \mathbf{C}_s \mathbf{x}(t) \\ \mathbf{x}(0) = \mathbf{0} \end{cases} \quad (62)$$

Finding the excitation forces, by integration of the pressure on the hull, implies the computation of $\tau_{FK+Diff}$ at each step; indeed, the computation must be carried out on the actual position of the hull, so it's possible only after updating it, integrating the motion equation.

We can apply several numerical methods to integrate both 61 and 62, for example a Runge-Kutta method.

The general algorithm to proceed with the integration is:

$$\begin{aligned} \xi(0), \dot{\xi}(0) &\rightarrow \mathbf{y}(0) \\ \xi(0) &\rightarrow \tau_{FK+Diff}(0) \\ \mathbf{x}(0) &\rightarrow \mu(0) \\ \left\{ \begin{array}{l} \mathbf{y}(0) \\ \tau_{FK+Diff}(0) \\ \mu(0) \end{array} \right. &\rightarrow \mathbf{y}(\Delta t) \end{aligned}$$

$$\begin{aligned} \xi(k\Delta t) &\rightarrow \tau_{FK+Diff}(k\Delta t) \\ \mathbf{x}(k\Delta t) &\rightarrow \mu(k\Delta t) \\ \left\{ \begin{array}{l} \mathbf{y}(k\Delta t) \\ \tau_{FK+Diff}(k\Delta t) \\ \mu(k\Delta t) \end{array} \right. &\rightarrow \mathbf{y}((k+1)\Delta t) \end{aligned}$$

The possibility to add a forward speed U is implemented. To add the drag force due to the relative motion, we can use empirical formulas: after finding the instantaneous relative velocity U_i of the vessel with respect to the water – adding to the forward speed the surge fluctuation and the water velocity – we can compute the Reynolds number and the global resistance coefficients C_{Drag} , expressed as a percentage of the friction coefficient C_f :

$$\begin{aligned} Re &= \frac{\rho U_i L_{pp}}{\mu} \\ C_f &= C_f(Re) \\ C_{Drag} &= \alpha C_f, \quad \alpha > 1 \end{aligned}$$

For example, we can use the Gabers formula to estimate the friction coefficient:

$$C_f = \frac{0.02058}{\sqrt[5]{Re}}$$

and consider the pressure resistance as the 50% of the friction one, so $C_{Drag} = \alpha C_f$ with $\alpha = 1.5$. To compute the drag force we can consider an equivalent plate with a wet surface of $S_{eq} = 2L_{pp}d$, so it results

$$D = \rho U_i^2 L_{pp} d C_{Drag}$$

The steady part of the resistance, due only to the forward speed U , is taken off from the overall resistance: for seakeeping simulations, the hypothesis that the propulsive system balances at each instant this component, to assure equilibrium, is assumed.

10 Maneuvering simulation

To perform ship maneuvering simulations, we have to change reference frames. Unable to define any equilibrium position the ship fluctuates around, every kinematics quantity must be referred with respect to an inertial frame $\{n\}$: η and ν are the generalized position and velocity vectors of the ship with respect of the origin of $\{n\}$, but while η is also expressed in the inertial frame, ν is expressed in the body coordinate system.

The frequency domain dynamical model for maneuvering is:

$$[\mathbf{M}_{RB} + \mathbf{M}_A(\omega)] \delta \dot{\nu} + \mathbf{N}(\omega) \delta \nu + \mathbf{C}_{RB} \delta \nu + \mathbf{G} \xi = \tau_{FK+Diff}^b + (\tau_{PID} - \bar{\tau})$$

with

$$\begin{aligned} \mathbf{M}_A(\omega) &= \mathbf{J}^{*T} \left[\mathbf{A}(\omega) - \frac{U}{\omega_e^2} \mathbf{B}(\omega) \mathbf{L}^* \right] \mathbf{J}^* \\ \mathbf{N}(\omega) &= \mathbf{J}^{*T} [\mathbf{B}(\omega) + U \mathbf{A}(\omega) \mathbf{L}^*] \mathbf{J}^* \\ \mathbf{C}_{RB} &= U \mathbf{M}_{RB} \mathbf{L}^* \end{aligned}$$

On the other hand, the related time domain version is:

$$[\mathbf{M}_{RB} + \mathbf{M}_{A,\infty}] \delta \dot{\nu} + \mathbf{N}_\infty \delta \nu + \mathbf{C}_{RB} \delta \nu + \int_0^t \tilde{\mathbf{K}}(t-t') \delta \nu(t') dt' + \mathbf{G} \eta = \tau_{FK+Diff}^b + (\tau_{PID} - \bar{\tau})$$

with

$$\begin{aligned} \tilde{\mathbf{K}}(t) &= \frac{2}{\pi} \int_0^\infty [\mathbf{N}(\omega) - \mathbf{N}_\infty] \cos(\omega t) d\omega \\ \mathbf{M}_{A,\infty} &= \mathbf{J}^{*T} \mathbf{A}_\infty \mathbf{J}^* \\ \mathbf{N}_\infty &= \mathbf{J}^{*T} [\mathbf{B}_\infty + U \mathbf{A}_\infty \mathbf{L}^*] \mathbf{J}^* \\ \mathbf{C}_{RB} &= U \mathbf{M}_{RB} \mathbf{L}^* \end{aligned}$$

The difficulties to overcome to implement the resolution are the same of the seakeeping case:

- Find a transfer function for $\tilde{\mathbf{K}}(t)$ and approximate the convolution term;
- Find \mathbf{A}_∞ and \mathbf{B}_∞ to compute $\mathbf{M}_{A,\infty}$ and \mathbf{N}_∞ .

10.1 Identification of $\mathbf{M}_{A,\infty}$, \mathbf{N}_∞ and Fluid Memory Effect

All the considerations we already made about the memory effect terms still hold; the difference in maneuvering is that the argument of the convolution operator is different: it's a linear combination of the frequency dependent matrices $\mathbf{A}(\omega)$ and $\mathbf{B}(\omega)$.

The method is similar to the seakeeping one. We start correlating the following expression

$$\mathbf{M}_A(\omega) \delta \dot{\nu} + \mathbf{N}(\omega) \delta \nu = \left[\mathbf{M}_A(\omega) + \frac{\mathbf{N}(\omega)}{j\omega} \right] \delta \dot{\nu} \quad (63)$$

with the related time domain one:

$$\mathbf{M}_{A,\infty} \delta \dot{\nu} + \mathbf{N}_\infty \delta \nu + \int_0^t \tilde{\mathbf{K}}(t-t') \delta \nu(t') dt'$$

Taking the Laplace transform of the former, we can write an equivalent form in the frequency domain:

$$\left[\mathbf{M}_{A,\infty} + \frac{\mathbf{N}_\infty + \tilde{\mathbf{K}}(s)}{s} \right] \delta \dot{\nu} \quad (64)$$

Considering each term of 63 and 64 separately, and approximating the retardation matrix with a rational function:

$$K_{ik}(s) \approx \tilde{K}_{ik}(s) = \frac{L_{ik}(s; \theta)}{G_{ik}(s; \theta)}$$

we define

$$\begin{aligned} M_{A,ik}(\omega) + \frac{N_{ik}(\omega)}{j\omega} &= \mathcal{T}_{ik}(j\omega) \\ M_{A\infty,ik} + \frac{N_{\infty,ik}}{s} + \frac{L_{ik}(s; \theta)}{sG_{ik}(s; \theta)} &= \hat{\mathcal{T}}_{ik}(s; \theta) \end{aligned}$$

We can form a discrete data set for each $\mathcal{T}_{ik}(j\omega)$, by having available the matrices $\mathbf{A}(\omega_l)$ and $\mathbf{B}(\omega_l)$. Indeed, both $\mathbf{M}_A(\omega)$ and $\mathbf{N}(\omega)$ are simple combinations of them:

$$\begin{aligned}\mathbf{M}_A(\omega_l) &= \mathbf{J}^{*T} \left[\mathbf{A}(\omega_l) - \frac{U}{\omega_{e,l}^2} \mathbf{B}(\omega_l) \mathbf{L}^* \right] \mathbf{J}^* \\ \mathbf{N}(\omega_l) &= \mathbf{J}^{*T} [\mathbf{B}(\omega_l) + U \mathbf{A}(\omega_l) \mathbf{L}^*] \mathbf{J}^*\end{aligned}$$

so

$$\mathcal{T}(j\omega_l) = \left[\mathbf{M}_A(\omega_l) + \frac{\mathbf{N}(\omega_l)}{j\omega_l} \right]$$

To find $M_{A\infty,ik}$, $N_{\infty,ik}$ and the polynomial functions of $\frac{L_{ik}(s;\theta)}{G_{ik}(s;\theta)}$, we can solve an optimization problem: starting with the definition of the degree of approximation of the retardation function, i.e. the degree of the functions $L_{ik}(s;\theta)$, or $G_{ik}(s;\theta)$, we try to find θ^* such that $\hat{\mathcal{T}}_{ik}(s;\theta^*)$ will fit in the best way possible – in the least mean square sense – the data $\mathcal{T}_{ik}(j\omega_l)$:

$$\theta^* = \arg \min_{\theta} \sum_l w_l \left| \mathcal{T}_{ik}(j\omega_l) - \hat{\mathcal{T}}_{ik}(s;\theta) \right|^2$$

the resulting $\hat{\mathcal{T}}_{ik}(s;\theta^*)$ has a rational form too:

$$\hat{\mathcal{T}}_{ik}(s;\theta^*) = \frac{M_{A\infty,ik}sG_{ik}(s;\theta^*) + N_{\infty,ik}G_{ik}(s;\theta^*) + L_{ik}(s;\theta^*)}{sG_{ik}(s;\theta^*)} = \frac{R_{ik}(s;\theta^*)}{S_{ik}(s;\theta^*)} \quad (65)$$

Therefore, after the fitting problem, we have $R_{ik}(s;\theta^*)$ and $S_{ik}(s;\theta^*)$.

As we already discussed, for the properties of the retardation functions, the relative degree between $L_{ik}(s;\theta^*)$ and $G_{ik}(s;\theta^*)$ is one and the former has the higher order. That means that we can directly find both $\hat{M}_{A\infty,ik}$ and $G_{ik}(s;\theta^*)$: the former is simply $\frac{1}{s}S_{ik}(s;\theta^*)$ and, on the other hand, $M_{A\infty,ik}$ is the highest degree coefficient of $R_{ik}(s;\theta^*)$, having $sG_{ik}(s;\theta^*)$ the highest order in the numerator of 65.

As already done, we can iterate until finding also $\hat{N}_{\infty,ik}$ and $L_{ik}(s;\theta^*)$: \mathbf{N}_{∞} can be initialized with the highest available frequency $\mathbf{N}(\omega_{max})$ and from the following

$$M_{A\infty,ik}sG_{ik}(s;\theta^*) + N_{\infty,ik}G_{ik}(s;\theta^*) + L_{ik}(s;\theta^*) = R_{ik}(s;\theta^*)$$

the first iterative step is

$$[L_{ik}(s; \theta^*)]_1 = R_{ik}(s; \theta^*) - M_{A\infty, ik} s G_{ik}(s; \theta^*) - N_{ik}(\omega_{max}) G_{ik}(s; \theta^*)$$

Then, defining the sum of the coefficients of the polynomials $G_{ik}(s; \theta^*)$, $L_{ik}(s; \theta^*)$ and $R_{ik}(s; \theta^*)$ as $\sum_j g_j = G$, $\sum_j l_j = L$ and $\sum_l r_j = R$, we can add the relation

$$M_{A\infty, ik} G + N_{\infty, ik} G + L = R$$

which means

$$(N_{\infty, ik})_{l+1} = M_{A\infty, ik} - \frac{R - L_l}{G}$$

to continue the iteration process, similarly as we already discussed. Clearly, the notation L_l represent the sum of the coefficients of the polynomial $L_{ik}(s; \theta^*)$ at the l th iteration.

As we found every components we needed, we can compute the error, i.e. evaluating the quality of the order. We will exploit the following properties: in analogy of the seakeeping motion equation, it holds

$$\tilde{\mathbf{K}}(t) = \frac{2}{\pi} \int_0^\infty [\mathbf{N}(\omega) - \mathbf{N}_\infty] \cos(\omega t) d\omega = -\frac{2}{\pi} \int_0^\infty \omega [\mathbf{M}_A(\omega) - \mathbf{M}_{A, \infty}] \sin(\omega t) d\omega$$

from which it derives

$$\begin{cases} \mathbf{N}(\omega) &= \mathbf{N}_\infty + \int_0^\infty \tilde{\mathbf{K}}(t) \cos(\omega t) dt \\ \mathbf{M}_A(\omega) &= \mathbf{M}_{A, \infty} - \frac{1}{\omega} \int_0^\infty \tilde{\mathbf{K}}(t) \sin(\omega t) dt \end{cases}$$

and the Laplace transform leads to

$$\tilde{\mathbf{K}}(j\omega) = \int_0^\infty \tilde{\mathbf{K}}(t) e^{-j\omega t} dt = [\mathbf{N}(\omega) - \mathbf{N}_\infty] + j\omega [\mathbf{M}_A(\omega) - \mathbf{M}_{A, \infty}] \quad (66)$$

Having found $\hat{N}_{\infty, ik}$ and $\hat{M}_{A\infty, ik}$, using 66 we can compare the points from the data set $N_{ik}(\omega_l)$ and $M_{A, ik}(\omega_l)$, with the approximated ones

$$\begin{cases} \hat{N}_{ik}(\omega_l) &= \hat{N}_{\infty, ik} + Re \left\{ \frac{L_{ik}(j\omega_l; \theta^*)}{G_{ik}(j\omega_l; \theta^*)} \right\} \\ \hat{M}_{A, ik}(\omega_l) &= \hat{M}_{A\infty, ik} + \frac{1}{\omega} Im \left\{ \frac{L_{ik}(j\omega_l; \theta^*)}{G_{ik}(j\omega_l; \theta^*)} \right\} \end{cases}$$

After computing the error, we can increase the order of $\frac{L_{ik}(s;\theta)}{G_{ik}(s;\theta)}$ and, at the end, choose the best trade off between a low error and a low order.

To convert this formulation in a state-space one, we proceed as before:

$$\begin{aligned}\mu_i(s) &= \hat{K}_{ik}(s) \delta\nu_k(s) \approx \frac{L_{ik}(s)}{G_{ik}(s)} \delta\nu_k(s) \\ \mu(s) &= \mathbf{C}_s' (s\mathbf{I} - \mathbf{A}_s')^{-1} \mathbf{B}_s' \delta\nu(s)\end{aligned}$$

and after the correlation we can find the constant matrices \mathbf{A}_s' , \mathbf{B}_s' and \mathbf{C}_s' .

10.2 Cummins equation resolution

The approach to integrate the maneuvering equation is the same of the seakeeping one: having the dynamical model

$$\begin{cases} \dot{\eta} = \mathbf{J}_b^n(\eta) \nu \\ [\mathbf{M}_{RB} + \mathbf{M}_{A,\infty}] \dot{\nu} + \mathbf{N}_\infty \nu + \mathbf{C}_{RB} \nu + \mu(t) + \mathbf{G} \eta = \tau_{FK+Diff}^b + \tau_{PID} \end{cases}$$

Rearranging the motion equation, the acceleration results:

$$\dot{\nu} = -[\mathbf{M}_{RB} + \mathbf{M}_{A,\infty}]^{-1} \mathbf{G} \eta - [\mathbf{M}_{RB} + \mathbf{M}_{A,\infty}]^{-1} (\mathbf{N}_\infty + \mathbf{C}_{RB}) \nu + [\mathbf{M}_{RB} + \mathbf{M}_{A,\infty}]^{-1} (\tau_{FK+Diff}^b + \tau_{PID} - \mu(t))$$

Defining the state vector $\mathbf{y}(t)$ and the matrices $\mathbf{W}(t)$ and $\mathbf{l}(t)$ as follows:

$$\begin{aligned}\mathbf{y}(t) &= \begin{bmatrix} \eta(t) \\ \nu(t) \end{bmatrix} \\ \mathbf{W}(t) &= \begin{bmatrix} \mathbf{0}_{6 \times 6} & \mathbf{J}_b^n(\eta) \\ -[\mathbf{M}_{RB} + \mathbf{M}_{A,\infty}]^{-1} \mathbf{G} & -[\mathbf{M}_{RB} + \mathbf{M}_{A,\infty}]^{-1} (\mathbf{N}_\infty + \mathbf{C}_{RB}) \end{bmatrix} \\ \mathbf{l}(t) &= \begin{bmatrix} \mathbf{0}_{6 \times 1} \\ [\mathbf{M}_{RB} + \mathbf{M}_{A,\infty}]^{-1} (\tau_{FK+Diff}^b + \tau_{PID} - \mu(t)) \end{bmatrix}\end{aligned}$$

the motion equation turns into:

$$\dot{\mathbf{y}}(t) = \mathbf{W}(t) \cdot \mathbf{y}(t) + \mathbf{l}(t) = \mathbf{f}(t, \mathbf{y}(t))$$

This time the matrix $\mathbf{W}(t)$ is time dependent, because of the presence of $\mathbf{J}_b^n(\eta(t))$.

The algorithm for integrating numerically the dynamics equation, are perfectly analogous to the seakeeping ones. The main difference is that the matrix $\mathbf{W}(t)$ must be computed each time step, after updating the position η and consequently $\mathbf{J}_b^n(\eta)$. After setting the initial conditions for position and velocity $\eta(0)$ and $\nu(0)$ we proceed in the following way:

$$\begin{aligned} \eta(0), \nu(0) &\rightarrow \mathbf{y}(0) \\ \eta(0) &\rightarrow \mathbf{J}_b^n(\eta(0)) \\ \mathbf{J}_b^n(\eta(0)) &\rightarrow \mathbf{W}(0) \\ \eta(0) &\rightarrow \tau_{FK+Diff}(0) \\ \mathbf{x}(0) &\rightarrow \mu(0) \end{aligned}$$

$$\left\{ \begin{array}{l} \mathbf{y}(0) \\ \mathbf{W}(0) \\ \tau_{FK+Diff}(0) \\ \mu(0) \end{array} \right. \rightarrow \mathbf{y}(\Delta t)$$

$$\begin{aligned} \eta(k\Delta t) &\rightarrow \mathbf{J}_b^n(\eta(k\Delta t)) \\ \mathbf{J}_b^n(\eta(k\Delta t)) &\rightarrow \mathbf{W}(k\Delta t) \\ \eta(k\Delta t) &\rightarrow \tau_{FK+Diff}(k\Delta t) \\ \mathbf{x}(k\Delta t) &\rightarrow \mu(k\Delta t) \end{aligned}$$

$$\left\{ \begin{array}{l} \mathbf{y}(k\Delta t) \\ \mathbf{W}(k\Delta t) \\ \tau_{FK+Diff}(k\Delta t) \\ \mu(k\Delta t) \end{array} \right. \rightarrow \mathbf{y}((k+1)\Delta t)$$

10.3 Sideslip stability

During maneuvering, ship experiences important sideslip angles, that is the misalignment between the velocity and the x body axis. The vessel response is opposite and it tends to realign itself with the velocity. In seakeeping that means static stability, but in maneuvering that can make the rudder capabilities inefficient.

According to the regression analysis of [Lee&Shin1998], we can add to our model the hydrodynamics derivatives in sway force Y and yaw moment N due to a sideslip δ .

Defining $k = \frac{2d}{L_{pp}}$ and the block coefficient $C_b = \frac{\Omega}{L_{pp}Bd}$, where d is the mean draft, L_{pp} the length of the ship and Ω the fluid displaced volume, [Lee&Shin1998] found:

$$\begin{aligned} Y_\delta &= -9.5114 + 30.278C_b - 36.8419k - 22.1929C_b^2 + 20.3124k^2 + 40.3232C_bk \\ Y_{\delta|\delta} &= 31.3506 + 3.622C_b + 318.2181\frac{B}{L} + 29.1844C_b^2 - 290.0526\left(\frac{B}{L}\right)^2 - 262.1299C_b\frac{B}{L} \\ N_\delta &= 0.0024 + 1.0272k \\ N_{\delta|\delta} &= -0.2149 + 4.6127k - 22.53k^2 \end{aligned}$$

Ultimately, we add the forces:

$$\begin{aligned} Y &= Y_\delta\delta + Y_{\delta|\delta}|\delta|\delta| \\ N &= N_\delta\delta + N_{\delta|\delta}|\delta|\delta| \end{aligned}$$

In our model we neglect the cross derivatives with the yaw angular velocity, i.e. $Y_{\delta r}$ and $N_{\delta r}$.

10.4 PD Controller

In a similar way we already did for seakeeping, we can add the resistance of the ship, starting from the instantaneous Reynolds number and using empirical formulas. Then, the steady resistance, required to assure a constant speed U , is balanced by the propulsive force and the remaining part acts autonomously.

Furthermore, to control the ship, in order to achieve simple maneuvering actions, a PD controller has also been implemented in the simulator. Selecting one or more target positions to reach, the error is computed by the means of the difference $\Delta\psi$ between the heading attitude the ship should have and the

one the ship actually has. Indeed, the x body axis of the ship should be aligned with the target point and, controlling a rudder, a yaw moment is generated to correct the attitude.

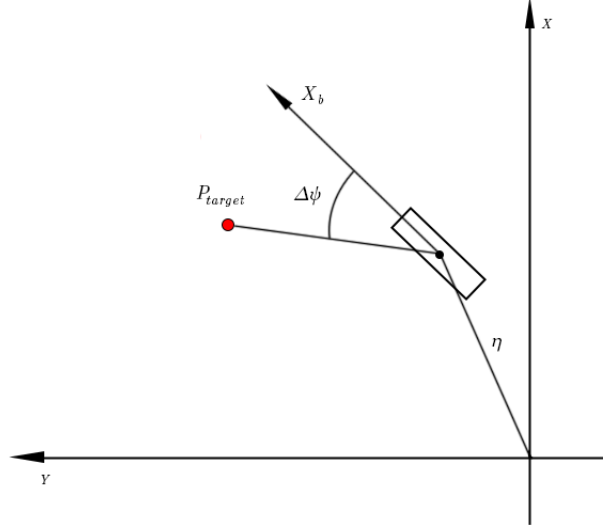


Figure 8: Error $\Delta\psi$ to correct by the PD controller

Once the error has been computed, the angle to command to the rudder is found by the means of the constant K_p and K_d :

$$\delta_{rudder} = K_p \Delta\psi + K_d \frac{d}{dt} (\Delta\psi)$$

The surface of the rudder S_{rudder} is assumed to be 2.5% of the longitudinal surface of the ship $L_{pp}d$, with a classic aspect ratio of $\lambda \sim 2/2.5$. The normal force coefficient is computed as:

$$C_{Fn} = \frac{6.13\lambda}{\lambda + 2.25}$$

To find the normal force generated by the rudder, the effective angle of attack α_{rudder} must be considered. Neglecting all the interaction with the hull, this angle is just the sum of the rudder deflection and the sideslip angle of the ship:

$$\alpha_{rudder} = \delta_{rudder} + \delta$$

Considering the instantaneous relative velocity of the vessel with respect to water, sum of the cruise – with respect to the inertial frame – and the sea one, the resulting normal force is found to be

$$F_n = \frac{1}{2} \rho U_i^2 S_{rudder} C_{Fn} \sin \alpha_{rudder}$$

The projection of F_n along the y body axes gives the sway force Y_{rudder} and the one along the x axis an added resistance; the sway component Y_{rudder} causes the yaw moment N_{rudder} , aimed to control the attitude of the ship, and also a reaction roll moment K_{rudder} due to the vertical distance of the rudder from the center of gravity Δz_{rudder} . Those forces, computed in the body reference frame, are respectively:

$$X_{rudder} = -|F_n \sin(\delta_{rudder})|$$

$$Y_{rudder} = -F_n \cos(\delta_{rudder})$$

$$N_{rudder} = -Y \frac{L_{pp}}{2}$$

$$K_{rudder} = Y \Delta z_{rudder}$$

11 Integration with WAFO

To create more realistic sea states we integrated WAFO, a Matlab toolbox for analysis of random waves and loads, with *FloBoS*.

This toolbox, created by a mathematical and engineering group of the University of Lund, can perform accurate and detailed statistical analysis about sea states and fatigue analysis; however we exploited very few features of this powerful software.

Using WAFO routines we can obtain a realistic wave spectrum just with three informations about the sea state:

- Significant waves height H_{m0} , defined as four times the standard deviation of the surface elevation;
- Peak period T_p , defined as the wave period associated with the most energetic waves in the total wave spectrum;
- Main direction of the waves θ_0 , with respect to our inertial frame.

11.1 Wave Spectrum

Waves on the sea surface are not simple sinusoidal but, with some simplifications, we arrive to the concept of the spectrum of ocean waves. A waves spectrum, statistically defined from a general sea surface, gives the distribution of the energy among different wave frequencies. There are many models for sea spectra, coupling both experimental data and theoretical concepts, and the state of art requires a good knowledge of the characteristics of the particular sea one wants to simulate to choose the best one. In *FloBoS* the main used spectrum is the JONSWAP; the former can also lead to a more sophisticated one, the Torsethaugen spectrum, by combining two of them. In what follows we will describe the main features of both.

JONSWAP spectrum

The JONSWAP (JOint North Sea WAVE Project), by [Hasselmann1973], is a result of a program to standardize wave spectra of the Southeast part of the North Sea.

This spectrum is particularly well suited for not fully developed sea states, but it can be used also to represent fully developed ones. His best validity range is when $3.6\sqrt{H_{m0}} < T_p < 5\sqrt{H_{m0}}$.

This spectrum is given in the form of

$$S^+(\omega) = \frac{\alpha g^2}{\omega^M} \exp\left(-\frac{M}{N} \left(\frac{\omega_p}{\omega}\right)^N\right) \gamma \exp\left(-\frac{(\omega - \omega_p)^2}{2\sigma^2 \omega_p^2}\right)$$

where

$$\sigma = \begin{cases} 0.07, & \omega < \omega_p \\ 0.09, & \omega > \omega_p \end{cases}$$

$$M = 5$$

$$N = 4$$

$$\alpha \approx 5.061 \frac{H_{m0}^2}{T_p^4} (1 - 0.287 \ln(\gamma))$$

$$\gamma = \exp\left(3.484 \left[1 - 0.1975 \frac{T_p^4}{H_{m0}^2} \left(0.036 - 0.0056 \frac{T_p}{\sqrt{H_{m0}}}\right)\right]\right)$$

The value of γ , the peakedness parameter, is limited by $1 \leq \gamma \leq 7$; a standard value that can be taken for it is $\gamma = 3.3$.

Torsethaugen spectrum

Torsethaugen proposed in [Torsethaugen1993] to describe a bimodal spectrum by the sum of two JON-SWAP spectra:

$$S^+(\omega) = \sum_{j=1}^2 S_j^+(\omega; H_{m0j}, T_{pj})$$

H_{m0j} and T_{pj} are the significant wave height and the angular peak frequency for the primary and secondary peak, respectively.

For more information about the definition of those spectra please consult the WAFO guide [WAFO2017].

The figure shows how an example of spectrum can appear:

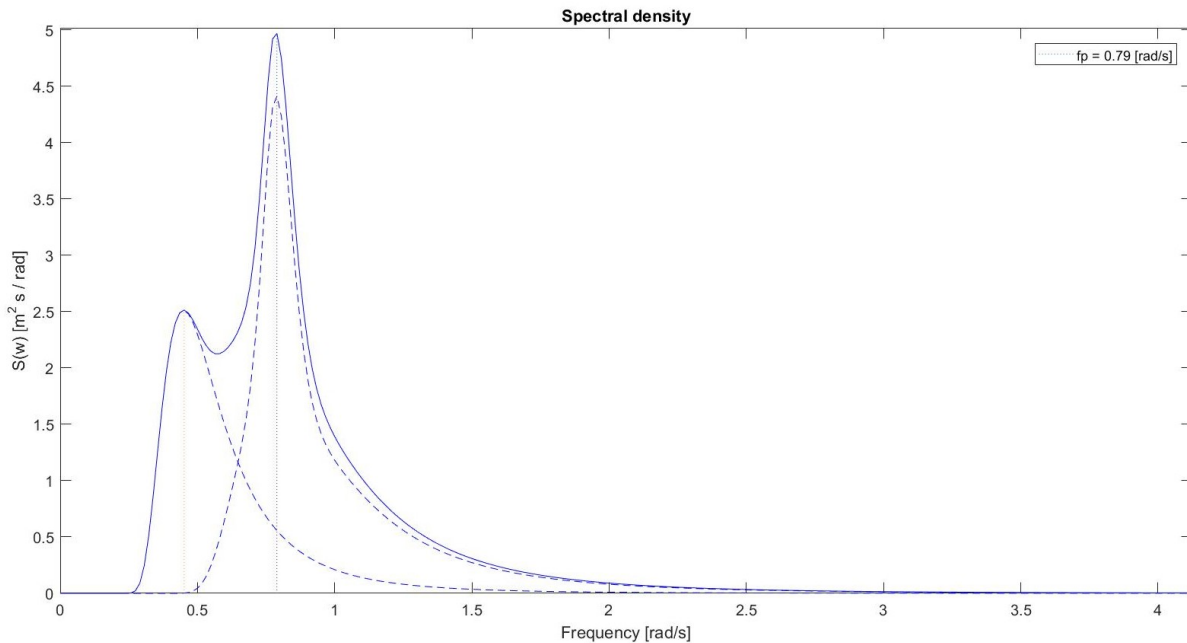


Figure 9: Example of Torsethaugen spectrum with parameters $H_{m0} = 6 \text{ m}$ and $T_p = 8 \text{ s}$

11.2 Directional spectrum

The wave train is also characterised by a main direction along it travels: the overall spectrum should also consider that. The way to describe the waves direction on the equilibrium water plane is the directional spectrum $D(\theta)$, a probability density function. It statistically describes the possible direction of a single harmonic of the whole spectrum. The resulting spectrum is simply the product of the energy spectrum

and the directional one:

$$S(\omega, \theta) = S(\omega) D(\theta)$$

A function that can be used is a *cos-2s* type, that for a mean direction of θ_0 is:

$$D(\theta; \theta_0) = \frac{\Gamma(s+1)}{2\sqrt{\pi}\Gamma(s+\frac{1}{2})} \cos^{2s}\left(\frac{\theta-\theta_0}{2}\right)$$

where $\Gamma(s)$ is the gamma function, the extension of the factorial function. We can see that $D(\theta)$ has a maximum centered in θ_0 and, as a probability density function, it holds

$$\int_{-\pi+\theta_0}^{\pi+\theta_0} D(\theta) d\theta = 1$$

One way to visualize $S(\omega, \theta)$ is a polar plot, which represents both the contour lines of the sea waves energy and their main directions in one fell swoop:

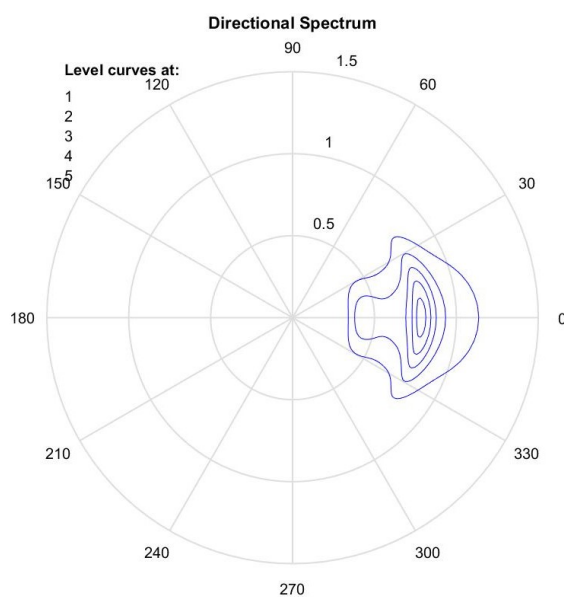


Figure 10: Example of polar plot: $H_{m0} = 6 m$ and $T_p = 8 s$

11.3 Spectra sampling

To integrate in *FloBoS* the spectra generated by WAFO, we need to extrapolate simple harmonics: that can be made by a sampling of $S(\omega, \theta)$. Indeed, after choosing a resolution number N_{res} , an approximated sea surface is defined by:

$$\omega_i = i \frac{\omega_{max} - \omega_{min}}{N_{res} + 1}$$

$$\zeta(t, x, y) = \sum_{i=1}^{N_{res}} \sqrt{2S(\omega_i, \theta_i)} \Delta\omega \cos[k_i(x \cos \theta_i - y \sin \theta_i) + \phi_i]$$

where $\sqrt{2S(\omega_i, \theta_i)} \Delta\omega$ is the amplitude of the i th harmonics, $k_i = \frac{2\pi}{\lambda_i}$ its wave number – equal to $\frac{\omega_i^2}{g}$ for infinite depth, θ_i is its direction and ϕ_i the phase.

The value of θ_i is chosen following the probability density function $D(\theta)$ and the phase is randomly sampled in the interval $[0, 2\pi)$

There are many possibility of carrying out the sampling: the discretization in N_{res} harmonics can be uniform along all the frequency range, as we saw, or not: in the former case we can choose smaller intervals where the spectrum function changes more sharply, i.e. near the peaks. In the case of uniform discretization, $\Delta\omega = \frac{\omega_{max} - \omega_{min}}{N_{res} + 1} = const.$

Part IV

FloBoS - An overview

The simulator assembles all the theoretical and technical apparatus mentioned before, implementing it in Matlab.

The first part of *SeaBoS* and *ManBoS* has been written starting from the seakeeping frequency domain Ship Response Simulator of [Musci2015]: the data pre-processing section of it has been adapted to new needs and recoded to make it more easily transferable in Python. Then, the time domain features has been added, as the optimization algorithms, the time integration of the motion equations, the manouvering simulator (possible only in time domain) with the related equations and the graphic part.

Starting from the shape of the vessel, given as a series of cross sections defined by points, every needed geometrical property is extrapolated: length of each strip element, mean and maximum draft, beam and freeboard, actual wet hull, normal and tangent unit vectors, each section's area, water plane area, area moments, buoyancy center, fluid displaced volume etc. To accomplish these tasks, the work of [Musci2015] has been adapted.

The software PDSTRIP solves a bidimensional boundary value problem for each j th cross section, which are globally n_{sec} , finding its bidimensional added mass and potential damping matrices, $\mathbf{a}_j(\omega_k)$ and $\mathbf{b}_j(\omega_k)$, for each of 52 frequencies ω_k that PDSTRIP chooses for each vessel, based on its dimension.

After an integration along the ship length, the tridimensional frequency dependent matrices of the whole hull, $\mathbf{A}(\omega_k)$ and $\mathbf{B}(\omega_k)$, are computed.

Once the vessel is completely defined with all the needed geometrical data, a static stability analysis is carried out: both longitudinal and transverse metacentric stability are evaluated and the restoring coefficients are computed.

To proceed with the real time domain simulation, the infinite frequency matrices \mathbf{A}_∞ and \mathbf{B}_∞ must be computed, as the definition of the state-space model matrices for the fluid memory effect term $\mu(t)$. In order to do that, specifying what simulator is intended to run, *SeaBoS* or *ManBoS*, is needed. The differences are in the algorithm to find \mathbf{A}_∞ and \mathbf{B}_∞ and in the motion equation integrated during the simulation.

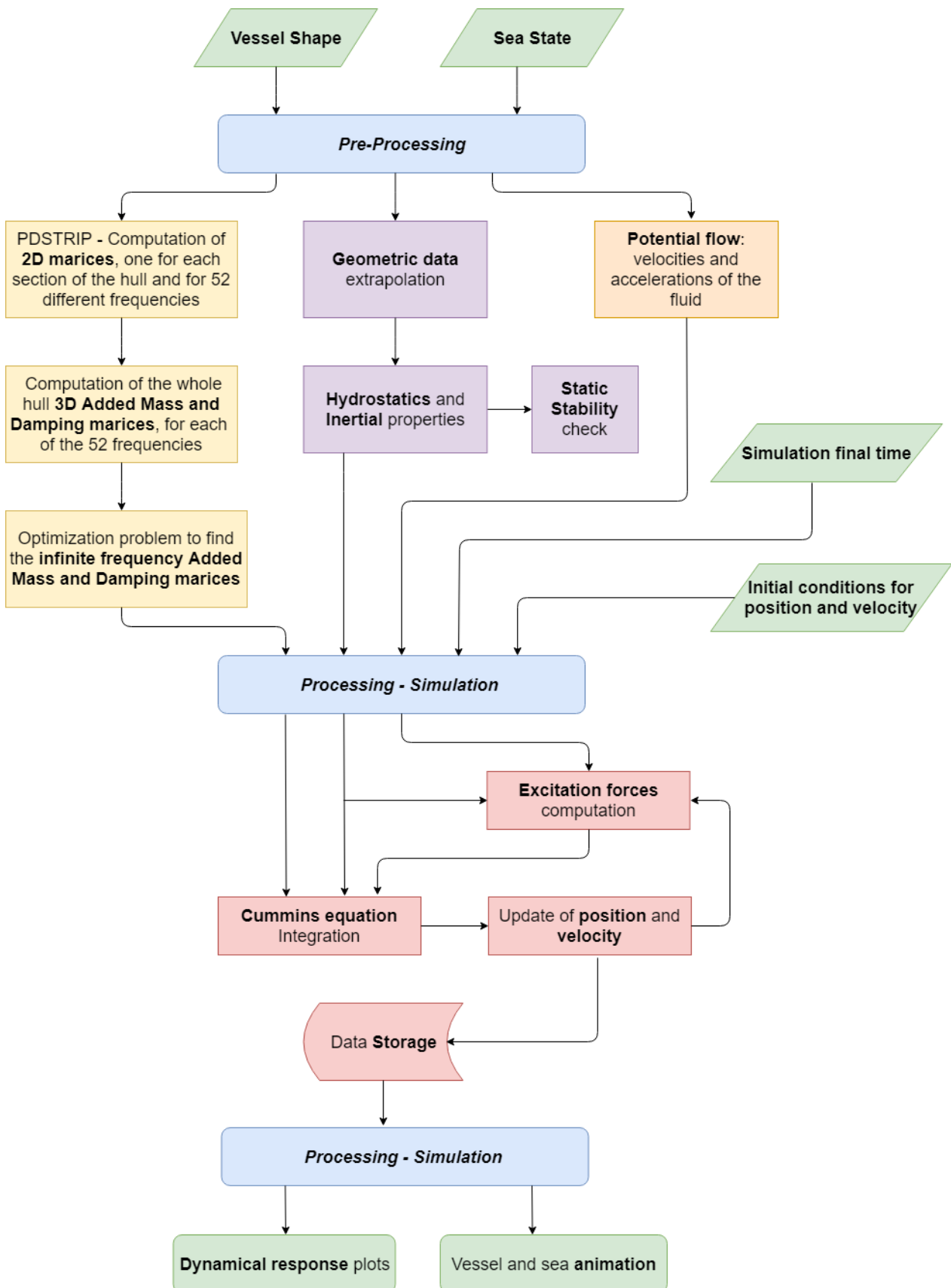
Moreover, to start a maneuvering analysis with *ManBoS*, a set of target points must be inserted: the vessel will be controlled with the rudder, by the means of the *PD* controller, with the objective to reach the target positions in the selected order.

Concerning the sea state, the waves harmonics can be defined manually or by uniform sampling of a Torsethaugen spectrum, which requires as inputs H_{m0} , T_p and θ_0 ; with the harmonics data, the computation of the excitation forces can be made during each time step of the simulation.

After the simulation, performed until the final time specified by the user, a post-processing phase starts. The dynamical responses are plotted and a vessel animation is shown.

In what follows we will give a more detailed description of *FloBoS*, taking a look in each of his part.

A scheme of how *SeaBoS* works is presented:

Figure 11: *SeaBoS* block diagram

12 Simulation setting

Before starting a simulation, a number of settings must be arranged. First of all, after choosing the case to simulate, PDSTRIP has to have the right input files to run. Then, the user has to set other simulation properties directly on the *FloBoS* script. The reference frames considered in *FloBoS* have the z vertical coordinate axis pointing upward, the x longitudinal one pointing from the stern to the bow, as the velocity, and the last cross one, the y axis, points from starboard to port:

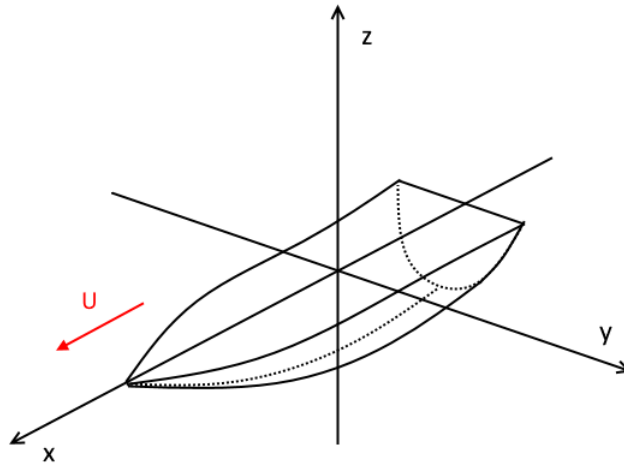


Figure 12: *FloBoS* frame of reference

Before going into the details, knowing how the simulator code is structured is suitable.

12.1 *FloBoS* folders structure

In the main *FloBoS* folder we can find three Matlab scripts – `FloBoS.m`, `SeaBoS.m` and `ManBoS.m`, and three subfolders – *FloBoS routine*, *PDSTRIP* and *WAFO*.

Among the scripts the user dedicated one is `FloBoS.m`, which is the one that, after setting in it all the simulation's properties, will launch one of the others, `SeaBoS.m` or `ManBoS.m`.

Concerning the subfolders, *FloBoS routine* contains routines to compute the excitation forces, to solve the optimization problem, to create the sea spectrum from WAFO results, the PD controller and some animation and graphic properties.

WAFO is the original December 2017 WAFO version folder, that can be downloaded from their official website <http://www.maths.lth.se/matstat/wafo/download/index.html>. Sea spectrum data are generated with these routines and then integrated in the simulator.

Finally, the folder *PDSTRIP* is where a subfolder for each case to simulate must be created, in order to specify the geometry of the hull.

In what follows, a more detailed section for *PDSTRIP* is dedicated.

12.2 *PDSTRIP* folder and cases subfolders

PDSTRIP is originally coded in FORTRAN 90, but a Windows-executable file, `pdstrip.exe`, is present in this subfolder. As we said, to allow *FloBoS* to run PDSTRIP, a folder for the case must be created and it must contain two input files and a post processing Matlab script, `SectionResults.m`. This script will take the output files of *PDSTRIP* and will make them compatible with the next step simulator elaboration – it is a routine of [Musci2015].

The first input file is the geometry one. The user can decide to write his own file, creating a personal hull, or to load a `.mgf` file from ShipX VERES list; in the former case it will be sufficient to specify it in `FloBoS.m`, as we will show below.

To write a geometry file, which must be called `geometry.out`, the structure to follow is:

```
n_s   T   d
x_1 n_p1 0
y_1 ... y_(n_p1)
z_1 ... z_(n_p1)
.
.
.
x_j n_pj 0
y_1 ... y_(n_pj)
z_1 ... z_(n_pj)
```

- *First line:* n_s , the number of the sections, indicates in how many sections the vessel has been discretized in; T refers to symmetrical sections – the only supported type by *FloBoS*, and d is the mean draft of the vessel.
- *Second line:* it refers to the first section, so x_1 is its x -coordinate, n_{p1} is the number of points of this section and the zero stands for simply connected sections – again, the only supported type by *FloBoS*.

- *Third and Fourth lines*: the lists of y and z coordinates of all the offset points of the section, from 1 to n_{pj} . It's fundamental to know that only half section must be identified, because the symmetrical sections hypothesis is always made. The order is from the bottom hull point to the port point.

Then, a block similar to the one formed by the 2nd, 3rd and 4th lines has to be repeated for each section, so n_s times. An important note is that the order of the sections must be from the stern to the bow, so that $x_{j+1} > x_j$.

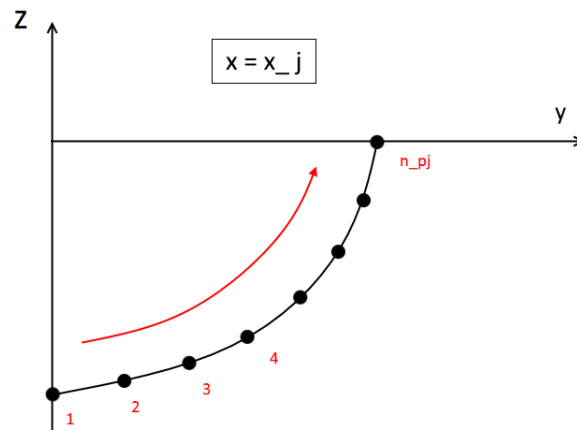


Figure 13: Generic j th section

The second input file, called `pdstrip.inp`, has this form:

```
0 t f f
// General description text
9.81 1.000 0 -1e6 999.
0
geomet.out

0/
```

The second line is irrelevant for PDSTRIP; the third one is composed by the following data: gravity acceleration g ; fluid density expressed in ton/m^3 (i.e. with respect to water density); z coordinate of the waterline, which is set to zero; the z coordinate of the sea bottom, which must be put to 10^6 to simulate infinite depth; the last number is irrelevant for us.

12.3 FloBoS.m settings

Once the case subfolder has been created, the final settings have to be made on the main script `FloBoS.m`. There are eight sections to be completed, each one with specific information and data about the simulation the user wants to perform. Any numerical value required to be inserted by the user must be expressed according to the International System of Units SI.

These sections are called:

- %% SET CASE NAME AND ROOT DIRECTORY. There are 6 variables to be assigned:

1. **Simulator:** the user has to choose between 'SeaBoS' for seakeeping simulations or 'ManBoS' for maneuvering;
2. **ispdstrip:** this variable must be set to 1 if the geometry file is structured for PDSTRIP, or 0 if the model follows the ShipX one, that is a file `.mgf`;
3. **pwd:** it is the path of the main *FloBoS* folder, for example 'C:\Users\...\FloBoS';
4. **casename:** this is the name the user gave to the case subfolder, in the PDSTRIP folder;
5. **namegeom:** this variable must contain the name of the geometry file in the 'casename' subfolder, which is 'geometry.out' for PDSTRIP or a generic 'vessel.mgf' otherwise.
6. **scaling:** this last variable allows to scale the hull geometry; if the user wants to simulate a vessel defined by the geometry file `namegeom`, but scaling it of a certain factor, this variable changes proportionally all the geometry. For example, to simulate a vessel which is a half of the one defined by `namegeom`, it will be sufficient to set `scaling = 0.5`;

- %% SIMULATION SETTING: There are 2 variables to be assigned, concerning possible user's manual tasks:

1. **Man_Order:** if this variable is set to 1, it enables the manual check of the order of the approximated fluid memory effect's transfer function. Otherwise, if it is set to 0, an algorithm will proceed with an automatic evaluation of the order. If the speed is non zero, it's recommended to check the fitting, setting the manual control on: 'Man_Order = 1';
2. **Man_Spec:** setting this variable to 0, a realistic Torsethaugen sea spectrum will be generated and sampled, to define the corresponding sea surface. Setting it to 1, the user can create a personalized sea surface, by adding manually each harmonics directly in the 'Simulator' script, under the

section `'% 1. CREATE THE SEA SPECTRUM'`. In this former case, the vectors to insert, which will define the sea and will be used for the computation of the excitation forces, are: `zeta`, containing each harmonics amplitude; `T`, for the corresponding periods; `beta`, for their heading angles with respect to the vessel.

- `% Ship` There are 3 variables to be assigned:
 1. `U`: the velocity of the vessel;
 2. `zg`: the vertical position of the center of gravity, relative to the mean sea surface;
 3. `d`: the mean draft of the vessel. In the geometry file the sections are entirely defined; then, specifying the draft, the actual wet part of the hull will be determined too. Please note that this variable is also the one in charge of the definition of the vessel load: a greater draft implies a greater displaced volume of fluid, which, in turn, corresponds to a greater mass.
- `% Fluid and environment properties` There are 3 variables concerning physical properties of the environment:
 1. `rho`: the density of the fluid where the vessel is supposed to float;
 2. `visc`: the dynamic viscosity of the fluid;
 3. `g`: the gravity experienced by the vessel. Please note that if the user wants to simulate a different gravity, it should be changed also in the PDSTRIP input file.
- `% Sea State - Waves spectrum` There are 4 variables needed to define the Torsethaugen spectrum and the sampling:
 1. `Hm0`: the significant waves height;
 2. `Tp`: the peak period;
 3. `Beta`: the primary direction of waves, expressed in radiant;
 4. `Nres`: this variable indicates the resolution the user wants to sample the energy Torsethaugen spectrum with. In other words, it defines the number of harmonics used to approximate the sea surface. Increasing `Nres` means having a higher precision of the sea surface definition, implying a more accurate excitation forces computation; on the other hand, the computational cost and the simulation time will be strongly affected by this parameter. Suggested values range between 15 and 25.

- %% Time data of simulation There is just one variable to insert in this section, that is the final time of the simulation: `T_fin`;
- %% Set initial conditions There are two vectors of dimension 6 to insert: they represent the initial conditions for the generalized position and velocity vector.
In the case of a seakeeping simulation, these vectors are `xi` and `xi_dot` ; for maneuvering they are `eta` and `ni`.
If there is a non zero vessel forward speed U , for seakeeping it does not have to be added at the vector of initial velocity, because `xi_dot` represents a perturbation from the equilibrium state, and the speed is considered part of this state; indeed, the problem is reduced to an equivalent one, where the vessel is at rest and the sea moves in the opposite direction, with a velocity $-U$.
For maneuvering, a non zero U should be taken into account too in the vector `ni`, because in this case velocities are taken with respect to an inertial frame. Nevertheless, this is done automatically; that means that the user has to set this vector different to zero just if there is an initial perturbation. In general these four vectors can remain null.
- %% Target position This vector has to be set only if a maneuvering simulation is going to be performed. In this case, its size must be $n_{target} \times 2$, where n_{target} is the number of consecutive target points the ship should reach. The general j th row represents the (x_j, y_j) position of the j th target point, taken on the mean sea surface plane.

13 Code Logic description

A brief summary of the simulator code is now presented. Only *SeaBoS* is considered; indeed, for a qualitative description, the two simulators structures are similar, except for small details.

SeaBoS is composed by 16 sections; we are going to quickly analyze each one

1. Create the Sea Spectrum

This first part of the code is dependent on the variable `Man_Spec`: if its value is 0, WAFO routines will be called to generate the sea spectrum, by the means of the variables specified in the section Sea State - Waves spectrum of *FloBoS*; then the discrete simple harmonics will be defined by a sampling. Otherwise the harmonics can be defined in this section by the user. Independently by `Man_Spec`, at the end of this first section the vectors `zeta`, `T` and `beta` will be assigned and therefore available to represent the approximated sea.

2. Time simulation Data

The variables concerning the simulation time are created: the size of the time step is set by default to 0.05 seconds; so the number of steps is computed as the ratio between the final time imposed by the user and this time step. A time vector is also defined, containing all the values from zero to the final time, all spaced by the size of the time step.

3. Prepare Input Data

Geometry data are extracted by the file `namegeom` and the first variables concerning the vessel are created. There is, of course, the dependence of the file format, that is if the file is structured for PDSTRIP or the if it's `.mgf`. Having the length of the ship, a check about the *Froude* number can be effectuated: the value should not be greater then 0.4.

4. Geometrical Properties of the Ship

The few geometrical data inserted by the user are processed to deduce all the other needed quantities. After all the other mentioned operations (like computing the strips spacing, the vessel draft, beam and center of buoyancy, the elements lengths, area moments and unit vectors) a deck is also added and the actual wet hull is obtained. A first plot of the vessel is showed, where the mean sea surface is visible too.

5. Run PDSTRIP

The software PDSTRIP is launched and the bidimensional added mass and damping matrices are found. If the file `namegeom` format is `.mgf`, a conversion must be carried out first. The results are elaborated by the function `SectionResults` and made ready to be elaborated.

6. 2D Added Mass and Damping Coefficients

The data from the 2D matrices are saved in dedicated variables. The matrices $\mathbf{a}_j(\omega_k)$ and $\mathbf{b}_j(\omega_k)$, $j = 1, \dots, n_{sec}$ and $k = 1, \dots, 52$, are all 6×6 and sparse matrices; that's why it's convenient to save these data in structures containing the same element of each matrix, for all the vessel sections n_{sec} and for all the 52 frequencies.

For example, a non zero element of the matrices \mathbf{a}_j is the (2, 2) one: we can create a matrix \mathbf{a}_{22} which contains all these elements (the added mass term in the second degree of freedom, the sway, due to a sway oscillation) for the all the strips and for all the simulated frequencies, so that $\mathbf{a}_{22} \in \mathbb{R}^{n_{sec} \times 52}$.

7. 3D Added Mass Coefficients

The vessel overall matrices are now computed. That is possible by integrating the contribution of the single sections ones along all the vessel length: in this way we will found one Added Mass matrix $\mathbf{A}(\omega_k)$ for each frequency. The formulas used for the integration, dependent also by the speed of the vessel, are the ones proposed by [Faltinsen1990].

8. 3D Damping Coefficients

For the Damping matrices the same integration process is carried out, finding the global ship matrices $\mathbf{B}(\omega_k)$.

9. Moments of Inertia

In this section, the moments of inertia in roll I_{44} , pitch I_{55} and yaw I_{66} are computed. The evaluation is made by the means of gyration radii, following the approximated formulas of [Faltinsen1990]. Indeed, the values of I_{jj} are computed as $I_{jj} = mr_{jj}^2$, where

$$r_{44} = 0.35 \cdot L_{pp}$$

$$r_{55} = 0.25 \cdot L_{pp}$$

$$r_{66} = 0.25 \cdot L_{pp}$$

10. Transverse Metacenter – Static Stability

To evaluate the static stability in roll, the hull is tilted until a maximum of 10 degrees, by steps of 0.5 degrees. At each iteration, the static pressure is integrated all over the wet surface, which changes as the vessel rolls, and the resulting reaction moment K is computed. For the small angles range considered during this process, the hydrostatics moment is basically linearly dependent on the roll angle ϕ . After the evaluation of K at each roll angle ϕ , the derivative K_ϕ in $\phi = 0$ is found by an interpolation of the computed curve $K(\phi)$. Thanks to the linear behaviour in this range, this value could also be found simply by a ratio. If this value is positive, then the vessel is unstable and the simulation is interrupted. Otherwise, the value $K_\phi < 0$ is also equal to the oppostie of the term G_{44} .

From the derivative K_ϕ it is also possible to find the value of \overline{GM}_T , as we saw. The inverse procedure is not really feasible, because the trasverse second water plane area moment J_T is not easy to calculate: indeed the discretization in strips is carried out in the longitudinal dierction. The direct tilting simulation to compute the roll moment at each angle is simpler.

11. Longitudinal Metacenter – Static Stability

Concerning longitudinal static stability, the geometrical data make possible a easy calculation of the longitudinal second moment:

$$J_L = \int_{A_w} x^2 dA \approx \sum_{j=1}^{n_{sec}} B_j x_j^2 \Delta x_j$$

where B_j is the beam, i.e. the length along y direction, of the j th section, x_j is its distance from the centroid of the water plane and Δx_j is the spacing along x with the $(j + 1)$ th section. Then, by exploiting the relations of the hydrostatics physics:

$$\overline{GM}_L = (z_b - z_g) + \frac{J_L}{\Omega}$$

The longitudinal static stability is basically always assured for conventional slender vessels.

12. Restoring Coefficients

The coefficients of the restoring matrix \mathbf{G} are computed following the formulas already seen:

$$G_{33} = \rho g A_{wp}$$

$$G_{35} = \rho g \int_{A_{wp}} x \cdot dA_{wp} \approx \rho g \sum_{j=1}^{n_{sec}} B_j x_j \Delta x_j$$

$$G_{44} = \rho g \overline{GM}_T$$

$$G_{53} = G_{35}$$

$$G_{55} = \rho g \overline{GM}_L$$

For slender moving vessels, a particular correction have to be made about yaw stability. If a yaw perturbation ψ appears, with respect to the equilibrium state, of course no hydrostatics reaction is manifested. Nevertheless, if the vessel has a forward speed U , and the velocity is not aligned with the x body axis, a stabilizing moment shows up. Indeed, in the seakeeping reference frame, a yaw angle ψ coincides also with a sideslip angle δ .

The former statement is completely true if the main direction of waves is zero. By contrast, if the waves are crashing on the vessel hull with a certain heading angle β , the correct approach would be to evaluate the sideslip angle δ_0 by a vectorial sum of the vessel velocity U , which is along the x seakeeping direction, and the sea one u_{sea} . Then, the effective sideslip angle δ would be the sum

of δ_0 and the eventual yaw angle ψ

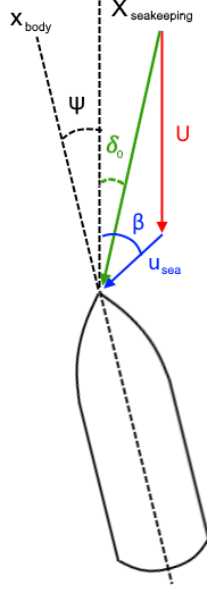


Figure 14: Effective sideslip angle $\delta = \delta_0 + \beta$ if waves income with a heading angle β

We can see that if the sea velocity is aligned with the x direction of the seakeeping frame, $\delta_0 = 0$ and we come back to $\delta = \psi$.

To simplify the analysis, we assume that u_{sea} is always negligible with respect to U , and the approximation $\delta \approx \psi$ is assumed. Indeed, from potential theory we know that the sea surface speed u_{sea} , which exponentially decreases with the depth, is limited by the value $\zeta\omega_0$:

$$\begin{aligned} u_{sea} &= Re \left\{ \sqrt{\left(\frac{\partial\varphi_I}{\partial x}\right)^2 + \left(\frac{\partial\varphi_I}{\partial y}\right)^2} \right\} = \\ &= \zeta\omega_0 Re \left\{ \sqrt{-\cos^2 \beta e^{2jk(x \cos \beta - y \sin \beta)} e^{2j\omega_e t} - \sin^2 \beta e^{2jk(x \cos \beta - y \sin \beta)} e^{2j\omega_e t}} \right\} \leq \zeta\omega_0 \end{aligned}$$

Neglecting u_{sea} amounts to saying $\zeta\omega_0 \ll U$, that for small amplitude waves with peak periods long enough can be a good approximation. In future versions, that can be treated with higher accuracy. For considering yaw stability and to point out the opposite reaction moment N and the cross force Y caused by the presence of a non zero sideslip angle δ , two coefficients are taken into account. Indeed, in order to compute the exact values of N and Y , one should solve the potential flow around the ship water plane section. But, to simplify, we will use the results of [Lee&Shin1998, Inoue et al. 1981] on this argument; defining a overall vessel aspect ratio $k_L = \frac{B}{L}$ and the block coefficient $C_b = \frac{\Omega}{L_{pp}Bd}$,

the following approximated derivatives are evaluated

$$N_\delta = -0.0024 - 1.0272 \cdot k$$

$$Y_\delta = \frac{\pi}{2}k + 1.4 \cdot C_b \cdot \frac{B}{L}$$

The reaction moment in yaw is stabilizing, so the derivative is negative; on the other hand, if a sideslip angle appears, the sway force has its same sign. From these values, we can compute the following terms

$$G_{16} = -\frac{1}{2}\rho U^2 L_{pp} d \cdot Y_\delta$$

$$G_{55} = -\frac{1}{2}\rho U^2 L_{pp} d \cdot N_\delta$$

Let us remember that the matrix \mathbf{G} is defined positive on the first side of the Cummins equation: that explains the opposite sign with respect the real forces. Furthermore, it is important to notice that these former two terms are not restoring coefficients due to hydrostatics physics, but they are dynamical coefficients, which appear in presence of a forward speed. They are just linearly dependent on an element of the generalized position vector, $\psi \approx \delta$, so that they can be incorporated in \mathbf{G} .

13. Infinite Frequency Matrices \mathbf{A}_∞ and \mathbf{B}_∞ and Transfer Function

The optimization problem is solved for a certain range of orders of the memory effect term approximated transfer function – from 2 to 20, and for each pair (i, k) of degrees of freedom separately; then the order choice will fall on the best trade off between a good fitting and a limited order.

Fixing the pair (i, k) , for every order in the range $\{2, \dots, 20\}$, the optimization problem will find $\hat{K}_{ik}(s)$, $\hat{A}_{\infty,ik}$ and $\hat{B}_{\infty,ik}$; in order to do that, the minimization algorithm is chosen in function of the speed – if it is zero or not, and according to what simulator is running, *SeaBoS* or *ManBoS*.

We saw how, after solving the problem for a certain approximation order, it is possible to carry out a quality control to evaluate the fitting; that is made by comparison of the data set discrete values for the 52 frequencies ω_l , $A_{ik}(\omega_l)$ and $B_{ik}(\omega_l)$, with the approximated ones:

$$\hat{B}_{ik}(\omega) = \hat{B}_{\infty,ik} + Re \left\{ \hat{K}_{ik}(j\omega) \right\}$$

$$\hat{A}_{ik}(\omega) = \hat{A}_{\infty,ik} + \frac{1}{\omega} Im \left\{ \hat{K}_{ik}(j\omega) \right\}$$

This weighted comparison is effectuated by computing both the mean relative distance of the points of the data set with the correspondent values of $\hat{A}_{ik}(\omega_l)$ and $\hat{B}_{ik}(\omega_l)$ and the difference of the trend – i.e. the first derivative:

$$err_A = \frac{1}{52} \left\{ 0.4 \cdot \sum_l \left| \frac{\hat{A}_{ik}(\omega_l) - A_{ik}(\omega_l)}{A_{ik}(\omega_l)} \right| + 0.6 \cdot \sum_l \left| \frac{[\hat{A}_{ik}(\omega_{l+1}) - \hat{A}_{ik}(\omega_l)] - [A_{ik}(\omega_{l+1}) - A_{ik}(\omega_l)]}{[A_{ik}(\omega_{l+1}) - A_{ik}(\omega_l)]} \right| \right\}$$

$$err_B = \frac{1}{52} \left\{ 0.4 \cdot \sum_l \left| \frac{\hat{B}_{ik}(\omega_l) - B_{ik}(\omega_l)}{B_{ik}(\omega_l)} \right| + 0.6 \cdot \sum_l \left| \frac{[\hat{B}_{ik}(\omega_{l+1}) - \hat{B}_{ik}(\omega_l)] - [B_{ik}(\omega_{l+1}) - B_{ik}(\omega_l)]}{[B_{ik}(\omega_{l+1}) - B_{ik}(\omega_l)]} \right| \right\}$$

The overall error is computed as the sum of the two former terms, multiplied by the order of the fitting:

$$err = (err_A + err_B) \cdot order$$

That will weight both the precision and the degree of the fitting function: for low orders a greater distance $err_A + err_B$ is found, but for higher orders the heaviness of the transfer function leads to other disadvantages. The algorithm will choose the order with the lowest accumulative error err . If the variable `Man_Order` is off, the simulator will proceed with all the degrees of freedom. Otherwise the user will be demanded each time for checking the fitting and the algorithm choice.

14. Time Simulation

This is the simulator core: after each time step Δt , the equation integration leads to the generalized position and velocity vector update. At first, there is a routine called `force_exc.m` responsible of the excitation forces computation: given the time and the vessel position and velocity, Froude-Krilov and diffraction forces are calculated on the body fixed frame, and then rotated in the seakeeping one.

We know that the motion equation can be written in the following linear form:

$$\dot{\mathbf{y}}(t) = \mathbf{W} \cdot \mathbf{y}(t) + \mathbf{l}(t) = \mathbf{f}(t, \mathbf{y}(t))$$

where $\mathbf{y}(t) = \begin{bmatrix} \xi(t) \\ \dot{\xi}(t) \end{bmatrix}$, the constant matrix \mathbf{W} is:

$$\mathbf{W} = \begin{bmatrix} \mathbf{0}_{6 \times 6} & \mathbf{I}_{6 \times 6} \\ -(\mathbf{M}_{RB} + \mathbf{A}_{\infty})^{-1} \mathbf{G} & -(\mathbf{M}_{RB} + \mathbf{A}_{\infty})^{-1} \mathbf{B}_{\infty} \end{bmatrix}$$

and the time dependent vector $\mathbf{l}(t)$ is:

$$\mathbf{l}(t) = \begin{bmatrix} \mathbf{0}_{6 \times 1} \\ (\mathbf{M}_{RB} + \mathbf{A}_\infty)^{-1} \left(\tau_{FK+Diff}^s - \mu(t) \right) \end{bmatrix}$$

To integrate this equation, a standard 4th order Runge-Kutta method (RK4) is applied; calling $t_j = j\Delta t$ and $\mathbf{y}_j = \mathbf{y}(j\Delta t) = \mathbf{y}(t_j)$, this method operates as follows:

$$\begin{aligned} k_1 &= \Delta t \cdot \mathbf{f}(t_j, \mathbf{y}_j) \\ k_2 &= \Delta t \cdot \mathbf{f}\left(t_j + \frac{\Delta t}{2}, \mathbf{y}_j + \frac{k_1}{2}\right) \\ k_3 &= \Delta t \cdot \mathbf{f}\left(t_j + \frac{\Delta t}{2}, \mathbf{y}_j + \frac{k_2}{2}\right) \\ k_4 &= \Delta t \cdot \mathbf{f}(t_{j+1}, \mathbf{y}_j + k_3) \\ \mathbf{y}_{j+1} &= \mathbf{y}_j + \frac{1}{6}(k_1 + 2k_2 + 2k_3 + k_4) \end{aligned}$$

We can notice that in order to apply this method, $\mathbf{l}(t_j + \frac{\Delta t}{2})$ and $\mathbf{l}(t_{j+1})$ must be computed, which means to evaluate $\tau_{FK+Diff}^s$ and μ at the instants $t_j + \frac{\Delta t}{2}$ and t_{j+1} .

The variable μ is updated by the means of another independent RK4 method, about the state variable $\mathbf{x}(t)$, and it is difficult to couple both integration: the approximation $\mu(t_j + \frac{\Delta t}{2}) \approx \mu(t_{j+1}) \approx \mu(t_j)$ is used.

Concerning the vector $\tau_{FK+Diff}^s$, the routine `force_exc.m` allows to compute it giving as input only the time t and the vector \mathbf{y} . To compute $\tau_{FK+Diff}^s$ at $t_j + \frac{\Delta t}{2}$ and t_{j+1} , the following process is carried out: approximating $\tilde{\mathbf{y}}_{j+1} = \mathbf{y}_j + \Delta t \cdot \mathbf{f}(t_j, \mathbf{y}_j)$, $\tau_{FK+Diff}^s(t_{j+1})$ is calculated giving $(t_{j+1}, \tilde{\mathbf{y}}_{j+1})$ as input to `force_exc.m`; then

$$\tau_{FK+Diff}^s\left(t_j + \frac{\Delta t}{2}\right) = \frac{1}{2}(\tau_{FK+Diff}^s(t_j) + \tau_{FK+Diff}^s(t_{j+1}))$$

The iterations go on until the final time `T_fin` is reached, that is after $\frac{T_{fin}}{\Delta t} = 20T_{fin}$ steps.

15. Post-Processing

After completing all the iterations, the dynamical responses are plotted: position, attitude, velocities and angular velocities in function of time.

16. Plot Vessel Dynamics – Time animation

To give a better physical sense of the results and of the vessel behavior, a 3D animation is available. It shows the vessel dynamics, while floating on the wavy fluid free surface

14 Examples

Now we will show some examples of results of *FloBoS*. More than standard simulations, we will also try to stress the code, pushing to the limit the cases concerning the validity range of the hypothesis.

Container S175 - *SeaBoS*

We present a set of simulation performed with the container ship S175, scaled differently in each case to decrease the computational cost. The data of the container and the hull geometry are presented below:

- Length $L_{pp} = 175\text{ m}$
- Beam $B = 25\text{ m}$
- Draft $d = 7.5\text{ m}$
- Free board $FB = 3.5\text{ m}$

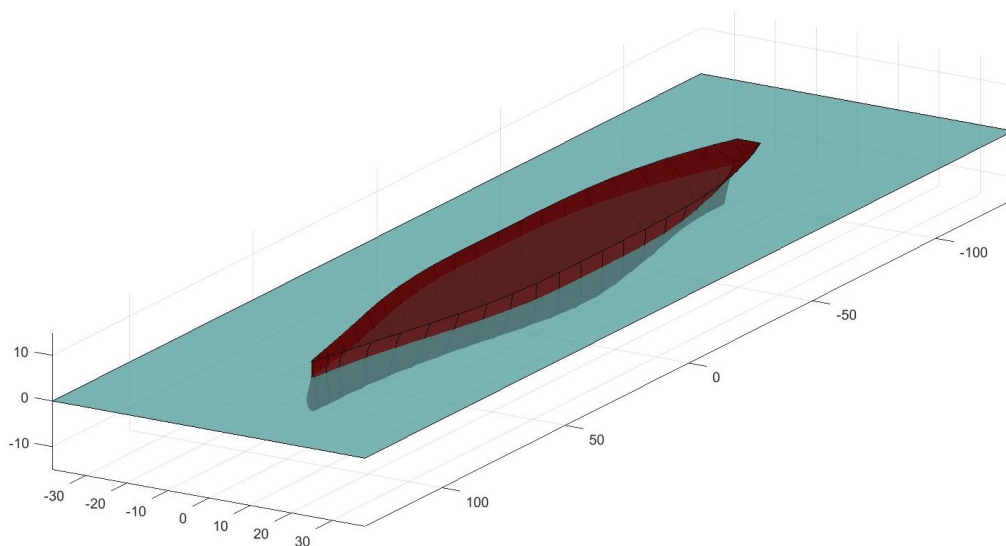


Figure 15: Container S175 with water free surface

Non-zero forward speed

This simulation has been performed with the 10% scaled container, so with a length $L_{pp} = 17.5 \text{ m}$. The speed of the ship is $U = 2.5 \frac{\text{m}}{\text{s}}$, so the Froude number is $Fr \approx 0.19$, in the limit of theory validity. The imposed sea state has been characterized by $H_{m0} = 0.6 \text{ m}$, $T_p = 6 \text{ s}$ and main direction $\theta_0 = 0^\circ$.

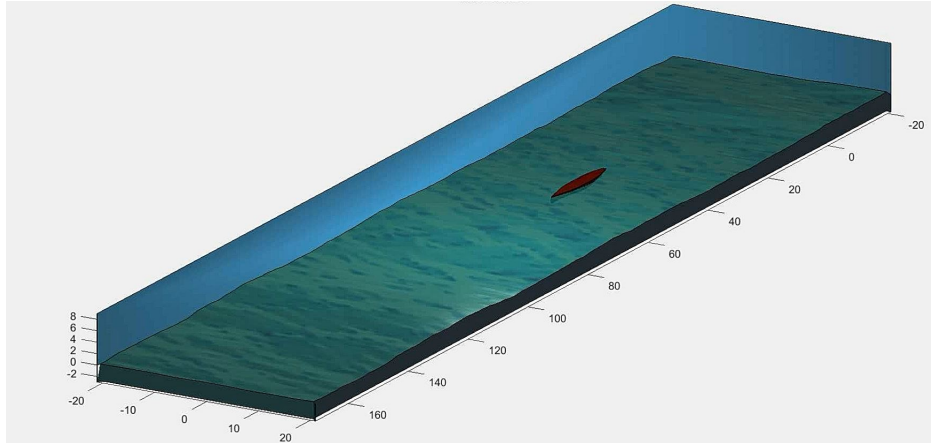


Figure 16: Container S175 and physical domain

After a 60 seconds simulation, the results of the vessel dynamics are:

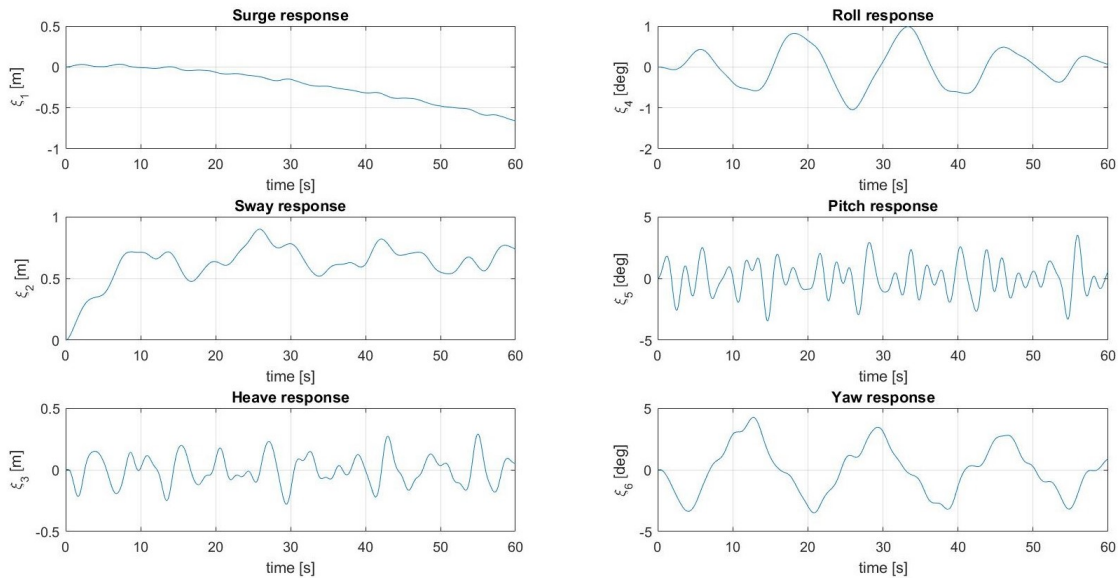


Figure 17: Position and attitude with respect to the seakeeping frame

We can see how sway and heave displacements are relatively small, while along the x direction there is a backwards drift caused by the resistance of the ship (friction and pressure) and by the excitation forces. However, the ship is moving forward: ξ_1 represents the displacement with respect the seakeeping

frame, which is moving along x with a positive speed of $U = 2.5 \frac{m}{s}$ in this case. Angular responses are limited enough to consider the linear small angles approximation valid.

Concerning velocities, linear ones are all small and with a zero mean. The most important dynamics contribution is due to pitch angular velocity, because of the incoming waves at zero heading.

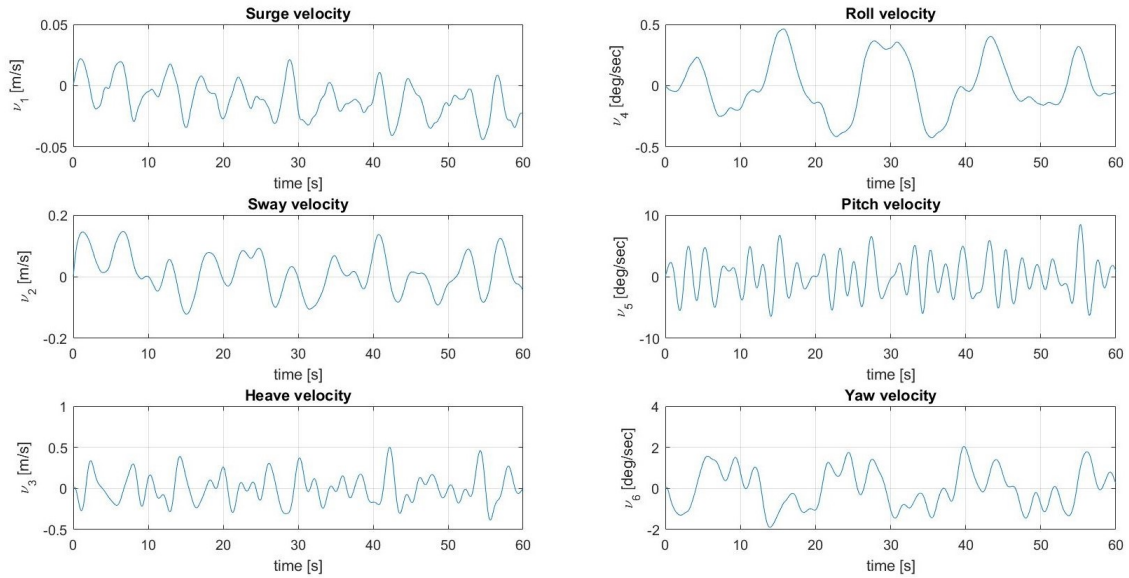


Figure 18: Velocities with respect to the seakeeping frame

The computed excitation forces are:

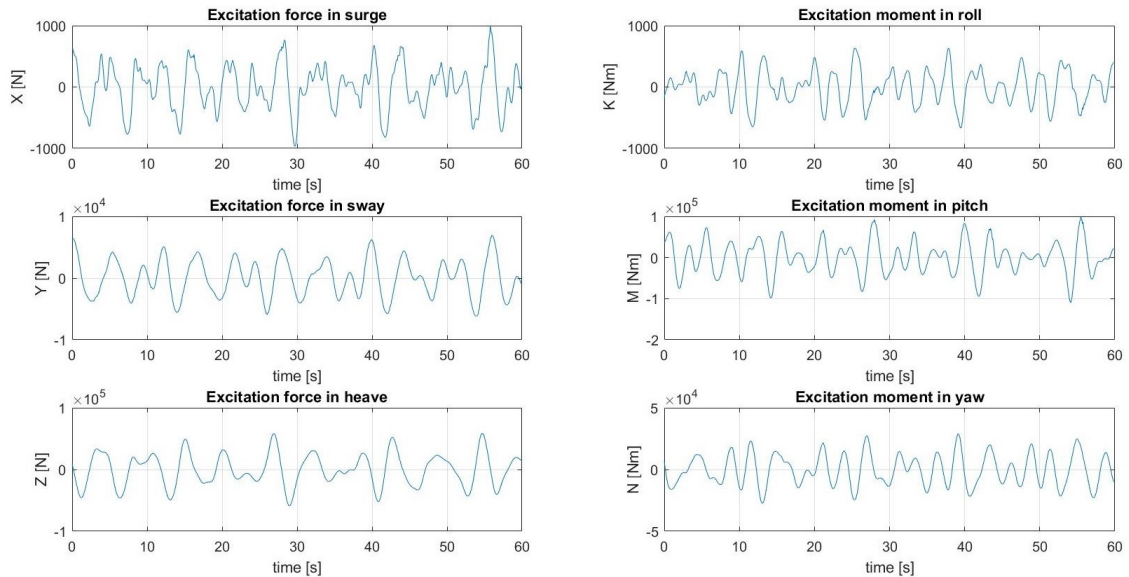


Figure 19: Waves excitation forces

Zero speed – green water

Trying to evaluate the simulator reaction to a rough sea condition, we imposed a spectrum with $H_{m0} = 2\text{ m}$ and $T_p = 8\text{ s}$, corresponding to a sea state Beaufort number 4, and main waves direction of $\beta = 20^\circ$.

The container, at zero speed $U = 0$, has been scaled at 33% :

- Length $L_{pp} = 57.75\text{ m}$
- Beam $B = 8.38\text{ m}$
- Draft $d = 2.47\text{ m}$
- Free board $FB = 1.15\text{ m}$

After simulating one minute, the results are:

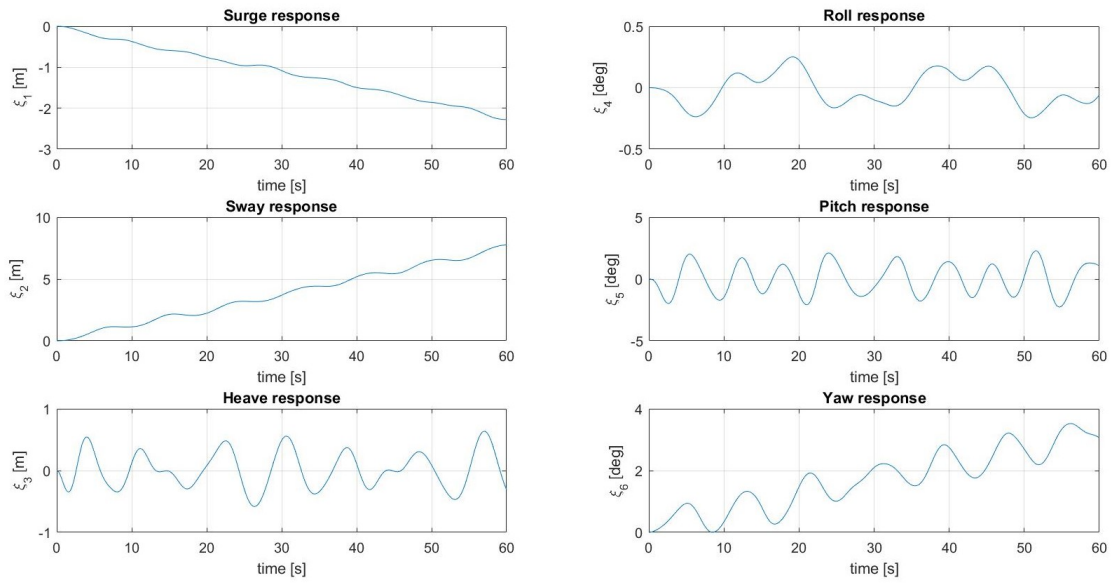


Figure 20: Position and attitude with respect to the seakeeping frame

Angles are small enough to consider them in the validity range of small oscillations theory. We can notice a drift both in surge (for the same reason as the first case) and in sway, because of the heading angle β . On the other hand, yaw angle increases in time, also if $\beta > 0$: in *FloBoS* a yaw stabilizing moment appears only if there is a speed $U > 0$, because the action of the sea is neglected – also in this case of zero speed, it can not be treated as negligible. Therefore, the only effect acting on yaw is due to the excitation forces: this can be confirmed by noticing the oscillatory trend of the yaw response. The integration of the dynamic pressure on the hull leads, evidently, to an increasing yaw angle.

For the velocities, as before, the most accentuated is the pitch one; the heading angle is too small to lead to important roll angular rate.

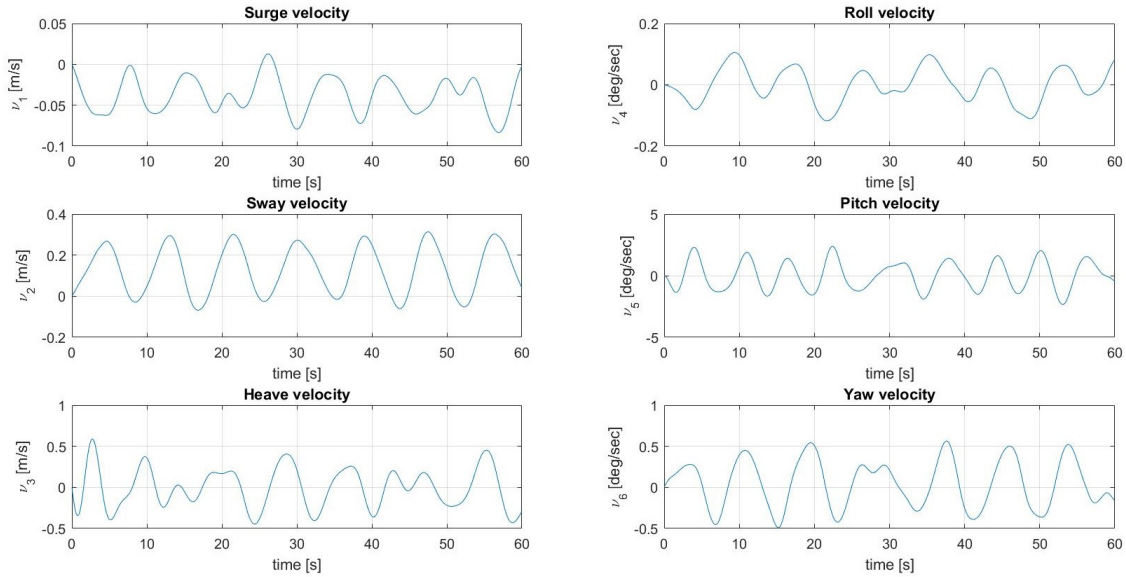


Figure 21: Velocities with respect to the seakeeping frame

The computed excitation forces are:

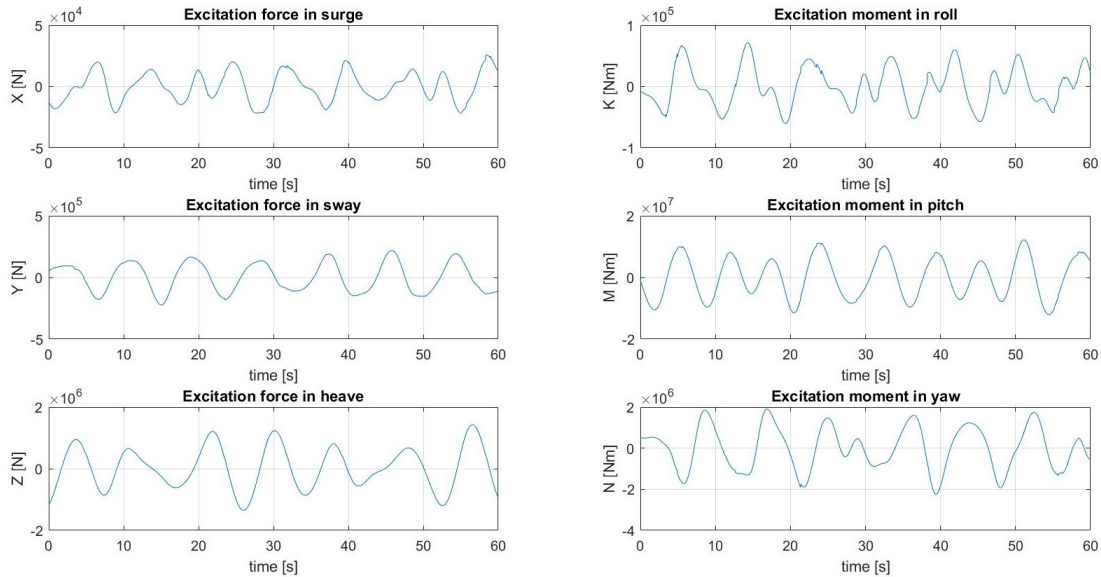


Figure 22: Waves excitation forces

Four frames of the animation are showed below, to relate the sea state to the vessel dimensions:

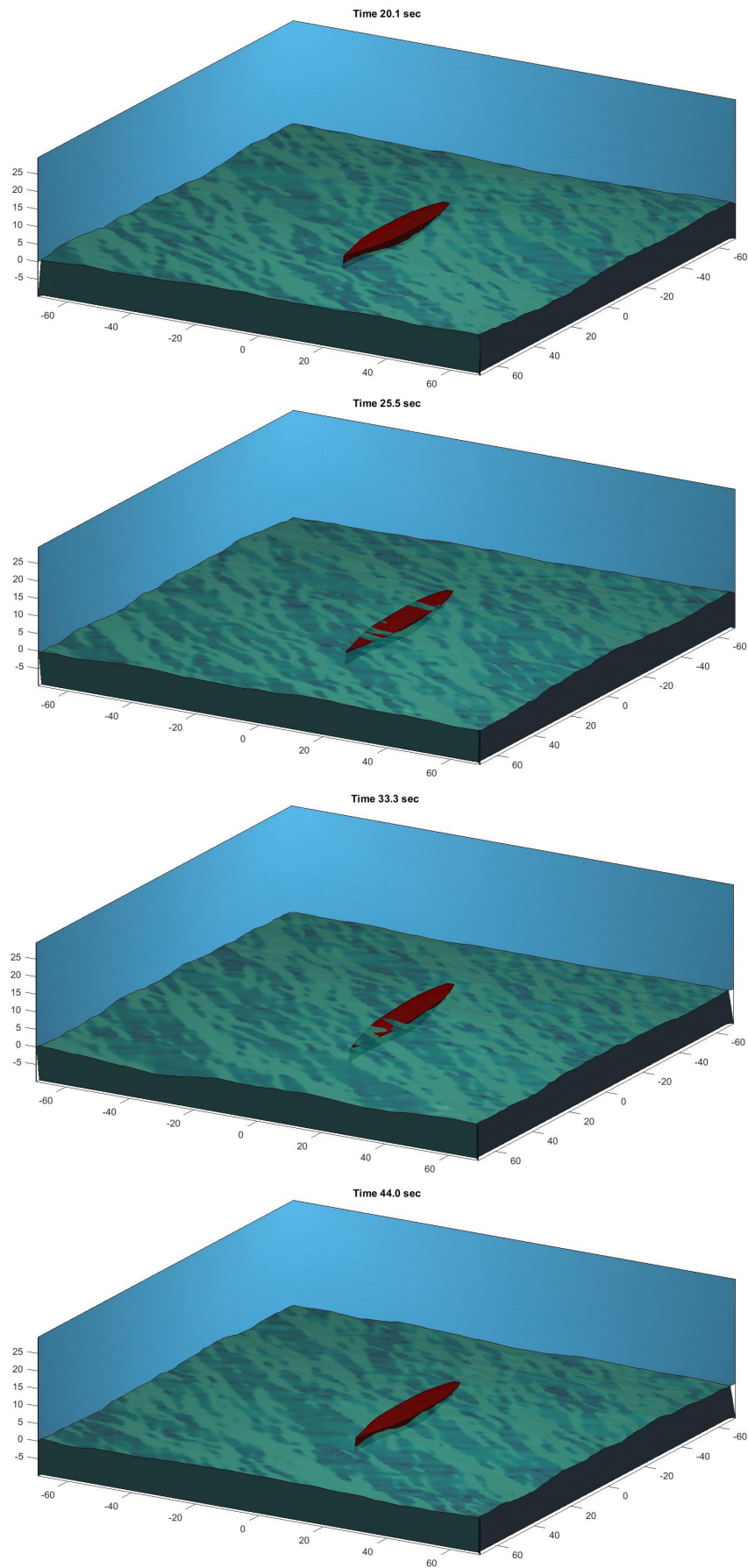


Figure 23: Container S175 scaled at 33% in a sea state Beaufort number 4

Container S175 - *ManBoS*

A similar simulation can be performed to evaluate how efficient is a solo rudder maneuver. The vessel is now scaled at 25% and the rudder geometric properties are:

- Surface equal to 5% of the longitudinal $L_{pp}d$;
- Aspect ratio of 2.5;
- Maximum angle of deflection $\delta_{max} = 30^\circ$

With relatively calm sea conditions, $H_{m0} = 0.1\text{ m}$ and $T_p = 5.5\text{ s}$, the vessel will try to reach two target points, one after the other: $P_1 = (150, 25)$ and $P_2 = (300, -15)$.

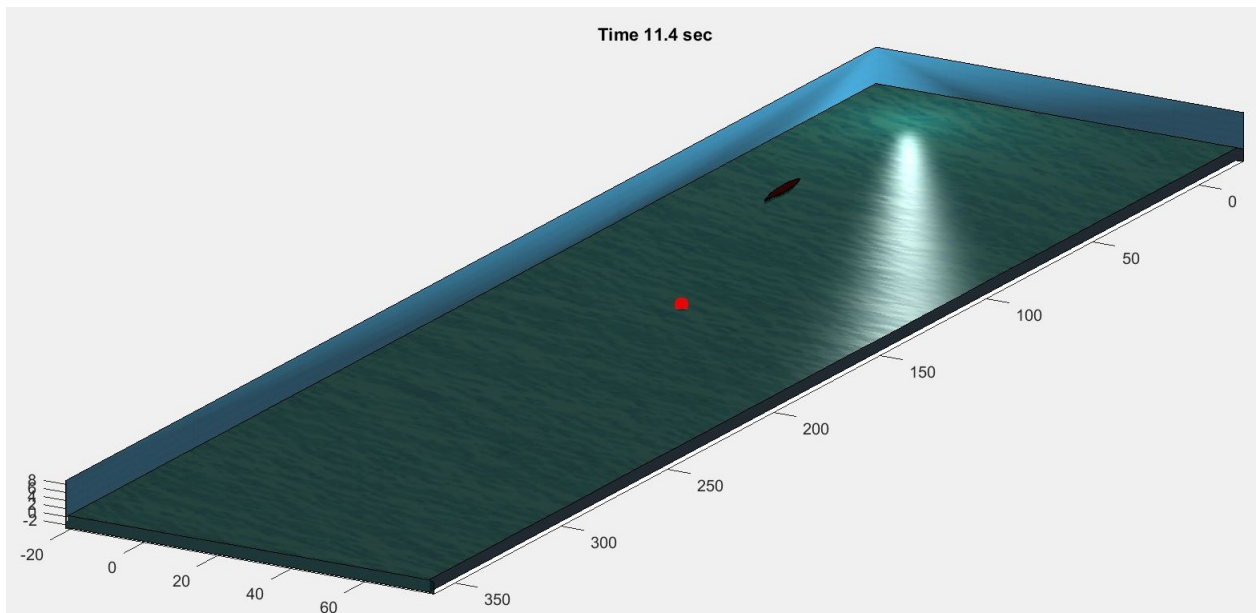


Figure 24: Container S175 with the first target point

After simulating, we can see how the rudder controls the vessel and it consequently follows and reach the target points. The results are good and the *PD* controller is functional; however the physical model of the controller is not realistic: it does not take into account neither the operational time of the actuator nor the hydrodynamics feedback. In spite of this, we can say that the *PD* controller design, based on the computation of the heading angle error, can be considered a good solution.

Looking at the dynamical responses, both the velocities and the positions are affected by the discontinuity after about 30 seconds, because of the sea lane change. The responses are pretty smooth, but after the second maneuvering action, with the purpose of reaching the second point, the roll response increases forcefully, remaining however in an acceptable range.

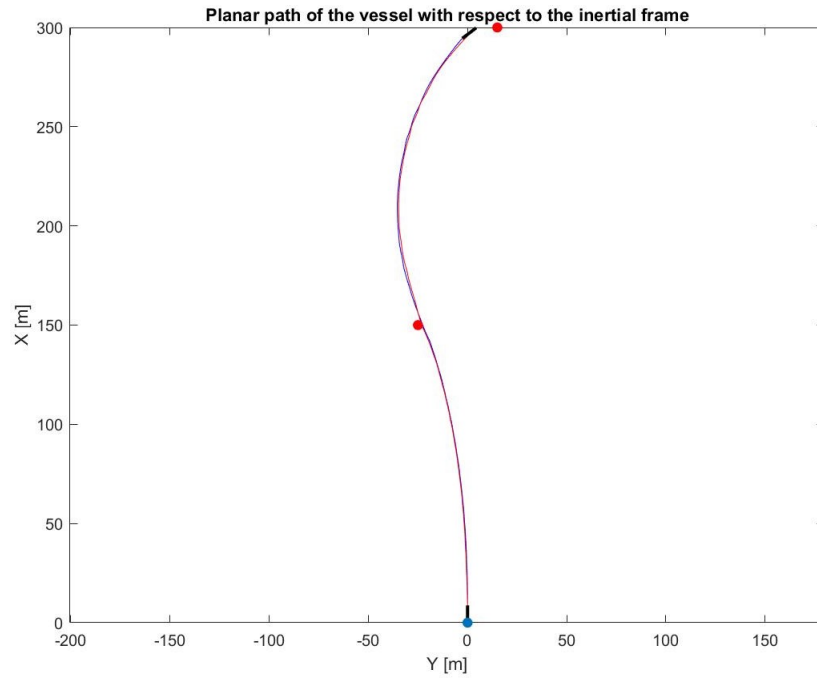


Figure 25: Vessel path

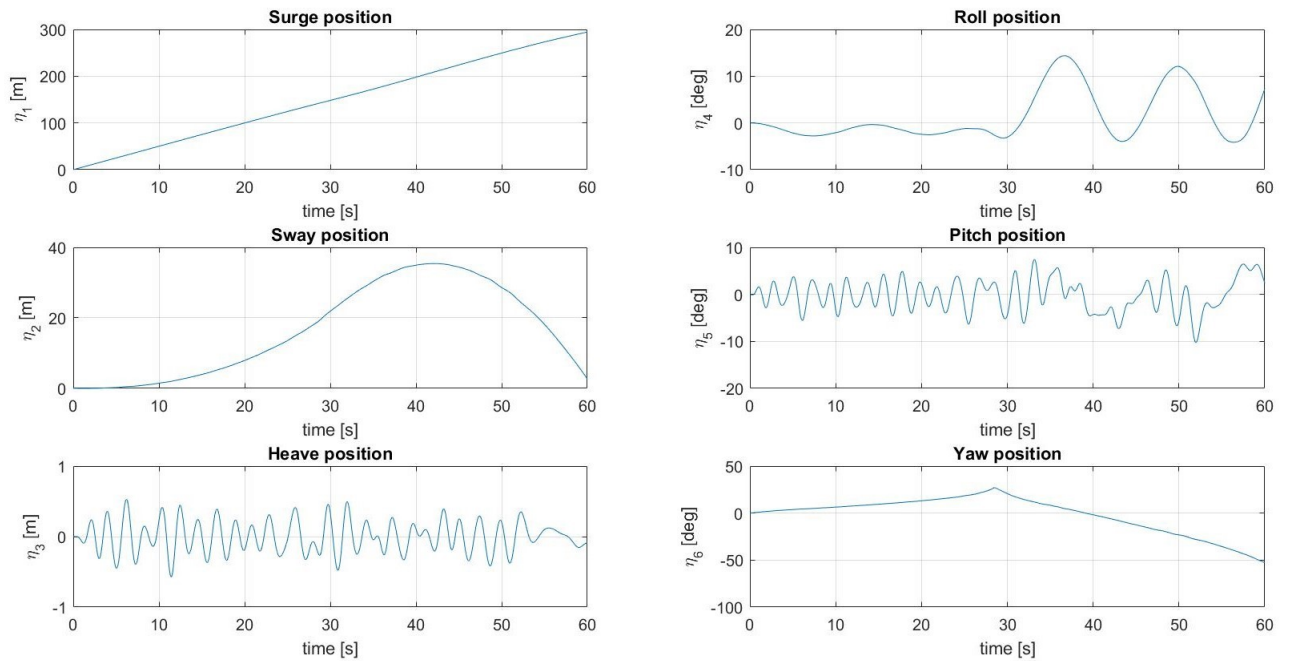


Figure 26: Position and attitude with respect to the seakeeping frame

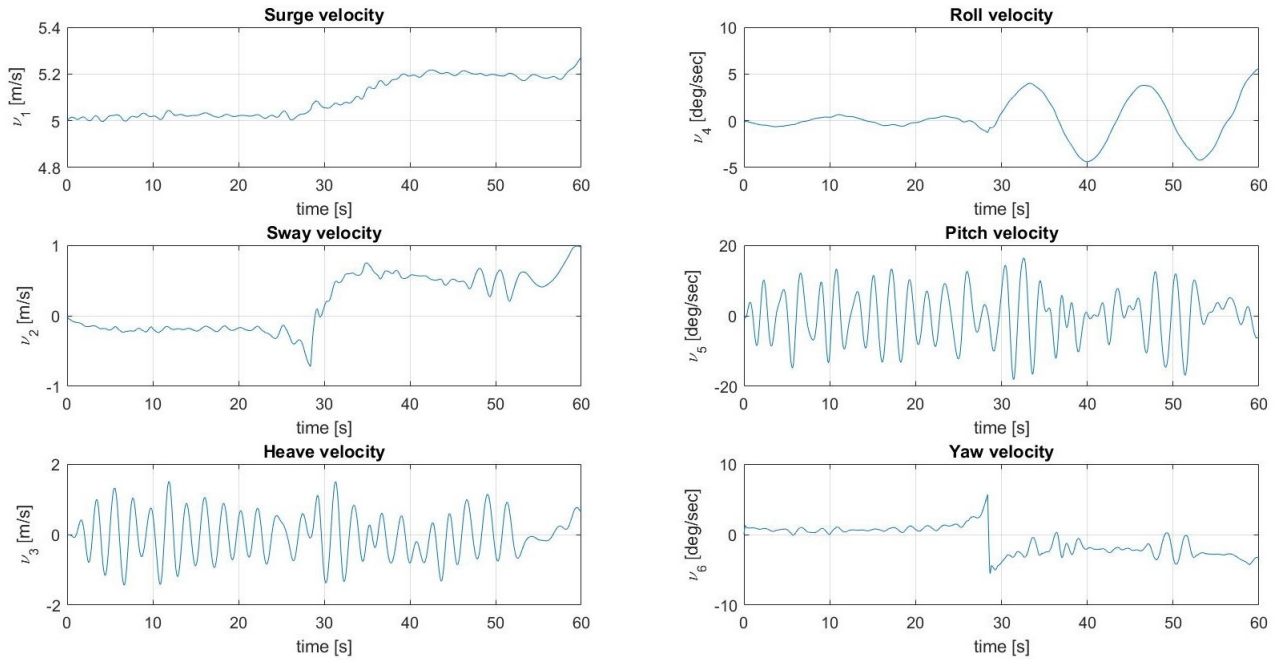


Figure 27: Velocities with respect to the seakeeping frame

The computed excitation forces are:

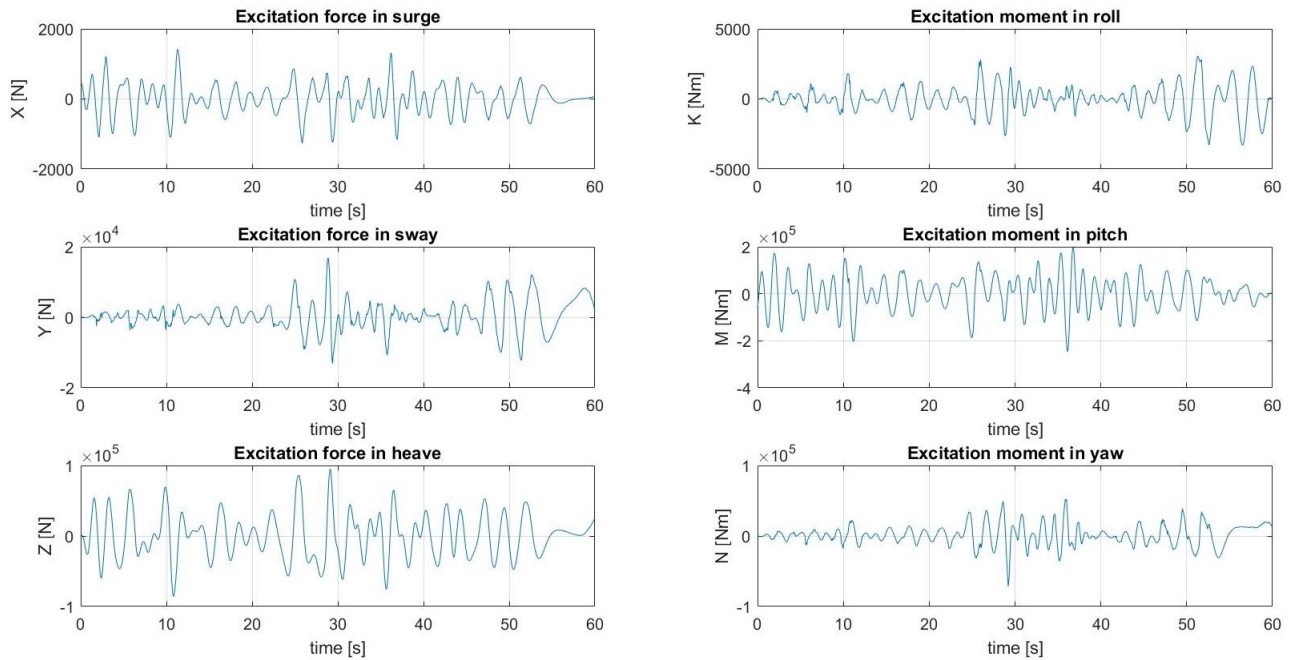


Figure 28: Waves excitation forces

TiME - *SeaBoS*

Another set of simulations has been run with a floating capsule for space exploration: the TiME – Titan Mare Explorer, a proposed design for a lander for Saturn’s moon Titan. The capsule is essentially composed by two truncated cones and, also if the hull is not conform with the hypothesis of slender body, the aim of simulating it has been to evaluate how strict the slender body assumption is.

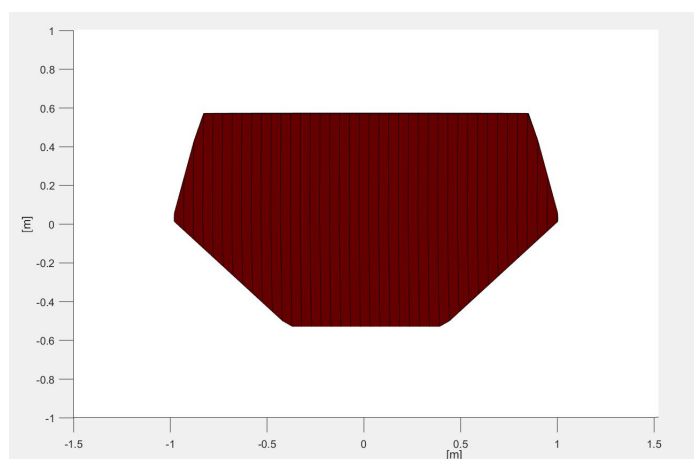


Figure 29: TiME capsule geometry

The simulation concerns the capsule response in a Titan hydrocarbons sea, composed by methane and ethane, to a simple harmonic wave excitation.

The results are compared with the analysis made by [Lorenz&Mann2015].

The density of the sea has been chosen as $\rho = 570 \frac{kg}{m^3}$ and the gravity on Titan is approximately $g = 1.35 \frac{m}{s^2}$. Concerning the wave, the amplitude is $\zeta_0 = 0.1 m$ with a period of $T = 5.5 s$. With a deep sea approximation the wave length should be $\lambda = \frac{2\pi}{k} = \frac{2\pi g}{\omega^2} = \frac{gT^2}{2\pi} = 6.5 m$, but to reproduce the same conditions of [Lorenz&Mann2015], the wave length is set to $\lambda = 2 m$.

The capsule is in the figure below: the diameter at the cones interface is $2 m$, while the other smaller diameters are about $1.7 m$, for the upper truncated cone, and $0.75 m$ for the lower one. The entire height is about $1.1 m$. The mass is $700 kg$ and the center of gravity is located at the interface.

These conditions imply a floating equilibrium position with the free liquid surface at the level of the cones interface.

It is important to notice that to evaluate oscillations caused by a simple harmonics, it is necessary to impose the sea direction to 90° . In a real situation, it would have been irrelevant, because of the symmetry of the capsule. However *FloBoS* is well suited for slender bodies: the strip theory does not allow to

analyze surge motion and the sway and roll dynamics are better captured. This means that, in order to increase the reliability of the simulation, it is more appropriate to choose $\beta = 90^\circ$.

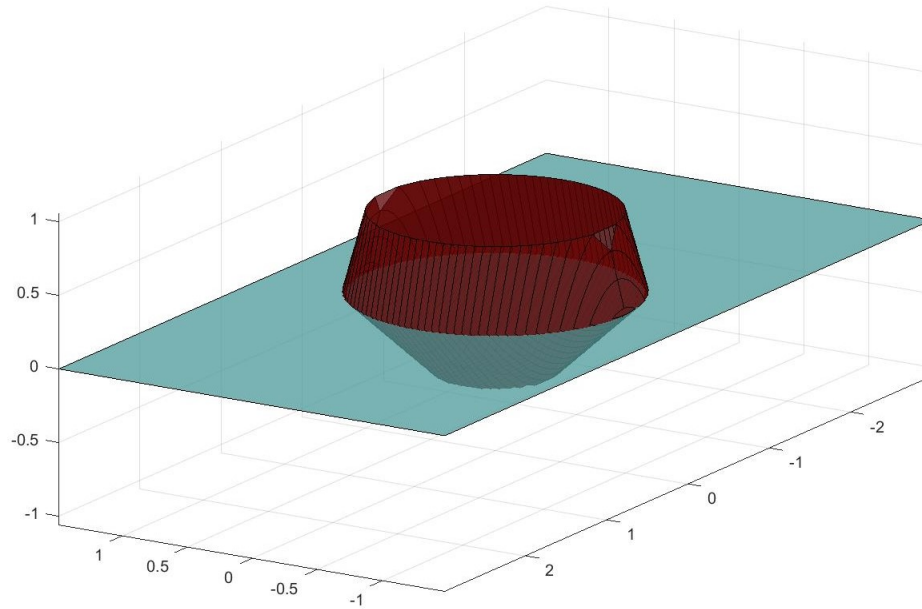


Figure 30: TiME capsule reproduction

The simulation is affected by an initial transitory phase, when the capsule starts to interact with the sea; after about 45 seconds the oscillations are periodic and stable. In the following figure the regime response is showed:

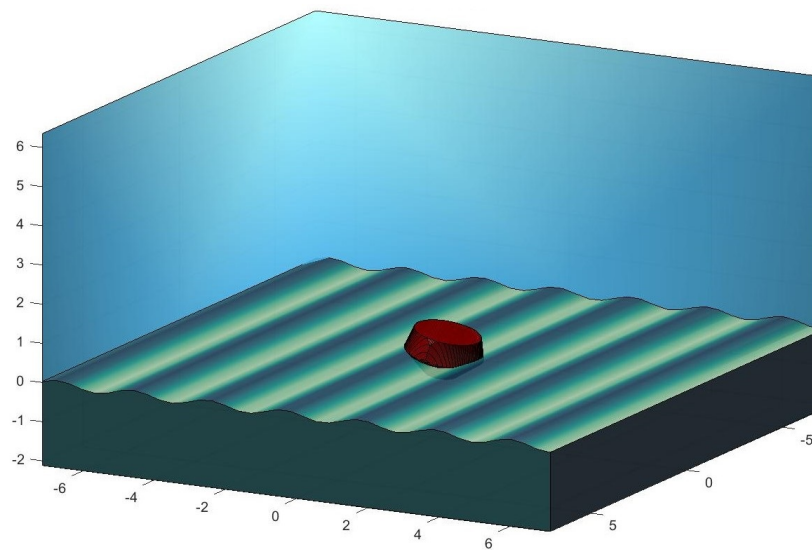


Figure 31: TiME capsule reproduction in the wavy sea

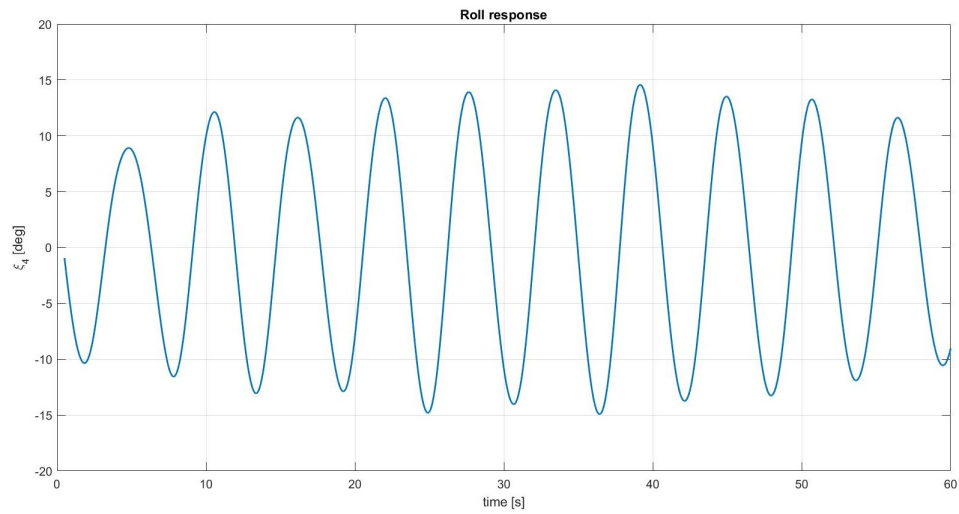


Figure 32: TiME regime response – *FloBoS* results

In the following figure the results of [Lorenz&Mann2015] are reported:

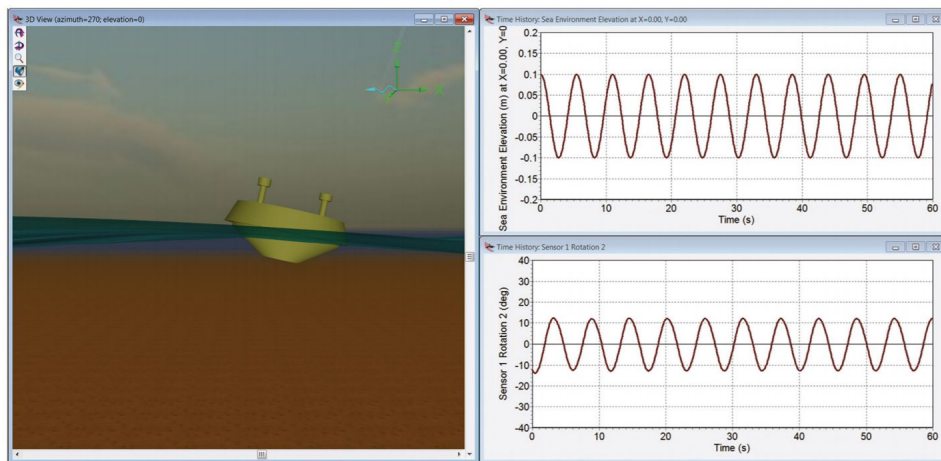


Figure 33: Simulation results of [Lorenz&Mann2015]

We can see that the response amplitude is comparable: 12° for [Lorenz&Mann2015] and around 14° obtained with *FloBoS*.

15 Conclusions

The simulator has been designed and tested, but a more intense validation process is needed. In order to make the results more reliable, a wide set of experimental data should be used for a cross control with the results, to improve and refine the simulator code. Moreover, viscous and non linear effect can be added in the model.

Concerning *ManBoS*, a more accurate controller can be implemented, both for the actuator physical model and a *PD* automatic tuning, by the means of the hydrodynamic derivatives of the vessel – see for example the well known autopilot model proposed by [Nomoto et al. 1957].

Finally, a possible future extension of *FloBoS* can implement a solver for the inverse problem, i.e. estimate the sea state from on-board measurements of the ship.

In conclusion, *FloBoS* is a starting point for the design of a more accurate simulator, which can give reliable feedback about vessel dynamical responses.

Acknowledgments

This research was carried out at NASA JPL – Jet Propulsion Laboratory, California Institute of Technology, during the internship sponsored by JVS RP – *JPL Visiting Student Research Program*, and NASA – *National Aeronautic and Space Administration*.

I would like to thank my mentor at JPL, Dr. Marco B. Quadrelli, who always motivated me, giving incitements to improve, both personally and professionally. His ideas, guidelines and suggestions made this experience and research project possible. I also thank the institution of Politecnico di Torino, which gave me this incredible opportunity, and my supervisor, prof. Lorenzo Casalino, for his help and support.

References

- [Cummins1962] W. E. Cummins. *The impulse Response Function and Ship Motions*. Technical Report 1661, David Taylor Model Basin–DTNSRDC, 1962.
- [Faltinsen1990] O. M. Faltinsen. *Sea Loads on Ships and Offshore Structures*. Cambridge University Press, 1990.
- [Fossen2002] Thor I. Fossen. *Marine Control Systems: Guidance, Navigation and Control of Ships, Rigs and Underwater Vehicles*. Marine Cybernetics, Trondheim, 2002.
- [Fossen2005] T. I. Fossen. *A Nonlinear Unified State-Space model for ship maneuvering and control in a seaway*. *Jurnal of Bifurcation and Chaos*, 2005.
- [Fossen2011] T. I. Fossen. *Handbook of Marine craft Hydrodynamics and motion control*. John Wiley & Sons Ltd. Publication, first edition, 2011.
- [Hasselmann1973] K. Hasselmann *et al.* *Measurements of wind-wave growth and swell decay during the Joint North Sea Wave Project*. *Deutschen Hydrografischen Zeitschrift*, 12, 9-95. 1973
- [Inoue et al. 1981] S. Inoue, M. Hirano and K. Kijima. *HYDRODYNAMIC DERIVATIVES ON SHIP MANOEUVRING*. *International Shipbuilding Progress* 28(321):112-125, 1981.
- [Levy1959] E. Levy. *Complex curve fitting*. *IRE Trans. Autom. Control*, 1959.
- [Lee&Shin1998] H. Y. Lee, S. S. Shin. *The Prediction of ship’s manoeuvring performance in initial design stage*. Elsevier Science B. V. *Practical Design of Ships and Mobile Units* M WC. Oosterveld and S. G. Tan, editors. 1998
- [Lorenz&Mann2015] R. D. Lorenz, J. L. Mann. *Seakeeping on Ligeia Mare: Dynamic Response of a Floating Capsule to Waves on the Hydrocarbon Seas of Saturn’s Moon Titan*. *Johns Hopkins APL Technical Digest*, Volume 33, Number 2, 2015.
- [Musci2015] V. Musci. *Development and Validation of a Ship Response Simulator*. *Jet Propulsion Laboratory*, MSc degree thesis at Poliecnico di Torino, 2015.
- [Newman1997] J. Newman. *Marine Hydrodynamics*. MIT Press, 1997.

- [Nomoto et al. 1957] K. Nomoto, T. Taguchi, K. Honda and S. Hirano. *On the Steering Qualities of Ships*. Technical report. International Shipbuilding Progress, Vol. 4, 1957.
- [Ogilvie1964] T. Ogilvie. *Recent progress towards the understanding and prediction of ship motions*. 6th Symposium on Naval Hydrodynamics, 1964.
- [Perez&Fossen] T. Perez, T. I. Fossen. *Time domain models of marine surface vessels based on seakeeping computations*. Centre for Ships and Ocean Structures, Department of Engineering Cybernetics. Norwegian University of Science and Technology.
- [Perez&Fossen2007] T. Perez, T. I. Fossen. *Kinematic Models for Manoeuvring and Seakeeping of Marine Vessels*. Modeling, Identification and Control, Vol. 28, No. 1, 2007.
- [Perez&Fossen2008] T. Perez, T. I. Fossen. *Joint identification of Infinite-Frequency Added Mass and Fluid-memory Models of Marine Structures*. Modeling, Identification and Control, Vol. 29, No.3, 2008.
- [Perez&Fossen2008bis] T. Perez, T. I. Fossen. *Time- vs. Frequency-domain Identification of Parametric Radiation Force Models for Marine Structures at Zero Speed*. Modeling, Identification and Control, Vol. 29, No.1, 2008.
- [Taghipour2008] R. Taghipour, T. Perez and T. Moan. *Hybrid frequency–time domain models for dynamic response analysis of marine structures*. Ocean Engineering, 2008.
- [Torsethaugen1993] K. Torsethaugen. *A two peak wave spectral model*. In Proc. 12th Int. Conference on Offshore Mechanics and Arctic Engineering, OMAE, Glasgow, Scotland, 1993
- [WAFO2017] WAFO group – Lund University. *Tutorial for WAFO version 2017*